

UNIVERSITY OF NAPLES FEDERICO II

Department of Pharmacy



Ph.D. thesis in Pharmaceutical Science

***In vitro biological characterization
of innovative anticancer
metal-based agents***

Candidate: Dr. Antonella Capuozzo

Tutor: Prof. Rita Santamaria

Coordinator: Prof. Maria Valeria
D'Auria

XXVIII cycle

2013-2016

*"One must still have chaos in
oneself to be able to give
birth to a dancing star"*

Friedrich Nietzsche

Index

ABSTRACT	8
1.BACKGROUND	10
1.1 Classical and epigenetic mechanisms involved in chemotherapy	11
1.1.1. Cancer: statistical data and the most used therapeutic approaches.....	11
1.1.2 Types of cell death induced by anticancer agents.....	13
1.1.2.a. Apoptosis.....	14
1.1.2.b. Autophagy.....	16
1.1.2.c. Necrosis and other types of cell death.....	18
1.1.3 The role of epigenetics in tumorigenesis and in cancer therapy.....	20
1.1.3.1. Epigenetic mechanisms.....	20
1.1.3.2. Histone modifications.....	21
1.1.3.2.a. The chromatin-forming proteins: the histones.....	21
1.1.3.2.b. Histone post-translational modifications.....	23
1.1.3.2.c. Histones localization.....	24
1.2. Anticancer metal-based drugs	26
1.2.1. Cisplatin and its analogs.....	26
1.2.2. New transition metals-based complexes.....	28
1.3. Nanovectors as innovative pharmaceutical forms for drug delivery	33
1.3.1. Liposomes and micelles.....	33
1.3.2 Supramolecular nucleolipids systems are good candidates for the drug delivery.....	38

2. Ruthenium-based nanovectors: comparison between neutral and cationic

liposomes	41
2.1. INTRODUCTION.....	42
2.1.1. The active principle: AziRu.....	42
2.1.2 ToThy, HoThy, DoHu: amphiphilic nucleolipids for the delivery of AziRu.....	43
2.1.3 Nuclelipidis based-Ru co-aggregate with the neutral liposome POPC.....	45
2.1.4 Nuclelipidis based-Ru co-aggregate with the cationic liposome DOTAP.....	46
2.2 AIM.....	47
2.3 MATERIALS AND METHODS.....	48
2.3.1 Cell cultures.....	48
2.3.2 Cell viability.....	48
2.3.3 Fluorescence microscopy.....	49
2.3.4 Flow cytometric analysis of autophagosomes formation.....	51
2.3.5 FACS analysis of apoptosis.....	51
2.3.6 DNA fragmentation assay.....	52
2.3.7 Western blot analysis of caspases expression.....	53
2.3.8 Statistical analysis.....	53
2.4 RESULTS.....	54
2.4.1 Antiproliferative activity.....	54
2.4.2 Cellular uptake.....	56
2.4.3 Apoptosis and autophagy activation.....	60

2.5 CONCLUSIONS.....	68
3. DOTAP-TothyCholRu: cholesterol improves the cellular uptake.....	70
3.1. INTRODUCTION.....	71
3.1.1. The role of cholesterol in natural and biomimetic membranes.....	71
3.1.2. ToThyCholRu/DOTAP.....	72
3.2 AIM.....	73
3.3 MATERIALS AND METHODS.....	73
3.3.1 Cell cultures.....	73
3.3.2 <i>In vitro</i> bioscreening.....	73
3.3.3 Fluorescence microscopy and cellular uptake of liposomes.....	74
3.3.4 Light Microscopy.....	74
3.3.5 DNA fragmentation assay.....	74
3.3.6. Statistical Analysis.....	74
3.4 RESULTS.....	75
3.4.1 <i>In vitro</i> bioscreening for anticancer activity.....	75
3.4.2. Cellular uptake.....	78
3.4.3. Cellular morphological changes and DNA fragmentation.....	82
3.5 CONCLUSIONS.....	85
4. de-LOS-POPC-TothyRu: an alternative liposome inspired to the bacterial wall...86	86
4.1 INTRODUCTION.....	87
4.1.1 Long-time circulation strategy for the new generation of liposomes.....	87
4.1.2 The LOS inclusion into the liposome.....	87

4.2 AIM.....	90
4.3. MATERIALS AND METHODS.....	90
4.3.1. Cell cultures.....	90
4.3.2. <i>In vitro</i> bioscreens for cell survival.....	91
4.3.3. Cellular uptake by fluorescence microscopy.....	91
4.3.4. Macrophage activation and nitric oxide production.....	91
4.3.5. Western blot analysis of iNOS expression.....	92
4.3.6. Statistical Analysis.....	92
4.4. RESULTS.....	93
4.4.1. Anticancer activity.....	93
4.4.2. Effect on healthy cells.....	93
4.4.3. Macrophage response to de-LOS liposomes.....	97
4.5 CONCLUSIONS.....	100
5. RDCs and ODCs: the role of epigenetic changes in their mechanism of action.....	101
5.1. INTRODUCTION.....	102
5.1.1. Ruthenium derived compounds (RDCs): state of the art.....	102
5.1.2 Osmium derived compounds (ODCs).....	104
5.1.3. Epigenetic role in the mechanism of action of metal-based compounds.....	105
5.2. AIM.....	107
5.3 MATERIALS AND METHODS.....	108
5.3.1 Cell viability.....	108
5.3.2. Comet Assay.....	108

5.3.3. Peptides binding.....	109
5.3.4. Western Blot analysis.....	109
5.3.5. Protein immunoprecipitation.....	110
5.3.6. Statistical analysis.....	110
5.4 RESULTS.....	111
5.4.1. Impact of organometallic compounds on cell viability.....	111
5.4.2. DNA damage induced by organometallic compounds.....	113
5.4.3. Binding of organometallic compounds to histones.....	115
5.4.4. Modification of H2A and H2B expression patterns in cells treated with organometallic compounds.....	118
5.4.5. Modification of H3 expression pattern in cells treated with organometallic compounds.....	121
5.4.6. Caspase-3 activation.....	123
5.4.7. H3-acetylation.....	125
5.5. CONCLUSIONS.....	127
6. DISCUSSION.....	129
BIBLIOGRAPHY.....	134
ACKNOWLEDGEMENTS.....	156

ABSTRACT

Cancer is the second leading cause of death. Although it is already validated the use of techniques such as radiotherapy, immunotherapy and chemotherapy, in the last decade the medical community has focused on the research of less invasive drugs, through the identification of new anticancer agents, as well as by the design of an innovative system for the drug delivery, like the liposomes, that allow the protection of the active principle until the achievement of molecular target, reducing the toxic effects. Among the new anticancer agents currently in clinical trials, there are the ruthenium-based compounds, NAMI-A and KP1019. These have emerged as promising alternatives to platinum compounds (Cisplatin, Oxaliplatin, Carboplatin) that constitute still an important class of chemotherapeutics, whose limit is the high toxicity. Although ruthenium and platinum belong to the same chemical series, the ruthenium complexes showed anticancer and/or antimetastatic activity, associated with fewer side effects. The difference between the derivatives of ruthenium and platinum is probably due to their different pharmacodynamics that, if is well known for Cisplatin and its analogs, it is not yet completely clarified for the other metal complexes. Also, the chemical characteristics like the redox potential, the charges and the lipophilicity are very different among the various classes of metal-based compounds, reflecting their different biological effects.

In this context, my Ph.D. aim was the validation of new metal-based agents for the cancer therapy; in particular I analyzed two different classes of compounds:

- The ruthenium complex inspired to the drug NAMI-A, AziRu, prepared (designed and developed) by the Department of Chemical Sciences of the University Federico II, Naples (Prof. Luigi Paduano, Prof. Daniela Montesarchio). Its pharmacokinetic profile was improved by the inclusion in liposomes, which should provide, by a *passive targeting*, for the protection of AziRu and its delivery to cancer cells.
- The C-N heterocyclic compounds Ruthenium-derived (RDC11) or Osmium-derived (ODC2, ODC16, ODC20), prepared (designed and developed) by the Department of Chemistry of University of Strasbourg (Prof. Michael Pfeffer).

Therefore, my research had different focuses: first, the validation of a nanotechnological platform of metal-based compounds by evaluation of biocompatibility and cellular uptake

of different types of liposomes, as innovative carriers for metal complexes. The second point was the analysis of cell death pathways induced by these compounds. Finally, the research evaluated the possible targets involved in the mechanism of action. In fact, even if these compounds are really largely characterized by biological investigations, their mechanism of action, that, as mentioned above, is also closely dependent on redox status and chemical ligands, needs further insights. This study was carried out in particular on the compounds of RDCs and ODCs families, during the period of my Ph.D. at INSERM (French Institute of Health and Medical Research) of Strasbourg (supervisor Dr. Christian Gaidon); in particular, it concerned the evaluation of the epigenetic changes correlated with the activity of such compounds and the identification of their specific targets.

All the results of this work are thus divided, according to the different chemical characteristics of the compounds, into four sections:

- Ruthenium-based nanovectors: comparison between neutral and cationic liposomes
- DOTAP-TothyCholRu: cholesterol improves the cellular uptake
- de-LOS-POPC-TothyRu: an alternative liposome inspired to the bacterial wall
- RDCs and ODCs: the role of epigenetic changes in their mechanism of action

1. BACKGROUND



1.1 Classical and epigenetic mechanisms involved in chemotherapy

Since its multifactorial nature, cancer is nowadays one of the most difficult pathologies to eradicate, despite the well validated therapeutic protocols, and the continuous emerging of new approaches. There is a wide range of different agents used in chemotherapy that, targeting DNA or protein components are aimed to block the DNA replication and, by the involvement of several pathways, lead to cell death. In this complex scenario, an important role of epigenetic processes has recently emerged, both in the process of carcinogenesis and in the mechanism of the anticancer drugs.

1.1.1. Cancer: statistical data and the most used therapeutic approaches

The term “cancer” indicates a complex scenario of pathological changes characterized by deregulation of cell cycle and metabolism, resulting in uncontrolled cell proliferation [Teicher et al., 2012]. Since it is a multifactorial disease in which genetic, environmental, and lifestyle factors have all together an important impact on the carcinogenesis, cancer is at the moment one of the pathologies with larger incidence. The last statistical data about the incidence of cancer worldwide are reported by the International Agency for Research on Cancer (IARC), the specialized cancer agency of the World Health Organization, and are related to 2012 (Fig. 1). An estimated 14.1 million new cancer cases and 8.2 million cancer-related deaths happened in 2012, compared with 12.7 million and 7.6 million, respectively, in 2008. The most frequent cancers were those of the lung (1.8 million, 13.0% of the total), breast (1.7 million, 11.9%), and colorectum (1.4 million, 9.7%). The most common causes of cancer-related death were cancers of the lung (1.6 million, 19.4% of the total), liver (0.8 million, 9.1%), and stomach (0.7 million, 8.8%). Based on these estimations it can predict a substantial increase to 19.3 million new cancer cases per year by 2025, due to growth and aging of the population [Ferlay J. et al., 2015]. Thus the data about the incidence of the cancer join also with a high incidence of death, although the research is focused on the identification of new approaches for the cancer therapy, and many protocols, based on different method, such as surgery, radiotherapy and chemotherapy, are already validated. More recently, the immunotherapy, which comprises a wide range of different agents, as immuno-modulatory drugs, vaccines, antibodies [Kocoglu and Badros, 2016] is entered in these protocols. The surgical removal of the

tumor is the oldest and most effective strategy, but requires that the cancer is localized or has limited loco-regional diffusion. Also, the radiation therapy is more efficient if the tumor is not largely diffused. Often it is used in combination with chemotherapy and / or surgery. It is based on the induction of cell damage by radiation of protons, electrons or neutrons, which, however, is nonspecific and increases the risk of secondary tumor [Muralidharan et al., 2015]. Chemotherapy has spread from the second half of the twentieth century, when research has led to the creation of a wide range of drugs aimed to block the DNA replication, such as: DNA alkylating agents (capable to form a covalent bond with the purine or pyrimidine bases of DNA), anti-metabolites (like folic acid analogs, pyrimidine and purine analogs), the antimetabolic agents, topoisomerase inhibitors, anti-tumor antibiotics, hormones. Chemotherapy is also the only possible approach for the treatment of metastases, which often develop before the tumor is diagnosed. However, chemotherapeutic agents have often some limitations, such as poor selectivity, several side effects, and onset of resistance mechanisms.

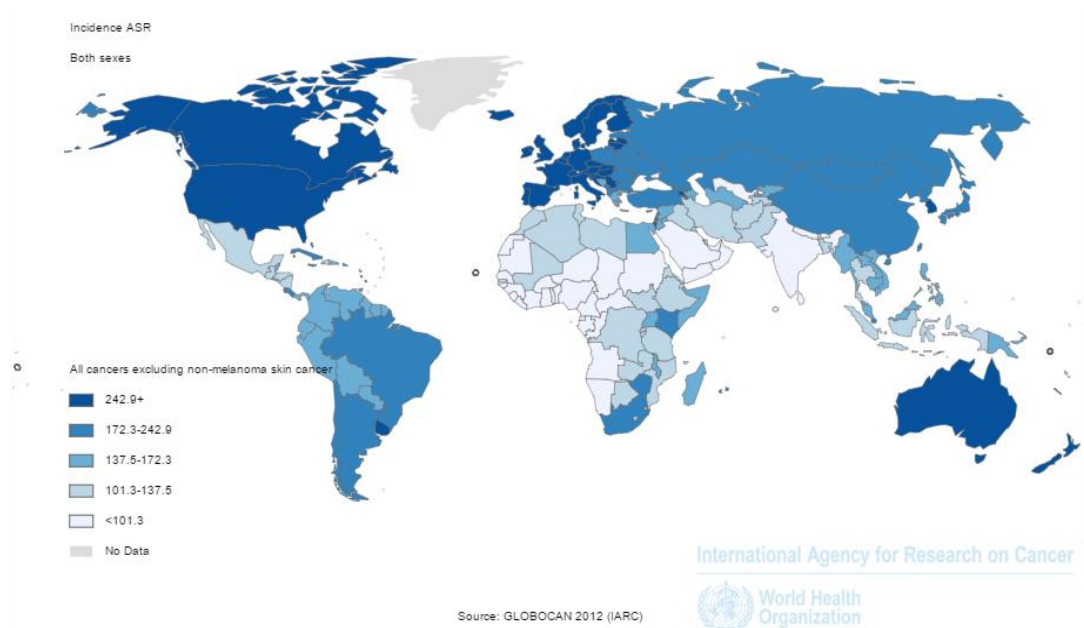
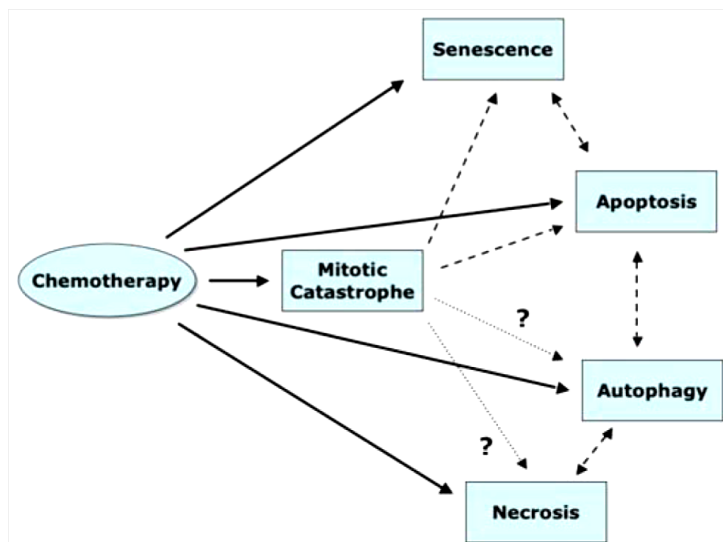


Fig. 1. Cancer incidence in the worldwide (2012); indicator: age-standardized rate per 100,000 (ASR)

1.1.2 Types of cell death induced by anticancer agents

Despite various cellular targets of chemotherapeutic agents, involving metabolic and genetic processes, the possible kinds of cell death to which the cancer cells undergo during the treatment are few, but however are very important to evaluate the cellular response to the drugs. The principal types of cell death are apoptosis, autophagy, necrosis, mitotic catastrophe and senescence (Fig. 2). Two of these, the apoptosis and autophagy, are considered programmed cell deaths, because of their strict genetic control [Danial and Korsmeyer, 2004; Lum et al., 2005]. Necrosis and mitotic catastrophe are generally considered passive responses to massive cellular insult. However, new evidence suggests that also these kinds of death undergo a genetic control [Castedo et al., 2004; Zong and Thompson, 2006]. Senescence is a process of aging, of which nevertheless the deregulation could represent a type of cell death in cancer cells [Robles and Adami, 1998; Schmitt et al., 2002; te Poele et al., 2002]. In the following paragraphs, an overview of the principal mechanism of cell death will be presented, particularly focused on their implications during the cancer therapy.



Ricci et al., Oncologist. 2006; 11(4): 342–357

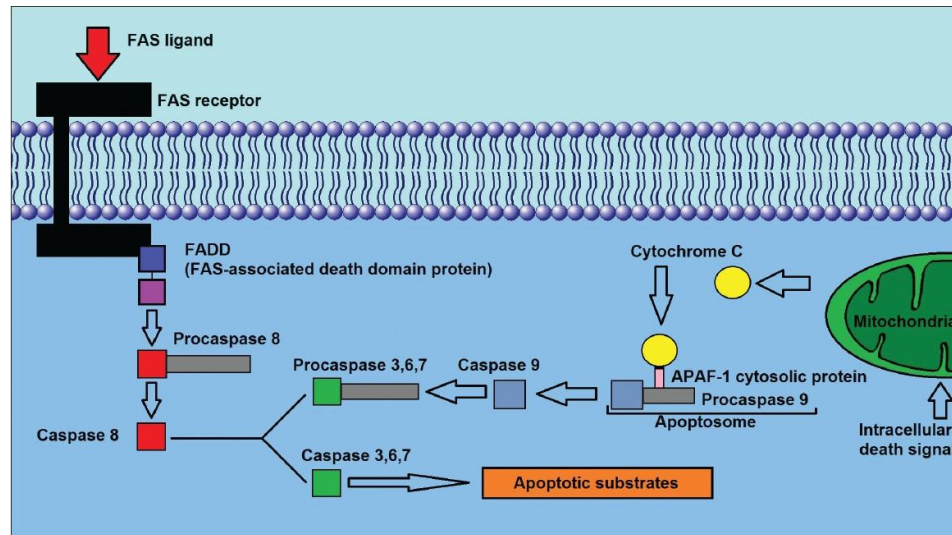
Fig. 2. Chemoterapy-induced cell death

1.1.2.a. Apoptosis

The typical morphological characteristics of apoptosis are cell membrane blebbing, cell shrinkage, chromatin condensation and nucleosomal fragmentation. In particular, cell shrinkage and pyknosis happen during the early process of apoptosis, while extensive plasma membrane blebbing occurs followed by karyorrhexis and separation of cell fragments into apoptotic bodies [Elmore, 2007]. Generally, there is no inflammatory process associated with the apoptosis, because the apoptotic cells don't release their cellular components into interstitial tissue and are rapidly phagocytosed, preventing secondary necrosis, as well as the phagocytic cells don't produce anti-inflammatory cytokines [Savill and Fadok, 2000; Kurosaka et al., 2003]. In fact, a typical biochemical aspect that occurs in the early state of apoptosis is the exposition of the anionic lipid phosphatidylserine (PS) on the external surface of cancer cells, as signal of “eat me”, important for the ordered and quick elimination of cell bodies by macrophages or other near normal cells [Hankins et al., 2015]. The apoptosis is an important process both in normal and cancer cells that has to be strictly controlled, for its potential damage in case of inappropriate activation in normal cells, as well as in case of deficient activation during the anticancer treatment, that represents an important mechanism of drug resistance [Fulda and Debatin, 2004]. Apoptosis in response to anticancer chemotherapy can be initiated as a result of the activation of receptors on plasmatic membrane (extrinsic pathway) or at the mitochondria (intrinsic pathway) [Fulda and Debatin, 2004] (Fig.3). The intrinsic pathway is usually activated in response to intracellular stress signals, such as DNA damage, high levels of the reactive oxygen species (ROS) [Ricci and Zong, 2006] and endoplasmic reticulum (ER) stress [Farooqi et al., 2015], all events that notoriously can take part in the mechanism of action of chemotherapeutic agents. ROS can also directly damage DNA by causing cleavage of DNA strands, DNA protein cross-linking, and oxidation of purines [Marnett., 2000]. The principal response of the DNA damage is the activation of p53 tumor suppressor protein, a transcriptional factor that has a key role in the control of cell cycle and apoptosis [Meek, 2015]. The extrinsic pathway is triggered by the binding of an extracellular ligand to a receptor on the plasma membrane. In particular, is activated by the binding of the members of the tumor necrosis factor (TNF) family with their receptors (TNFR) [Ricci and Zong, 2006]. Both pathways activate the proteolytic enzymes named caspases, containing a nucleophilic cysteine residue involved in the cleavage of aspartic

acid-containing motifs [Thornberry and Lazebnik, 1998]. There are two groups of caspases, the initiator caspases (caspase-2, caspase-8, caspase-9, and caspase-10), and the effector caspases (caspase-3, caspase-6, and caspase-7). They are expressed as inactive precursors (procaspases) that form active oligomers after cleavage events, by a cascade mechanism that leads to the cleavage of different substrates in the cytoplasm or nucleus and thus to the degradation of organelles and disassembly of cellular architecture. For example, proteolysis of several cytoskeletal proteins such as actin or fodrin leads to loss of cell shape, whereas degradation of lamin results in nuclear shrinking; the DNA fragmentation is mediated by the cleavage of ICAD (Inhibitor of Caspase-Activated DNase), with subsequent activation of the inhibitor of the endonuclease CAD (Caspase-Activated DNase) that cleaves DNA into the characteristic oligomeric fragments [Degterev et al., 2003]. Stimulation of the TNFR superfamily such as the cluster of differentiation 95 CD95 (also known as apoptosis antigen-1 APO-1 and Fas) or TNF-related apoptosis-inducing ligand (TRAIL) receptors results in activation of the initiator caspase-8 which can propagate the apoptotic signals by direct cleavage of downstream effector caspases, such as caspase-3 [Walczak and Krammer, 2000]. On the other hand, the stimuli that initiate the intrinsic pathway lead to the activation of two pro-apoptotic B-cell lymphoma 2 (BCL2) proteins, such as Bax (Bcl-2-associated X protein) and Bak (Bcl-2 homologous antagonist killer), that migrate to the mitochondria, where homodimerize to expose cryptic dimer-dimer binding sites and introduce pores into the surface of the mitochondria [Koff et al., 2015]. This event results in changes in the inner mitochondrial membrane, with increased mitochondrial outer membrane permeabilization (MOMP) and loss of transmembrane potential, causing the release of pro-apoptotic proteins into the cytosol [Elmore, 2007], including cytochrome c and Smac/DIABLO [Saelens et al., 2004]. Once in the cytosol, these apoptogenic proteins trigger the execution of cell death by promoting caspase-9 activation [Kim et al., 2015] and subsequently caspase cascade, or by acting as caspase-independent death effectors [Saelens et al., 2004]. Links between the extrinsic and intrinsic pathways exist at different steps. For example, after the binding of the death receptors, activation of caspase-8 may result in the cleavage of Bid, another Bcl-2 family protein, which in turn translocates to mitochondria, releasing cytochrome c and thus initiating a mitochondrial amplification loop [Adams and Cory, 2002]. In addition, cleavage of caspase-6 downstream of mitochondria may feed back to the receptor pathway by cleaving caspase-8 [Cowling and Downward, 2002]. However, the concept that caspases have a

central role in the mechanism by which chemotherapy kills cancer cells may not universally be valid, and both caspase independent-apoptosis and other modes of cell death have to be considered as cellular response to anticancer therapy [Brown and Attardi, 2005].



Palade et al., Asian J Neurosurg. 2013; 8(2):106-11

Fig. 3. Extrinsic and intrinsic apoptotic cascades

1.1.2.b. Autophagy

The involvement of autophagy in chemotherapy cancer treatment is very complex. On one hand, autophagy has a protective role so that autophagy inhibitors have potential use as drugs to overcome anticancer therapy resistance. On the other hand, this process participates in cell death and its induction may help to eliminate cancer cells [Notte, 2011]. Autophagy is a highly regulated and evolutionarily conserved process that is activated in response to metabolic stresses, such as nutrient starvation and hypoxia, differentiation, endoplasmic reticulum (ER) stress, oxidative stress, expression of aggregate-prone proteins, glucose deprivation, with the results of intracellular degradation of proteins and organelles [Shintani and Klionsky, 2004]. During autophagy, a portion of the cytoplasm, that can include various proteins and organelles, are encapsulated in vesicles called autophagosomes, which fuse with the lysosomes, allowing the degradation of the cytoplasmic components by lysosomal hydrolases. In physiological conditions this is an adaptive response to the stress that contributes to the normal turnover of cytoplasmic

components and to maintain the homeostasis [Ricci and Zong, 2006]. However it can lead to cell death, if the stress is persistent or excessive. Excessive autophagy is also shown to promote cell death following treatment with specific chemotherapeutic agents, either because it directly leads to cell death or by an autophagy-mediated induction of apoptosis [Sui et al, 2013]. In the first case, autophagy could degrade large parts of the cytosol and organelles, leading to irreversible cellular atrophy with a consequent cellular collapse; in fact, the large volume occupied by autophagic vacuoles can be approximately equal to, or greater than the volume of normal cytosol [Baehrecke, 2005]. In the second case, autophagy develops as primary response to stress stimuli and then triggers apoptotic or necrotic cell death [Maiuri et al, 2007]. In addition, since the autophagic catabolic process is believed to restore ATP levels [Katayama et al., 2007] it could help the apoptosis that in turn requires ATP, i.e. for the activation of caspase-9 [Maiuri et al, 2007]. Even if the molecular mechanisms by which autophagy mediates its effects on both normal and cancer cells are not yet fully clarified, various signaling pathways have been individuated in the upregulation or downregulation of autophagy [Glick et al., 2010; Cecconi and Levine, 2008]. For example, the phosphatidylinositol 3-kinase/mammalian target of rapamycin (PI3K/mTOR) and AMP-activated protein kinase (AMPK) signaling pathways have emerged as important regulatory processes of autophagy [Din et al., 2012; Yu et al., 2010]. Several of the known tumor-suppressor genes, like p53, and tumor-associated genes (p21, Akt) also respectively stimulate or inhibit autophagy [Glick, et al., 2010]. Interacting with these pathways, several cross-talks are possible between autophagic and apoptotic pathways [Maiuri et al, 2007]. Many anticancer drugs stimulate autophagy by inhibiting the PI3K/Akt/mTOR pathway or altering genetic/epigenetic phenotype of cancer cells [Ciuffreda et al., 2010; Botrugno et al., 2012; Shubassi, 2012], suggesting a synergic role of autophagy and apoptosis in the induction of cell death [Notte A., 2011]. In fact, the role of autophagy in cell death has been described on different cancer cell lines for several drugs, such as etoposide [Cosse et al., 2010; Lee et al., 2007] doxorubicin [Lambert et al., 2008], carboplatin [Sun et al., 2009] gemcitabine [Mukubou et al., 2010] paclitaxel [Zou et al., 2011; Eum et al., 2011]. Also, the histone deacetylase (HDAC) inhibitors, which constitute a new class of potential anticancer agents [Gołabek et al., 2016] are recently involved in the control of DNA damage response (DDR) and autophagy [Sui et al, 2013]. These different observations show that autophagy takes part in cell death induction in

apoptosis competent cells while it becomes the major death inducing pathway in apoptosis deficient cells [Notte, 2011].

1.1.2.c. Necrosis and other types of cell death

Even if autophagy and apoptosis are considered the principal mechanism of cancer cell death in response to chemotherapy, the involvement of other processes cannot be excluded. In fact, crosstalk between apoptosis, autophagy and necrosis have been found [Nikoletopoulou et al., 2013]. Also, some evidence indicates that necrosis and apoptosis represent morphologic expressions of a shared biochemical network described as the “apoptosis-necrosis continuum” [Zeiss, 2003]. The term necrosis collects different kinds of cell death due to a massive insult, that leads to common morphological changes, including cell swelling and plasma membrane rupture, disorganization of structure of organelles, without chromatin condensation [Green and Llambi, 2015]. The loss of cell membrane integrity results in the release of the cytoplasmic material outside the cells, drawing the attention of chemotactic factors and thus with the recruitment of inflammatory cells [Elmore, 2007]. While apoptosis is well defined at the molecular level, necrosis has not a specific molecular signature and has been referred as uncontrolled and pathological form of cell death. Necrosis can be induced by inhibition of cellular energy production, imbalance of intracellular calcium flux, generation of ROS, and activation of non-apoptotic proteases. These events often potentiate each other and synergize to cause necrosis [Ricci and Zong, 2006]. In fact, excessive production of ROS is cause of oxidative stress, DNA damage, protein oxidation and lipid peroxidation. Lipid oxidation can lead to the loss of integrity of both the plasma membrane and intracellular membranes of organelles, that may lead to the influx of Ca^{2+} , event that in turn induces cell death by the activation of Ca^{2+} -dependent proteases and mitochondrial Ca^{2+} overload [Waring, 2005]. Recent discoveries revealed that also regulated forms of necrosis exist, as in the case of necroptosis [Dunai et al., 2011], a programmed cell death fashion, in which specific signaling pathways have been individuated and the loss of caspases involvement represents the main difference respect to the classical apoptosis [Christofferson and Yuan, 2010]. Several anticancer compounds have been reported to initiate necroptosis in cancer cells [Fulda, 2014]. In the contest of cell death induced by chemotherapy, also mitotic catastrophe and senescence are noteworthy. Mitotic catastrophe is referred to the activation of cell death

directly from mitosis. Morphologically, mitotic catastrophe is associated with the formation of giant cells with either many micronuclei [Ricci and Zong, 2006]. Instead, the senescent cells appear large in size, flattened and often vacuolated. The senescence is normally considered a process of aging, due to the physiologic erosion of the telomeric sequence after a high number of cellular divisions, with subsequent DNA damage. DNA damage response could be triggered by other cellular stresses, i.e. some chemotherapeutic agents induce a premature senescence [Schmitt et al., 2002; te Poele et al., 2002].

1.1.3 The role of epigenetics in tumorigenesis and in cancer therapy

The term epigenetic was for the first time coined in the 1942 by Waddington [Waddington, 2012] as a link between the genotype and the phenotype development. From the mid-seventies, epigenetics became a real branch of science whose molecular bases are well understood. The epigenetic field is constantly evolving, according to the growing understanding of DNA methylation, chromatin modifications, and noncoding RNA processes, as well as of their effects on gene expression [Choudhuri, 2011]. At the molecular level, cancerous phenotype is the result of an altered network of transcriptional and post-translational events, regulatory interactions of histone and non-histone proteins and chromatin remodeling, in response to dynamic and persistent upstream signals [Kumar, 2016]. Thus, in the light of the recent evidences about the role of epigenetic factors in carcinogenesis and tumor growth, many researches are pointing to the development of new anticancer agents whose targets are chromatin-modifying enzymes and proteins involving in the epigenetic processes, as well as to revise the role of epigenetics in the mechanism of action of drugs already in use [Davey GE and CA, 2008].

1.1.3.1. Epigenetic mechanisms

Modifications of DNA, non-coding RNA and histones are considered the principal mechanisms involved in the epigenetic regulation. The most common DNA modification is the methylation, especially in a specific region rich in cytosine-guanine bases (CpG islands) [Bird, 2002]. This is considered gene repressive, preventing the transcription process [De Smet et al., 1999] and it is implicated both in physiological cellular functions and in several pathological conditions, among which different kinds of cancer [Shinjo and Kondo, 2015]. The modifications of non-coding RNA (ncRNAs) can include the ribosomal RNA (rRNAs), micro RNA (miRNAs) and long non-coding sequences (lncRNAs). miRNAs play a central role in repression of mRNA stability and translation, de-adenylation and also regulation by the recruitment of specific proteins to the nucleus [Mikhed et al., 2015]. lncRNAs is a family of molecules with different functions, involved for example in the cell differentiation and stability of chromosome [Bartel, 2004]. Epigenetic modifications observed on histones are methylation, acetylation, ubiquitination, sumoylation, ADP-ribosylation [Kouzarides, 2007] phosphorylation and citrullination

[Tessarz and Kouzarides, 2014]; each of these has a specific impact on the chromatin condensation and on activating or silencing transcription signals [Mikkelsen et al., 2007]. Moreover, recently many studies have correlated the redox signaling and the oxidative stress with the epigenetic regulation of genes by changes in function of histones and DNA modifying enzymes, and thus altering the phenotype of the cells [Mikhed et al. 2015].

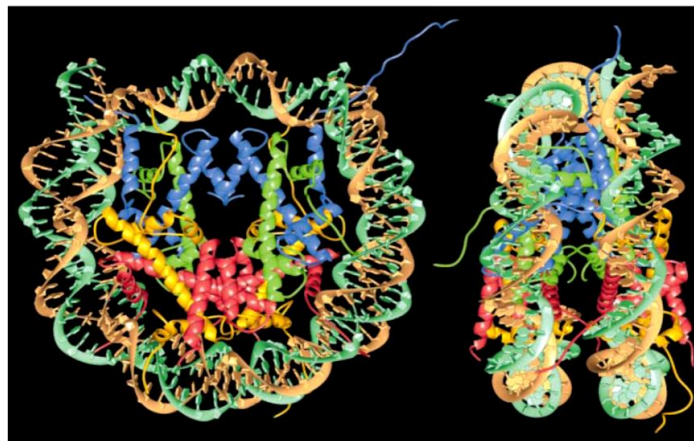
1.1.3.2. Histone modifications

Among the class of molecules epigenetically regulated, there are the chromatin-forming proteins namely histones. If before only a "static" action of histones in the DNA packaging was known, increasingly discoveries have led to new insights into their role, as a "dynamic" system capable of influencing biological cellular processes, like the transcription. In performing such function, histone post-translational modifications are essential to change the chromatin condensation state and thus the DNA accessibility [Falahi et al., 2014]. Since the inhibition of transcription is one of the principal mechanisms of action to obtain an antiproliferative effect, histones and the histone-modifying enzymes, represent nowadays one of the most protein machinery studied as possible target for the cancer therapy.

1.1.3.2.a. The chromatin-forming proteins: the histones

The histones are basic proteins that interact with the DNA by non-covalent interactions, allowing its packaging [Felsenfeld, 1978]. In particular, they form an octamer, composed by two H2A-H2B dimers and one H3-H4 tetramer, around which 146 bp of supercoiled DNA is wrapped in 1,67 turns, to form the nucleosome core particle (NCP) [Luger et al., 1997; Andrews and Luger, 2011] (Fig.4). The linker histone H1 (or H5, in some case [Chen et al., 2014]) completes the DNA compaction, binding to the species-dependent fragments of DNA of about 50 bp, close to the entry and exit points of the NCP; together, H1 linker and NCP, form the nucleosome, the repetitive unit of chromatin [White et al., 2016]. Histone H1 is the poorly conserved during the evolution [Kasinsky et al., 2001] and has a different structure consisting of a short amino-terminal tail, a central winged-helix and a carboxy-terminal intrinsically disordered domain [Roque et al., 2009]. Conversely,

the core histones is highly conserved in the evolution [Postberg et al., 2010; Slesarev et al., 1998], and share a common structural motif, termed "histone fold", consisting of three α -helices ($\alpha 1$, $\alpha 2$, $\alpha 3$) separated by not structured loops (L1-L2) [Arents et al., 1991]. The interactions that stabilize the dimers are mainly of hydrophobic nature, and elapse over the entire region of the histone fold. Moreover, two H3-H4 further associate to form a tetramer, which has an important role at the beginning of the nucleosome assembly, whereas the H2A-H2B doesn't form tetramer. Also, thermodynamic study on H2A-H2B showed that the histones are stable only when they are in dimers [Chen et al., 2014]. The histone fold domain is joined to two tail regions which protrude from the nucleosome [Arents et al., 1995]. These tail regions undergo post-translational covalent modifications which are of crucial importance for nucleosome stability [Cascone et al., 2012].



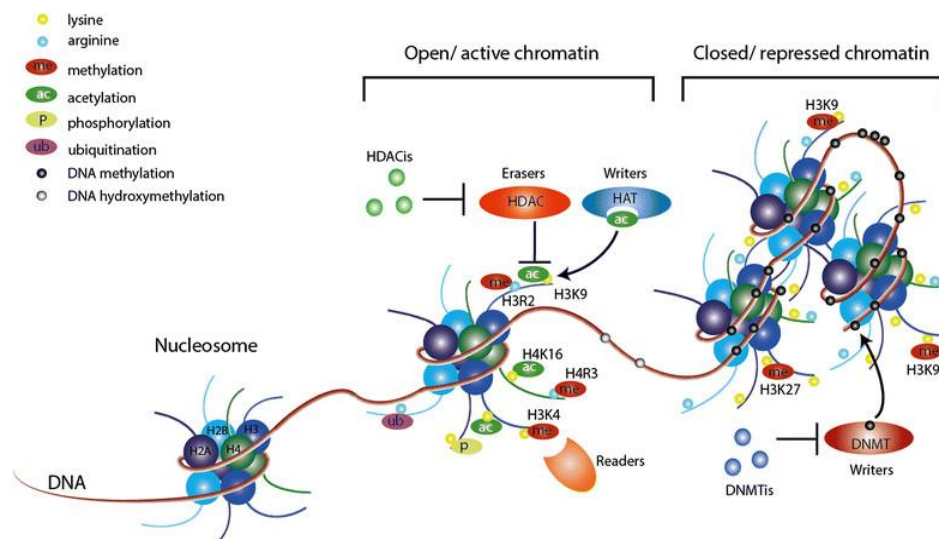
Luger et al., Nature. 1997; 389(6648):251-60

Fig. 4. X-ray crystal structure of nucleosome core particle of chromatin: phosphodiester backbones of 146-bp DNA (brown and turquoise) and histone octamer (blue: H3; green: H4; yellow: H2A; red: H2B).

1.1.3.2.b. Histone post-translational modifications

Chromatin has two forms, named euchromatin and heterochromatin. Heterochromatin is the most packed form, usually close to the transcriptionally inactive region, while euchromatin is the more relaxed form, typically located in transcriptional initiation regions, such as promoter and enhancer elements of the gene [Chen et al., 2014]. These two different forms can be switched by means of epigenetic modifications on histones, which lead to gene repression or activation [Jiang and Pugh, 2009] (Fig. 5). Modifications may impact the chromatin state by changing the contact between different histones in adjacent nucleosomes or the interaction of histones with DNA, and, depending on the type of such modifications, enzymatic proteins, that can further modify chromatin, are facilitated to bind chromatin, or are occluded from it. Epigenetic modifications observed on histones are methylation, acetylation, ubiquitination, sumoylation, ADP-ribosylation, deimination, proline isomerization [Kouzarides, 2007] phosphorylation and citrullination [Tessarz and Kouzarides, 2014], that often act in combination, being subjected to cross-regulations [Latham and Dent, 2007]. They are prevalently introduced on lysine or arginine residues of the N-terminal tails, because of their accessibility [Mikhed et al., 2015]. Histones can undergo different kinds of modifications in several times or the same modification at different residues. All possible combination patterns of histone modifications give reason to coin the expression "histone code" [Jenuwein and Allis, 2001], as an extended pool of information to add to the genetic code, in order to better understand the transcription process. One of the most known modifications is the acetylation, that has a strong potential to unfold the chromatin, since it neutralizes the positive charge of basic aminoacids [Saikusa et al., 2015], reducing the interaction between the positive-charged histones and the negative-charged DNA. In fact, acetylation is correlated with the formation of the euchromatin, and thus making the DNA more accessible to the gene transcription [Dekker, 2009]. Conversely, histone deacetylation causes chromatin condensation and inhibition of transcription [Marks et al., 2001; Gallinari, 2007]. In this context, the enzymes of the family histone deacetylases (HDACs) and histone acetyltransferases (HATs) play a central role. In fact, many HDACs are over-expressed in malignant cells and they have been closely correlated with acquisition of malignant phenotypes in cancerogenesis. In particular, depending on the classes of HDACs, they can inhibit apoptosis and induce angiogenesis in cancer cells, induce cell proliferation, inhibit differentiation and cause also

cell motility, leading to metastasis [Yoon and Eom, 2016]. Moreover, a specific group of HDAC, named sirtuins, has a crucial role in the redox signaling, since they are, unlike the other classes, NAD^+ - rather than Zn-dependent enzymes [Webster et al., 2012]. For all these observations, HDAC inhibitors are nowadays object of studies for making targeted anticancer agents, many of which are in clinical trials [Xu et al., 2007], and some are already approved [Gryder et al., 2012].



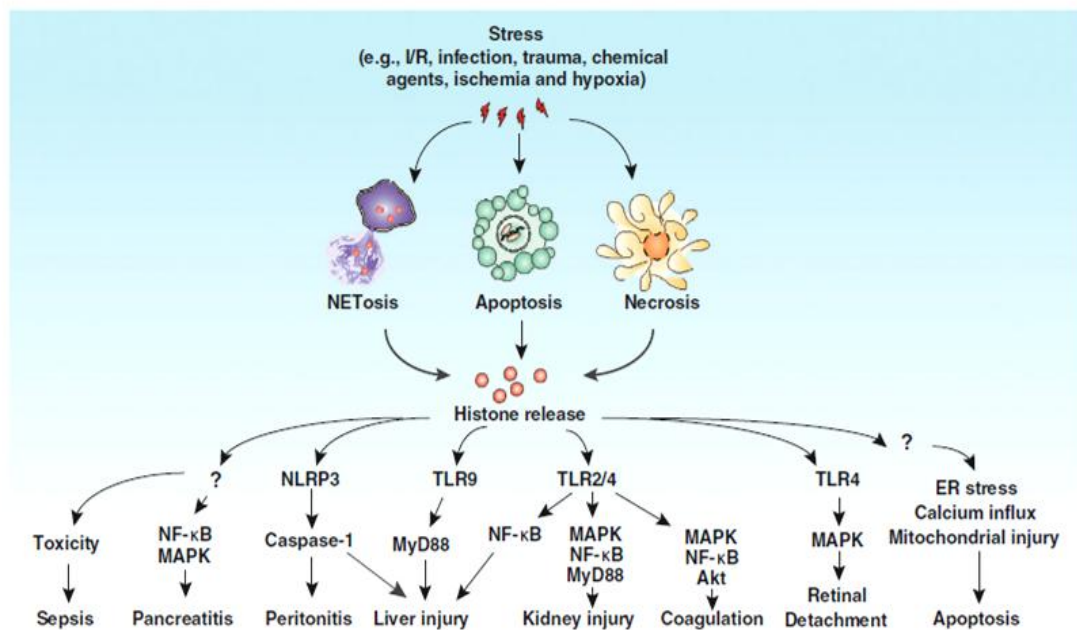
Falahi et al., Breast Cancer Research 2014; 16:412

Fig. 5. The two forms of chromatin (active euchromatin and repressed heterochromatin) and their interaction with epigenetic players, classified in enzymes that induce modifications (writers) or removing them (erasers) or factors that bind these modifications (readers) and recruit further re-enforcing complexes. The role of DNA methyltransferases (DNMTs) and their inhibitors (DNMTis), as well as histone acetyltransferases (HATs), histone deacetylases (HDACs) and their inhibitors (HDACis) is highlighted.

1.1.3.2.c. Histones localization

Beside the well known nuclear functions, recently new roles of the histones in extra-nuclear compartments have emerged. In fact, histones can be released by stressed cells in intracellular space, where they can act as endogenous danger signals in different pathological conditions [Chen et al., 2014] (Fig. 6). Histones release by neutrophils in the context of neutrophil-mediated cell death was the first reported example in literature

[Brinkmann et al., 2004]. Also apoptotic or necrotic cells can release extracellular histones [Jahr et al., 2001]; generally, nuclear components are not released during apoptosis, but increasing evidence indicates that cells undergoing apoptosis possess this ability. In particular, in response to apoptotic signals, core and linker histones can separate from DNA, with subsequent histone cytoplasmic translocation and then their release into the extracellular space, phenomena that are not necessarily connected to the apoptotic DNA fragmentation [Wu et al., 2002]. Moreover, the chromatin damage could be an early cause of histones release preceding the apoptosis [Gabler et al., 2003], and lead to an accumulation of cytoplasmic histones inducing the intrinsic pathways of apoptosis by destabilization of the mitochondrial membranes [Cascone et al., 2012]. Also, extracellular histones can in turn act as apoptotic signals for the neighboring cells, by means of different mechanisms, including induction of calcium influx, enhancement of the endoplasmic reticulum unfolded protein response, and increase of mitochondrial toxicity [Chen et al., 2014]. Nevertheless, the specific extracellular signaling capable of inducing apoptosis by histones release has yet to be clarified.



Chen et al., *Cell Death Dis.* 2014; 5:e1370

Fig. 6. Scheme of all the possible signaling pathways induced by extracellular histones in different pathological conditions

1.2. Anticancer metal-based drugs

The anticancer metal-based drugs constitute nowadays an important and heterogeneous class of compounds, of which the common thread is the presence of an inorganic active principle. The classical platinum-based agents are an important class of chemotherapeutics, and several studies are still focused on giving a complete view of their mechanism of action, as well as on making modification of their structure, in order to ensure the pharmacokinetics and pharmacodynamics. On the other hand, a series of new transition metal-based compounds, such as ruthenium and osmium-based, are object of numerous studies for their more attractive cytotoxic profile, including a high antiproliferative activity associated with less side effects.

1.2.1. Cisplatin and its analogs

Even if they don't have an alkyl group, the platinum compounds are classified in the class of alkylating agents, for their capacity to intercalate the DNA. The potential anticancer activity of platinum was serendipitously discovered, by Rosenberg and co-workers [Rosenberg et al., 1969]. During an experiment aimed to understand the effects of electric field on the growth of *Escherichia coli* bacteria, they observed that the passage of current between two platinum electrodes prevented the proliferation of *E. coli*. The antiproliferative effect was attributed to the formation of platinum-containing compounds in the presence of inorganic ammonium ions and chlorine. Rosenberg hypothesized that if these complexes inhibited bacterial cell division, they could also stop tumor cell growth. The more active among these substances in experimental models of tumor was the diamminodichloro cis-platinum (II) Cis- $[\text{PtCl}_2(\text{NH}_3)_2]$ (Fig.7). Indeed, in 1978, six years after clinical trials conducted by the NCI and Bristol-Myers-Squibb, the U.S. Food and Drug Administration (FDA) approved cisplatin for treating patients with metastatic testicular or ovarian cancer in combination with other drugs and also alone for treating bladder cancer [Monneret, 2011]. The first mode of action proposed for these compounds, that represent still the principal mechanism recognized for their action, is the DNA binding. When cisplatin enters the cell is hydrolyzed, forming a positively charged molecule that reacts with nucleophilic groups present on the DNA. In particular it binds the N-7 of the guanine [Bernges and Holler, 1991] forming intra and inter-strand crosslinks

[van den Berg and Roberts, 1975], that is the cause of DNA distortion, inhibition of DNA replication and transcription. On the other hand, the DNA damage causes the activation of transduction pathways, involving the Ataxia telangiectasia mutated and Rad3-related (ATR) protein kinase, p53 and p73 proteins, and the mitogen-activated protein kinases (MAPK), leading to the apoptosis [Siddik, 2003]. Bristol-Myers Squibb also licensed carboplatin, a second-generation platinum drug with fewer side effects [Sharma et al., 2011]. Carboplatin is formed by replacing the chloride with 1,1-cyclobutanedicarboxylate ligand, which increases the stability of the leaving groups [Muggia et al., 2015]. Numerous platinum derivatives have been further developed and the third derivative to be approved in 1994 was oxaliplatin. Respect to cisplatin, the two amine groups are replaced by cyclohexyldiamine to improve antitumor activity [Ramachandran et al., 2009], while the chlorine ligands are replaced by the oxalate-bidentate derived from oxalic acid in order to improve water solubility. Differently from cisplatin and carboplatin, oxaliplatin in plasma rapidly undergoes non-enzymatic transformation into reactive compounds because of displacement of the oxalate group. Most of these formed compounds appear to be pharmacologically inactive, but dichloro-platinum complexes enter the cell, where carry out their mechanism of action [Alcindor and Beauger, 2011]. Oxaliplatin was the first platinum-based drug to be active against metastatic colorectal cancer in combination with fluorouracil and folinic acid [Monneret, 2011].



Fig. 7. Cisplatin and its derivatives

Nevertheless, platinum compounds are mutagenic, teratogenic and show a high toxic profile (i.e. nausea and vomiting, diarrhea, myelosuppression, neuropathy, ototoxicity, hepatotoxicity and nephrotoxicity) [Apps et al., 2015]. Moreover, among the long-term effects of cisplatin treatment, has been mentioned an increased risk of development acute

myeloid leukemia (AML) [Philpott et al., 1996]. Also, the cancer cells have demonstrated resistance phenomena to cisplatin and its analogs. The principal platinum resistance mechanisms are: reduced cellular uptake and up-regulated drug efflux from cells, increased degradation and detoxification of the drugs by glutathione (GSH) activity, reduced formation of drug-DNA adducts and an increased tolerance or repair of the damaged DNA [Galluzzi et al. 2012].

1.2.2. New transition metals-based complexes

Metal complexes, in particular transition-metal-based complexes, have potential advantages respect to the organic-based drugs, including the possibility to occupy a high number of spatial positions due to their octahedral coordination geometry, the possibility of functionalization with different ligands that could change the thermodynamic and kinetic characteristics, and an important role of the oxidation/reduction state that allows them to be present in the biological fluids [Clarke et al., 1999]. The current platinum drugs, that are nowadays still one of the most used classes of chemotherapeutics, have some limitations: they are efficient only for a limited range of cancers and often cause severe side effects; in addition, some tumors showed acquired or intrinsic resistance [Köberle et al., 2010]. Although other platinum compounds are in clinical trials, they have not been able to overcome the drawbacks associated with cisplatin [van Rijt and Sadler, 2009]. Thus the research focused on the individuation of other transition metals, which have a similar chemical profile to platinum, but with fewer side effects. The ruthenium compounds are considered suitable candidates for anticancer drug design, because they have a similar spectrum of ligand substitution kinetics as platinum (II). After the pioneer works of Clarke [Clarke et al., 1980], Sava and co-workers were the first designers of one of the most promising complexes of low molecular weight based on ruthenium (III), called NAMI-A [Sava et al., 1998]. Subsequently, the same group has also tested the compound KP1019, made by Keppler and co-workers [Kersten et al., 1998; Bergamo et al., 2009]. These compounds have entered in the clinical trials in the 1999 and 2003 respectively [Galanski et al., 2003]. NAMI-A, now in the phase II of clinical trials [Bergamo and Sava, 2015], has been proposed for the combination therapy with gemcitabine as a second line therapy for the metastatic non-small cells lung cancer (NSCLC) [Leijen et al., 2015]. Despite the

structural similarities to NAMI-A, the compound KP1019 (Fig. 8) showed different pharmacological profiles.

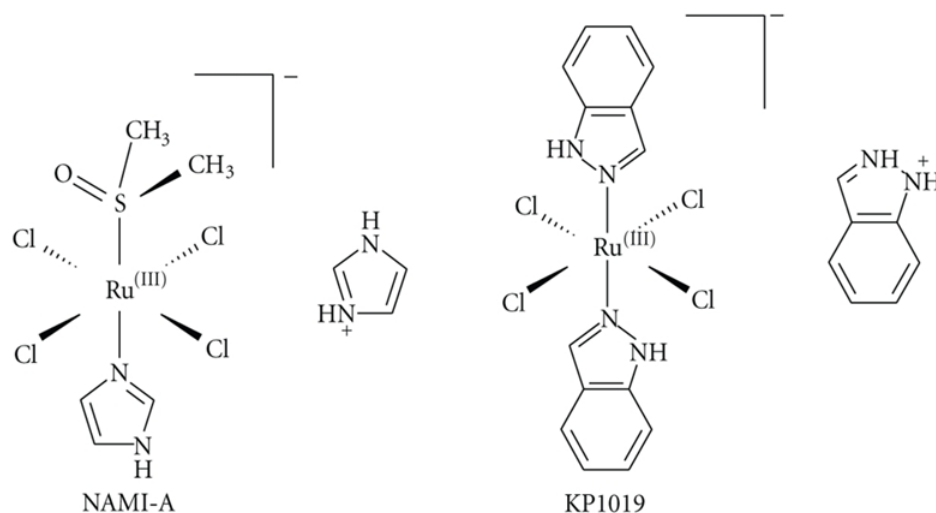


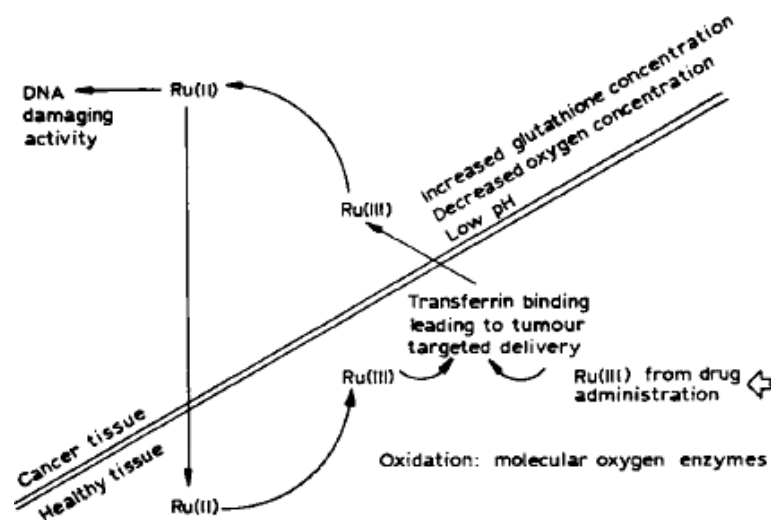
Fig. 8. Molecular structure of NAMI-A and KP1019

While KP1019 has a high cytotoxic effect on primary tumors [Kapitza et al, 2005], NAMI-A seems prevalently to be able to reduce metastases from solid tumors [Sava and Bergamo, 2000; Sava et al., 2003]. Also, NAMI-A is less toxic respect to cisplatin. An hypothesis for this difference lies in the diverse capacity to bind serum proteins. In fact, even if they bind approximately the same serum proteins, the NAMI-A binding is more reversible [Khalaila et al., 2006]. Differences between NAMI-A and cisplatin have been showed also for the mechanism of action. In fact, even if a binding to DNA by NAMI-A was found, this is weaker than that of platinum complexes [Pluim et al., 2004.], excluding thus the role of DNA as the primary target for its activity on metastases. Its antimetastatic activity seems due to an intricate network of actions, including the transforming growth factor beta 1 (TGF- β 1)-dependent fibrosis induction, the reduction of the release of the matrix metalloproteinases (MMPs) in the primary tumour and the extracellular matrix (ECM) remodeling, probably because it interacts more with targets outside the cells (like α 5 β 1 integrin) than inside the cells [Brescacin et al., 2015; Pelillo et al., 2015]. In the case of KP1019, the induction of apoptosis via the mitochondrial pathway, also generating ROS species, was found [Hartinger et al., 2006]. A confirmation of the involvement of ROS is

given by the suppression of the cytotoxicity of KP1019 by the pre-treatment of cells with the antioxidant N-acetylcysteine [Kapitza et al., 2005]. Although the mitochondrial pathway is considered responsible at least for its *in vitro* effect, a role of DNA binding is not excluded, as shown by the studies with DNA repair inhibitors [Hartinger et al., 2006].

Despite the differences observed in their activity, some aspects of this first generation of ruthenium compounds are believed in common:

- i)* The hypothesis of activation by reduction: ruthenium can be in the oxidation states of Ru (II), Ru (III) and Ru (IV) under physiological conditions. It is believed that Ruthenium (III) and Ru (IV) are less active and act as a pro-drug converted in the active form Ru (II) prevalently in the redox microenvironment of cancer cells [Clarke et al., 1999], as well as by the higher levels of glutathione present in these cells [Allardyce and Dyson, 2001] (Fig.9).
- ii)* Transport by transferrin: serum proteins as albumin, transferrin and globulins are believed to play a crucial role in the transport, delivery, and storage of anticancer metallodrugs. In particular, ruthenium complexes demonstrated high affinity for the protein transferrin [Groessl et al., 2010; Brabec and Nováková, 2006] the main transport protein of iron, whose request increases in tumor and metastatic cells [Corcé et al., 2016]. In fact, due to their intensive proliferation, tumor cells require large quantities of nutrients, particularly iron, that has a central role in numerous biological processes, and it is an essential part of many proteins and enzymes, such as the ribonucleotide reductase, responsible for the conversion of ribonucleotides into deoxyribonucleotides for the DNA synthesis [Lammers and Follmann, 1983].
- iii)* DNA binding: although the pharmacological targets for ruthenium compounds have not been unequivocally identified, the cytotoxicity of many of these complexes correlates with their ability to bind DNA. Several ruthenium compounds bind DNA and modify it differently than cisplatin or its analogues [Brabec and Nováková, 2006]. However NAMI-A and KP1019 showed a low profile of interactions, that is not enough to explain the wide range of their effects [Pluim et al., 2004; Bergamo et al., 2012].

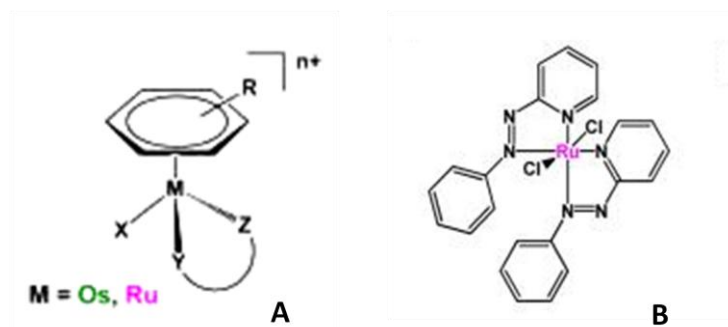


Allardyce and Dyson, *Platinum Metals Rev.* 2001; 45(2): 62-69

Fig.9. Different ruthenium activities in cancer and healthy cells due to the transferrin transport and the "activation by reduction" in cancer cell environment.

Nevertheless, these assumptions are currently only hypotheses, that, as well discussed recently by Bergamo and Sava [Bergamo and Sava, 2011], need further investigations to be validated. After the promising results on NAMI-A and its analogs, many works have focused on the identification of other kinds of ruthenium-based compounds, playing to modify the structure-relationship. In particular, these compounds can be divided into two general classes: the ruthenium arene complexes and the bifunctional complexes with polypyridyl and arylazopyridine ligands (Fig. 10). The half-sandwich Ru (II) arene complexes in which ruthenium is bound to an aryl group, two ligands YZ such as two amino groups, and a good leaving group X, such as chlorine, offer great scope for the design, with the potential to vary each of the building blocks, allowing modifications of thermodynamic and kinetic parameters [van Rijt et al., 2009]. Also, the arene has a crucial role in the mechanism of action because it works as a DNA intercalator [Liu et al, 2006]. The RAPTA family ($\text{Ru}[\eta^6\text{-arene}][\text{PTA}]\text{X}_2$), PTA = 1,3,5-triaza-7-phosphaadamantane) is an evolution of this class, and includes promising compounds [Murray et al., 2016; Nowak-Sliwinska et al., 2011]. Among these, the complex RAPTA-C showed stronger and more selective affinity to protein targets than platinum compounds [Casini et al., 2009]. Recently, RAPTA compounds were also conjugated with polymeric micelles to improve

the drug delivery [Lu et al., 2015; Blunden et al., 2013]. In addition, the class of the bifunctional complexes with polypyridyl and arylazopyridine ligands show promising cytotoxic activity that is structurally-dependent [Besker et al., 2007; van Rijt and Sadler, 2009]. It was proved that the cytotoxicity of some of these compounds depends on the activation of mitochondria-mediated apoptosis pathway [Chen et al., 2010].



van Rijt et al., *Drug Discov Today*. 2009; 19(10):1640-8

Fig. 10. [A] Sandwich model for metal-based drugs; [B] Azopyridine ruthenium-based

Although osmium has a reputation for its toxicity (OsO_4), the anticancer potential of this metal has recently been explored. In fact, some complexes inspired to the structure of the ruthenium compounds, as azole complexes [Kuhn et al., 2014], arene complexes [Peacock and Sadler 2008; van Rijt et al., 2009], and RAPTA analogs [Hanif et al., 2014] were designed and developed. Osmium complexes have different kinetics and thermodynamics of the reaction respect to the ruthenium compounds and showed more stability in aqueous solution [Hanif et al., 2014]. Also, they don't give cross-resistance with cisplatin towards cancer cells, suggesting a possibility to overcome the problem of intrinsic or acquired resistance in chemotherapy [Peacock and Sadler, 2008]. As for the ruthenium compounds, the DNA binding is not considered the principal mechanism of action; conversely, there are many evidences about their redox activity and apoptosis activation mediated by ROS production [Maillet et al., 2014; [Hanif et al., 2014; Hearn et al., 2012]. At this point it's clear that the comprehension of the mechanism of action of the transition metal-based compounds, and more in general of their pharmacodynamics, must take account of the complex structure-activity relationships, the different kinetics of ligand substitution reactions, as well as the different metal redox potential. Therefore, each compound can have a specific pool of interactions with various proteins/enzymes, playing a crucial role in inducing the observed variegate biological effects [Casini, 2012].

1.3. Nanovectors as innovative pharmaceutical forms for drug delivery

Classical cancer chemotherapy showed several drawbacks, such as adverse pharmacokinetic profiles, poor aqueous solubility, low therapeutic index, rapid clearance, instability, various collateral effects, and emergence of multidrug resistance (MDR) phenotypes [Chidambaram et al., 2011]. For this reason the research is focusing not only on the individuation of new active principles, but also on the discovery of new systems for drug delivery. In this contest, the application of the nanotechnologies on the medicine field seems to be very successful. In the following paragraphs, the principal supramolecular assemblies used in nanochemotherapy, as well as some of the most suitable materials for their realization, are described.

1.3.1. Liposomes and micelles

As reported by the U.S. National Institute of Health (NIH), nanotechnology will completely change the scenario of cancer diagnosis, treatment, and prevention [<http://nano.cancer.gov>] because of the easiness to modulate the physical parameters of the nanoparticles, like size, shape and surface physiochemical propriety, making them suitable for many applications. For these reasons nanovectors result very versatile, allowing for example the drug delivery by mechanism of passive or active targeting, the improvement of the drug passage through biological barriers, the protection of the active principle in the blood and thus also the reduction of the drug cytotoxicity [Jhaveri and Torchilin, 2016]. The main forms of nanovectors are dendrimers, vesicles, micelles, core-shell particles, microbubbles, and carbon nanotubes [Janib et al., 2010]. In particular, there is a growing interest for lipid-based nanoformulations, for the advantages related to the high degree of biocompatibility [Matougui et al., 2016]. Among the lipids used for this purpose, there is the zwitterionic POPC (1-palmitoyl-2-oleoyl-sn-glycero-3-phosphocholine) [Stano et al., 2004], a very stable lipid synthetically provided (Fig. 11). The fatty acid composition, i.e. saturated chain in the sn-1 position and unsaturated chain in the sn-2 position, mimics mammalian phospholipid composition. Since the major constituent in eukaryotic cell membranes is 1-palmitoyl-2-oleoyl PC, POPC is an excellent synthetic substitute.

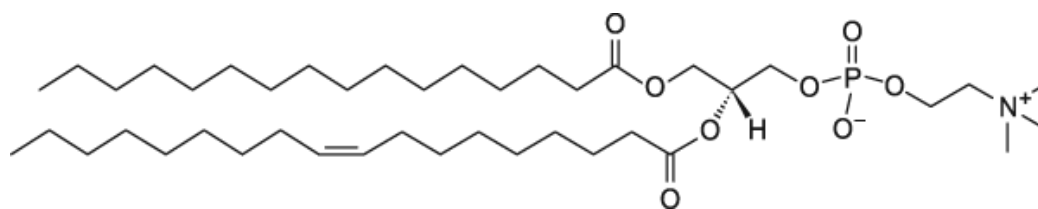


Fig. 11. Molecular structure of POPC

The ionic lipid DOTAP (N- [1- (2,3-dioleoilossi) propyl] -N, N, N-trimethylammonium methyl-sulfate) contains two chains of oleic acid linked with a propyl-amine [Marsh, 2012] (Fig. 12). This synthetic lipid has been recently studied to make cationic aggregates, that should better interact with the cell membranes, negatively charged because of the presence of anionic sugar residues of glycoproteins and glycolipids. [Stebelska et al., 2006].

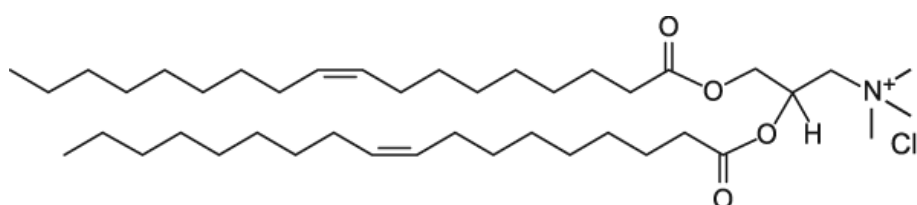
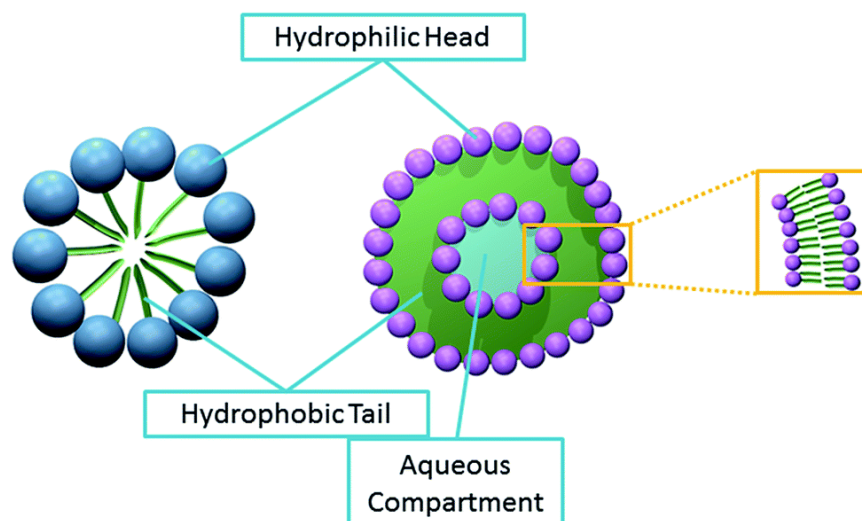


Fig. 12. Molecular structure of DOTAP

The main formulations that lipids are able to form spontaneously are micelles and liposomes.

- **Micelles:** the amphiphilic molecules consist of a single acyl chain forming a conical shape. At concentration values equal to the Critical Micelle Concentration (CMC) [Toh HS and Compton RG, 2015; Corrin et al., 1947] they can aggregate in micelles with the polar heads towards the outside and the hydrophobic tails towards the interior, without forming a double layer (Fig. 13). Consequently, the micelles have a lipophilic core.
- **Liposomal vesicles:** phospholipids or surfactant molecules containing two acyl chains, which have cylindrical geometry, ordering in planar sheet, forming a double layer (bilayer) which shapes a spherical structure, thermodynamically favored, with a central aqueous compartment [Monteiro et al., 2014] (Fig. 13).



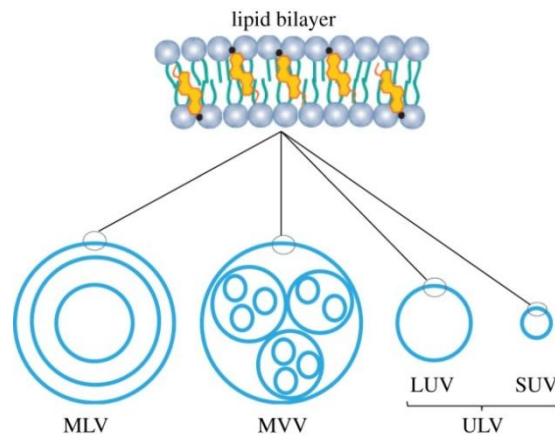
Toh and Compton, Chem Sci. 2015; 6:5053-5058

Fig. 13. Simplified model of aggregation in micelle (on left) and the liposome (on right)

Liposomes were initially designed by the biophysicist Bangham as simplified models of cell membranes [Bangham et al., 1965] and only later it was evaluated the possibility of using them as vectors in diagnostics, immuno-modulation, genetic engineering and chemotherapy [Gregoriadis et al., 1974]. Therefore, the liposomes can incorporate both hydrophilic (in the aqueous core), and lipophilic drugs (between the alkyl chains). Moreover, they can be divided according to their size and number of lamellae [Monteiro et al., 2014] (Fig. 14):

- MLVs, multilamellar vesicles (0.1–15 μm). These vesicles are formed by more bilayers, which can incorporate high amounts of lipophilic drugs, but they are easily recognized by the reticulo-endothelial system. The presence of more lamellae can also be exploited for a prolonged drug release.
- MVVs, multi-vesicular vesicles (1.6–10.5 μm). Complex systems of vesicles that contain inside more vesicles.
- LUVs, large unilamellar vesicles (100 nm to 1 μm), constituted by a single lamella. They are useful for incorporating macromolecules and hydrophilic drugs, but are easily recognized by the reticulo-endothelial system.

- SUV, small unilamellar vesicles (25–50 nm), constituted by a single bilayer. They have very long half-life because of their small size and thus are not recognized by the reticulo-endothelial system.

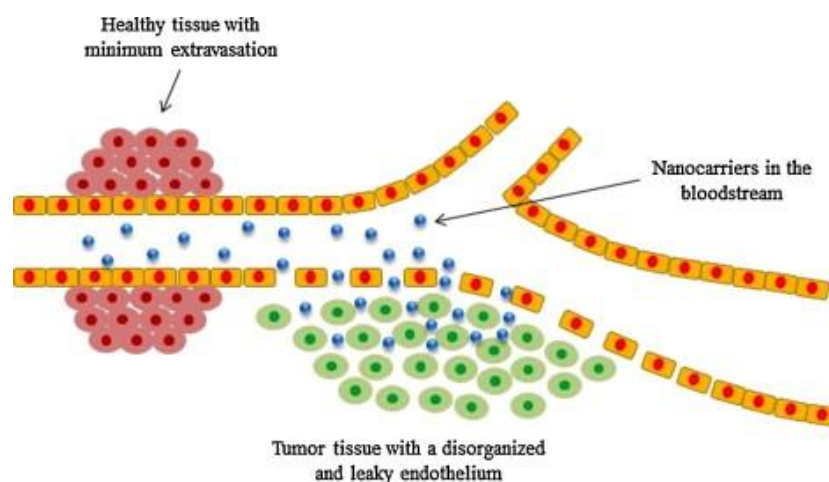


Monteiro et al., *J R Soc Interface*. 2014; 11(101): 20140459

Fig. 14. Representation of various types of liposomal vesicles

An important parameter for the liposomes is the lipid phase transition temperature (T_m) [Kraft et al., 2014], that is the temperature at which an ordered and rigid lipid membrane (gel phase) changes in a more disordered, fluid membrane (sol phase). T_m depends on: the kind of lipids (liposomes with saturated fatty acids are better compacted and therefore have a high T_m), the temperature of liposomes preparation, the presence of cholesterol. The cholesterol, similarly to its function in biological membranes, intercalates between the acyl chains, giving a double effect: condensing at a higher T_m (reduces the freedom of movement of the chains) or fluidifying at lower T_m (prevents intermolecular bonds between lipids). Therefore, by modulating parameters such as the size, composition, charge density, membrane fluidity, steric hindrance and permeability, it is possible to influence the interaction of the liposome with the tissues and the drug release. It was assumed that the liposomes can interact and/or penetrate cells through several mechanisms. In particular, some experiments conducted both *in vitro* and *in vivo* showed that the main interactions of liposomes with cells are simple adsorption (by specific interactions with cell-surface components, electrostatic forces, or by non-specific weak hydrophobic forces) or following endocytosis [Akbarzadeh et al., 2013]. Liposomal aggregates of nanometer size (between

10-1000 nm), represent an efficient therapeutic formulation combining the advantages of their shape with the small size and the ability to carry the drug. Thanks to the small size and the shape, the delivery of the drug is then favored to the cancer cells which, having different characteristics from the other tissue, allow the accumulation of the nanoparticles and make possible the "passive targeting" (Fig.15).



Estanqueiro et al., Colloids Surf B Biointerfaces, 2015; 126:631-48

Fig. 15. Illustration of the nanoparticles passive accumulation in the cancer tissue, due to the EPR effect

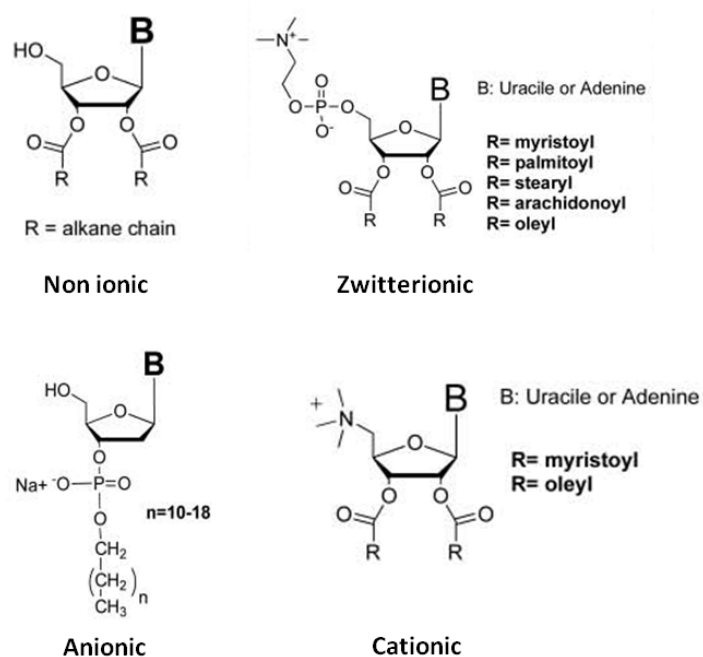
This process is called EPR (Enhanced Permeability and Retention) effect [Gill et al., 2015; Maruyama, 2011]. The tumor undergoes an angiogenic process by which develops a network altered blood, with widely fenestrated capillaries and reduced lymphatic drainage; this can lead to accumulation of molecules transported from the bloodstream into the interstitial space of the tumor cells [Seymour et al., 1994]. In addition, it is possible an "active targeting" by inserting of further components on the surface of nanovector, making it selective for a specific type of tumor. For example, the inclusion of hyaluronic acid causes a selective interaction with ovarian and colon cancer cells, overexpressing the receptor for hyaluronic acid. [Luo et al., 2002]. Also, liposomal formulations can be easily designed with *ad hoc* modifications in order to modulate their pharmacokinetics; for example, by adding a chain of polyethylene glycol (PEG), prolongs the half life of the drug because, due to its high hydrophilicity, interposes in the external versant of liposomal surface, obstructing the binding with other macromolecules and preventing recognition by the reticulo-endothelial system and thus the macrophages-dependent phagocytosis

[Gabizon et al., 2004]. These "pegylated" liposomes, able to evade the immune system by prolonging the half-life of the drug, belong to the second generation of liposomes, called "stealth liposomes" [Immordino et al., 2006; Cattel et al., 2003]. For example, nanoparticles of polyethylene glycol phosphatidyl ethanol amine (PEG-PE) containing doxorubicin have shown an increase of the antiproliferative effect of the drug, in addition to a lower cardiotoxicity [Tang et al., 2007]. Liposomal doxorubicin was the first nanovector approved by the Food and Drug Administration (FDA) for the Kaposi's sarcoma [Presant et al., 1993; Masood et al., 1993]. Currently there are more than 50 anticancer nanovectors in clinical trials [Wang and Thanou, 2010] among which the SPIO (superparamagnetic iron oxide) to diagnose pre-operative stage of pancreatic cancer [Flexman et al., 2008] and also lyso-thermosensitive liposomal doxorubicin as a novel activated therapy using radiofrequency ablation [Poon and Borys, 2009]. Interesting, several systems, i.e. liposome, micelles and dendrimers are studied also as carrier of platinum compounds [Oberoi et al., 2013; Parker et al., 2016].

1.3.2 Supramolecular nucleolipids systems are good candidates for drug delivery

There are numerous natural and synthetic molecules with amphiphilic properties that can be used for the preparation of supramolecular aggregates. Among these, the amphiphilic nucleolipids obtained considerable interest in recent years [Gissot et al., 2008]. Consisting of a purine or pyrimidine nucleoside, these compounds are used as a polyfunctional "scaffold", of which the ribose can be functionalized with aliphatic chains of variable length. The discovery of these systems started from the study of natural hybrid nucleolipids and recognition of their biological relevance. In fact, there are many nucleolipidic complexes that in both eukaryotic and prokaryotic cells have important physiological roles. Just think of the coenzyme CDP-DAG (diacyl glycerol citidin-phosphate) that plays a central role in the metabolism of the membrane lipids phosphoinositides and the mitochondrial membrane components cardiolipins [Heacock and Agranoff, 1997]. Based on its structure, several synthetic analogues were then obtained, initially with the only purpose of blocking the RNA transcription and of using them as anti-cancer drugs or anti-viral, as false substrates of the RNA polymerase [Gissot et al., 2008]. The inclusion of lipid chains improves the cellular uptake (indeed the phospho-ester bond is hydrolyzed directly in the cytoplasm, reducing the toxicity) and allows also the aggregation between the polar

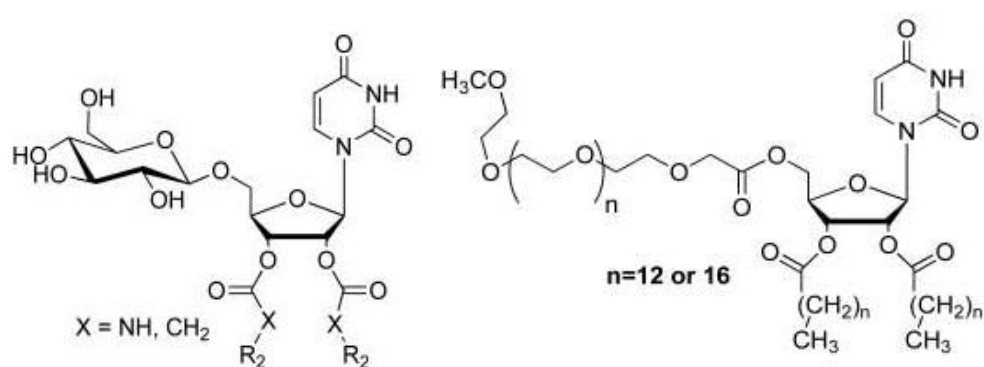
heads and the hydrophobic chains. The result is that the formulations, compared to classical amphiphilic compounds, have a polar head (adenine, thymine, guanine, uracil or similar) capable of forming hydrogen bonds and π -stacking that improve recognition with other nucleobases and thus the self-assembly. For these reasons, in the mid 80' these complexes were investigated not only for their pharmacological activity, but also for their ability to auto-aggregate under suitable conditions, forming vesicles, micelles and monolayers, which can act as carriers for the drug delivery [Rubas et al., 1986; Schwendener, et al., 1985]. These complexes interact easily with biological membranes and thus promote the cellular uptake of the active ingredients, reducing the premature release in the bloodstream and also protecting it from enzymatic degradation. Since 2002 were tested new complexes in which, in place of the functionalization of the position 5' of ribose with fatty acids, the positions 3' and 2' were derivatized, to analyze any changes in the physico-chemical characteristics of the complex, as well as its ability to self-assembly. Therefore, by modulating the three functionalizable positions, prototypes with different ionic characteristics (amphiphilic, anionic, zwitterionic, nonionic) were obtained [Gissot et al., 2008] (Fig. 16).



Gissot et al., *Org. Biomol. Chem.*, 2008; 6(8):1324-33

Fig. 16. Nucleolipidic prototypes with different ionic characters

Other promising compounds are the neutral glycosylated derivatives in which the interactions for the self-assembly occurs not only between the nitrogenous bases but also between the phosphate-sugar groups [Arigon et al., 2005], or the neutral nucleoside functionalized with the poly-ethylene glycol [Barthelemy et al., 2005] (Fig. 17).



Gissot et al., Org. Biomol. Chem., 2008, 6(8): 1324–1333

Fig. 17. Nucleolipids in which the position 5' is functionalized with glucose or PEG

The use of oligonucleotides was tested on the first time for the antisense antiviral therapy [Wilson and Keefe, 2006]. Also these complexes, known by the initials ONA (oligonucleotide-based amphiphiles), showed ability in auto-aggregation in micelles or vesicles [Alemdaroglu and Herrmann, 2007]. Often the oligonucleotides are functionalized with cholesterol; in fact it is recognized by receptors of low-density lipoprotein (LDL) facilitating the endocytosis process [Krieg et al., 1993].

**2. Ruthenium-based nanovectors:
comparison between neutral and
cationic liposomes**



2.1. INTRODUCTION

2.1.1. The active principle: AziRu

AziRu is the low molecular weight ruthenium-based complex (Fig.18) synthesized by Prof. Paduano and Prof. Daniela Montesarchio (Federico II University, Naples); this is a NAMI-A analog in which, instead of the imidazole, there is the pyridine. This substitution gives more lipophilicity to the complex that should more easily interact with the cell membrane; in fact, under the same conditions, the IC_{50} relative to AziRu are lower than those calculated for NAMI-A [Mangiapia et al., 2012].

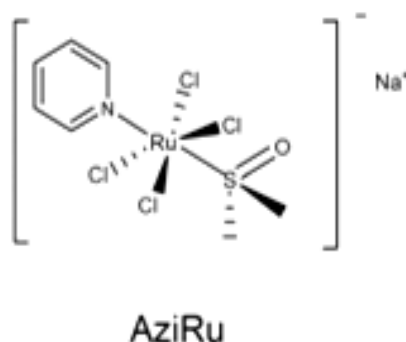


Fig.18. The low molecular weight complex AziRu

Also, both AziRu and NAMI-A are able to selectively interact with GG-containing DNA model systems, but AziRu is sensibly more reactive than NAMI-A [Musumeci et al., 2015]. Thus, this only change in the structure is responsible for the increase in the reactivity of the metal, able to form stable adducts with guanine-containing oligonucleotides. Interestingly, AziRu and NAMI-A showed different profiles of reaction with model proteins, such as the egg white lysozyme (HEWL). These two Ru-compounds, which are structurally very similar, making different adducts with HEWL, with distinct metalation sites [Vergara et al., 2013; Messori and Merlino, 2014]. Although the metal ligands could be eventually lost in the final products of the reaction, these findings remark the importance of them in the interaction of Ru-based drugs with proteins and in the kind of the adducts that are formed, thus changing also the pharmacological activity. Moreover,

by crystallographic studies, an inhibition of the RNAase A by AziRu was found [Vergara et al., 2013], suggesting that other enzymes could be inhibited "*in vivo*" and that this activity may have a central role in the AziRu mechanism of action. However, as the NAMI-A, AziRu are not stable over time in physiological solutions at neutral pH [Mangiapia et al., 2012]. Also, the IC₅₀ of AziRu is still too high to be considered an antiproliferative agent. Considering these aspects, the inclusion in nanocarriers could improve its stability. It may represent a good strategy both to evaluate a new platform of nanotechnological agents, and to individuate the pharmacodynamics of the ruthenium complex, whose the most part could be directly vehiculated inside the cells, by-passing all the physio-chemical implications and the pharmacokinetic processes to which these compounds are subjected in the blood [Levina et al., 2009].

2.1.2 ToThy, HoThy, DoHu: amphiphilic nucleolipids for the delivery of AziRu

Self-assembled amphiphilic aggregates represent nowadays a new strategy for the delivery of the anticancer agents. The advantages of these nanostructures are: the capacity to delivery in a safety way the active principle in the blood, to be "stealth" to the human immune system, increasing thus the life-time of the drug, to be selective toward cancer cells by passive or active targeting and the possibility of easily changing the shape and size both by directly modulating their molecular structure or external physicochemical parameters, like pH and ionic strength [Mangiapia et al., 2004; Vaccaro et al., 2006]. In this context, our research group has designed and tested different nanoaggregates, belonging to a new bio-technological platform in which the active principle is AziRu [Mangiapia et al, 2012; Simeone et al., 2011]. In particular, three different types of amphiphilic nucleolipidics are used for the self-assembly, each one functionalized with AziRu (Fig.19): **Tothy**: 3- [4-pyridylmethyl] -30-O-oleoyl-50-O (monomethoxy) triethylene glycol-acetyl-thymidine; **HoThy**: 3- [4-pyridylmethyl] - 30- O- oleyl 50-O (benzyloxy) exaetilen glycol-acetyl-thymidine; **DoHu**: 3- [4-pyridylmethyl] 20, 30 of O-oleil- 50-O- (benzyloxy) esaetilen glycol-acetyl-uridine

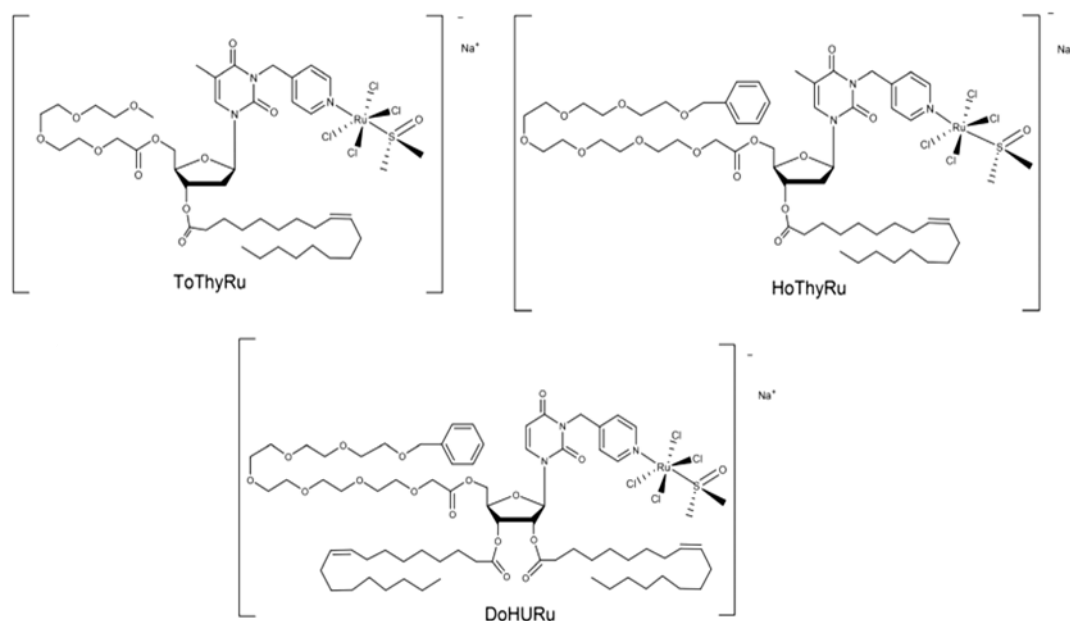


Fig.19. Amphiphilic nucleolipids ruthenium-based

We can thus describe their structure activity relationships (SARS):

- The pyrimidine deoxyribo- or ribo-nucleoside (Thymidine, as in the case of ToThyRu and HoThyRu; Uridine, for DoHURu) constitutes the central scaffold on which to place different functions.
- The active principle, AziRu, is bound to the N3 of the methyl-pyridine arm.
- One (or two groups in the case of DoHu) lipophilic chain attached at the hydroxy 3' (and 2') of the ribose. It is used to induce the self-assembly in aqueous solutions. The choice of the oleic acid as "building block" is due to its commercially available and also for its structural similarity with the components of cell membranes.
- An oligo ethylene-oxide chain at the hydroxy 5' of the ribose not only serves to optimize the hydrophilic-lipophilic balance, but also to prevent the extracellular degradation; in fact, like the widely used polyethylenglycol (PEG), this hydrophilic chain could have the capacity to mask the system in the blood, make it a "stealth liposome"

Both hydrophilic and lipophilic components are linked to ribose through ester linkages, stable in neutral and extracellular media but easily degradable by cellular esterases, thus promoting the release of the drug. Previous results [Simeone et al., 2011] showed that

ToThy, HoThy, DoHu self-assembled in pure water or under pseudo-physiological conditions, as well as *in vitro* experiments confirmed their biocompatibility, essential condition to use these aggregates as inert carriers of the drug. In particular, they were analyzed by dynamic light scattering (DLS) to estimate aggregate dimension and small angle neutron scattering (SANS) to analyze the aggregate morphology and to determine their geometrical characteristics. They showed a strong ability to organize into vesicles, whose hydrodynamic radius is between 50 and 400 nm. In pure water they can also be organized in cylindrical micelles; it should be noted that the vesicles are preferable because they have a larger and more stable architecture when their size is maintained in a range from 50 to 100 nm. The *in vitro* bioscreening conducted on a panel of cell lines, including murine fibroblasts (3T3-L1), human neuroblastoma cells (SH-SY5Y), rat glioma cells (C6), human cervical cells (HeLa), and human colorectal adenocarcinoma cells (Caco-2), demonstrated that the nucleolipids can be used as biocompatible vectors, showing in all the treatments IC₅₀ higher than the range of μM [Simeone et al., 2011].

2.1.3 Nuclelipidis based-Ru co-aggregate with the neutral liposome POPC

It is important to highlight that the complexes DoHuRu, ToThyRu and HoThyRu, as well as ruthenium derivatives of low molecular weight, are not very stable, showing phenomena of degradation, within a few hours in saline buffer or a few days in pure water, that, as illustrated in the Figure 20, are visible to the naked eye because the solution changes color from yellow to dark green. Moreover, after 5 h in saline and 78 h in pure water, they form small dark precipitates. These complexes are susceptible to hydration and hydrolysis due to the presence of chlorine ions and the residual dimethyl sulfoxide (DMSO). In particular, the EPR method showed that the single hydrophobic tail, as in the complexes ToThyRu and HoThyRu, destabilizes more the phospholipid bilayer respect to the presence of two hydrophobic chains (DoHuRu) [Mangiapia et al., 2012]. In order to increase their stability, the nucleolipids ruthenium-based aggregates were mixed with the lipid POPC, well known for its ability to form stable liposome [Stano et al., 2004]. This co-aggregation allows modulating the quantity of metal to be included and ensure the protection from extracellular degradation. Previous experiments have excluded the cytotoxicity of POPC alone and of the co-aggregates without ruthenium (ToThy/POPC, DoHu/POPC, HoThy/POPC), confirming the usability of POPC in the preparation of pharmaceutical

formulations. Moreover, the co-aggregates, including even the metal, have resulted stable for months [Mangiapia et al., 2012].



Mangiapia et al., Biomaterials. 2012; 33(14):3770-82.

Fig.20. DoHuRu just prepared in pure water (left) and after 120 h (at the center); DoHuRu complexed with POPC the physiological solution, 10 months after (right).

The POPC self-assembled prevalently in the liposomal vesicles, more stable than the micelles. The data obtained through the methods SANS and DLS are similar to those obtained with the POPC only, since the amount of this compound is very high compared to that of ruthenium (molar ratio 85:15). On the other hand, this means that the nucleolipids do not destabilize the structure of the POPC liposomes. In addition bioscreening *in vitro*, showed that the POPC liposomes ruthenium-based had similar effects to that of AziRu, although they enclose only 15% of ruthenium in moles. This means that these formulations have the same cytotoxicity of AziRu, but at a ruthenium concentration 6 times smaller. Also, by fluorescence experiments, they showed an efficient kinetics of cellular uptake, presumably with a localization in the cytoplasm [Mangiapia et al., 2012].

2.1.4 Nuclelipidis based-Ru co-aggregate with the cationic liposome DOTAP

In order to enhance the antineoplastic activity, we tested the coaggregation of the nucleolipids with the cationic lipid DOTAP in the mixture 50:50 (Fig.21). The cationic liposomes are emerged as alternative to the neutral vesicles, and could bring several advantages, first of all the major interaction with the cell membranes [Wiethoff et al.,

2001]. In our case, the cationic charge of DOTAP can also enhance the aggregation with the negative charges of the nucleolipids forming the amphiphilic ruthenium complex, as described for the formation of DOTAP complex with the DNA [Hayes et al., 2006] and thus make a more stable liposome. These aggregated are well chemically characterized by different techniques, like dynamic light scattering (DLS), small angle neutron scattering (SANS), neutron reflectivity and zeta potential, and electron paramagnetic resonance (EPR), and have presented high stability in aqueous environment even at high Ru-complex content.

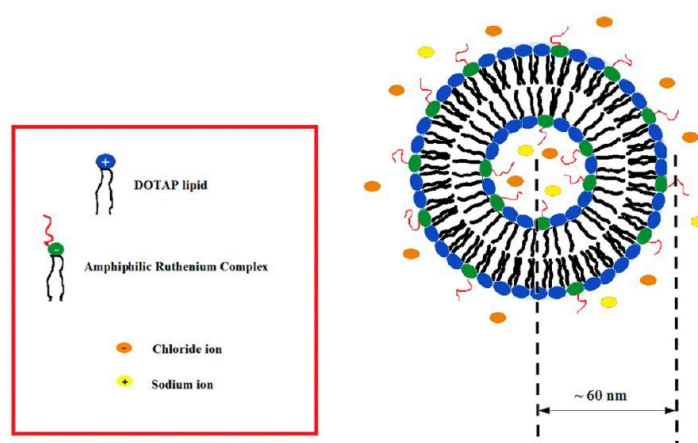


Fig. 21. Simplified representation of DOTAP liposome ruthenium-based

2.2 AIM

Previous results obtained by our research group have shown that the co-aggregation between amphiphilic nucleolipids and the neutral lipid POPC forms stable liposomes that are good candidate for the delivery of the ruthenium complex. In fact, the effect of this "nanovectorization" is an increment of the bioactivity of AziRu. Also, in order to optimize this system we made a cationic liposome, based on DOTAP lipid. The aim of this work is thus the *in vitro* biological characterization of the ruthenium-based DOTAP liposome. Considering the promising results about the stability of such liposomes, the first objective was to explore the bioactivity of the ruthenium-based DOTAP liposomes, as well as their cellular uptake, and to compare the data with those previously obtained by the co-aggregation with the neutral liposomes. For this purpose, cell viability assays and fluorescence microscopy experiments have been conducted. Indeed, it assessed that these compounds have antiproliferative effects and this is imputable exclusively to the vehiculated active principle. The question is what happens after the cellular uptake of the

liposomes, when the metal is released into the cells. In fact, as well as the other ruthenium compounds, it is not fully understood their mechanism of action. On the other hand, it is probable that, unlike NAMI-A [Bergamo and Sava 2015], the ruthenium-delivered complex interacts more with intracellular than extracellular targets. In addition, the liposomal formulations and the nucleolipidic scaffold could be responsible of different pharmacodynamics. Thus, in view of a more in-depth analysis of the specific target involved in their mechanism of action, the second objective was to identify the cell death pathways induced by both cationic and neutral liposomes, by means of the FACS analysis of autophagy and apoptosis, the evaluation of the DNA damage, and the Western Blot analysis of the caspases expression.

2.3 MATERIALS AND METHODS

2.3.1 Cell cultures

Human WiDr epithelial colorectal adenocarcinoma cells, MCF-7 breast adenocarcinoma cells, and rat C6 glioma cell line were purchased from ATCC (American Type Culture Collection, Manassas, Virginia, USA). C6 cells were grown in Dulbecco's modified Eagle's medium (DMEM, Invitrogen, Paisley, UK) containing high glucose (4.5 g/l), while MCF-7 and WiDr were grown in RPMI 1640 medium (Invitrogen, Paisley, UK). Media were supplemented with 10% fetal bovine serum (FBS, Cambrex, Verviers, Belgium), L-glutamine (2 mM, Sigma, Milan, Italy), penicillin (100 units/ml, Sigma) and streptomycin (100 mg/ml, Sigma), according to ATCC recommendations. All cells were cultured in a humidified 5% carbon dioxide atmosphere at 37 °C.

2.3.2 Cell viability

To evaluate the antiproliferative activity of the nanovectors, both the MTT Assay and the cell count were performed. WiDr, MCF-7 and C6 cells were washed with PBS buffer solution (Sigma), collected by trypsin (Sigma) and then inoculated in a 96-microwell culture plates at density of 10^4 cells/well. Cells were allowed to grow for 24 h, then the medium was replaced with fresh medium and cells were treated for further 48 h with a range of concentrations (10→100 μ M) of AziRu and of the liposomes DOTAP,

DoHuRu/DOTAP, HoThyRu/DOTAP and ToThyRu/DOTAP. Cell viability was evaluated with the MTT assay procedure, which measures the level of mitochondrial dehydrogenase activity using the yellow 3-(4,5-dimethyl-2-thiazolyl)-2,5-diphenyl-2H-tetrazolium bromide (MTT, Sigma) as substrate. The assay was based on the redox ability of living mitochondria to convert dissolved MTT into insoluble purple formazan. Briefly, after the treatments the medium was removed and the cells were incubated with 20 μ l/well of an MTT solution (5 mg/ml) for 1 h in a humidified 5% CO₂ incubator at 37 °C. The incubation was stopped by removing the MTT solution and by adding 100 μ l/well of DMSO to solubilize the purple formazan. Finally, the absorbance was monitored at 530 nm by using a microplate plate reader (iMark microplate reader, Biorad, Milan, Italy). For the count of the viable cells, the method of Trypan Blue Exclusion was used. Briefly, cells were grown at 1.0×10^5 in 48 well-plate for 24 h and treated with the compounds, at the same condition used for the MTT assay. The cells are then trypsinized, centrifuged and resuspended in the medium. An aliquot of cell suspension (10 μ l) is mixed 1:1 with Trypan Blue and the number of viable cells was evaluated using an automatic counter (TC20 Automated Cell Counter, Bio-Rad, Milan, Italy), providing an accurate and reproducible total count of the cells and the live/dead ratio. The calculation of the concentration required to inhibit the cell the viability by 50% (IC₅₀), arising both of MTT assay and cell count, is based on plots of data carried out in triplicates and repeated three times. IC₅₀ values were obtained using a dose-response curve by nonlinear regression using a curve fitting program, GraphPad Prism 5.0, and are expressed as mean \pm SEM.

2.3.3 Fluorescence microscopy

To evaluate the cellular uptake of the liposome, rhodamine B lipid derivative, 1,2-dioleoyl-sn-glycero-3-phosphoethanolamine-N-(lissamine rhodamine B sulfonyl) ammonium salt (λ_{ex} 560 - λ_{em} 583 nm) (Fig.22), was used as a fluorescent probe by adding 2% mol during the synthesis of DoHuRu/DOTAP liposome. To directly follow the ruthenium fate in the cell, the fluorogenic group of the dansyl (λ_{ex} 370 - λ_{em} 450 - 550 nm) was used, directly bound to the ruthenium complex (HoThy-DansRu) (Fig.23), that is then normally co-aggregated with DOTAP. Sterile coverslips were placed in twenty-four-well plates. MCF-7 cells were seeded at a concentration of 5×10^4 /ml in the same twenty-four-well plates. Following a growth period of 24 h at 37 °C in RPMI 1640 medium

containing 10% FBS, the medium was replaced with serum-free RPMI 1640 medium, which was followed by the addition of fluorescent liposomes at final concentration 100 μM or free PBS saline solution to each well. The cells were incubated for additional times (30 min, 1, 3 and 6 h) with liposomes and washed with PBS three times to remove unassociated liposomes. The cells were then fixed at room temperature in 4% paraformaldehyde for 20 min. After washing with PBS three times, the cells were treated with diaminophenylindole (DAPI) (Sigma) to stain the cell nuclei. The coverslip from each well was mounted onto a glass microslide with 80% fluorescence-free glycerol mounting medium. Finally, the interaction of liposomes with MCF-7 cells and the cellular uptake was monitored using a fluorescent microscope (Leica Microsystems GmbH, Wetzlar, Germany) to visualize DAPI (345/661 nm) and fluorescent liposomes (557/571 nm). Images were taken using an AxioCam HRc video-camera (Zeiss) connected to an Axioplan fluorescence microscope (Zeiss) using the AxioVision 3.1 software.

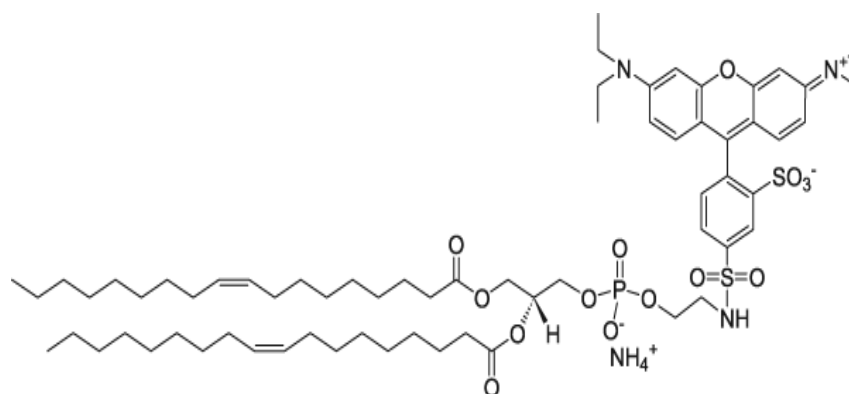


Fig.22. Molecular structure of rhodamine-based fluorescent probe

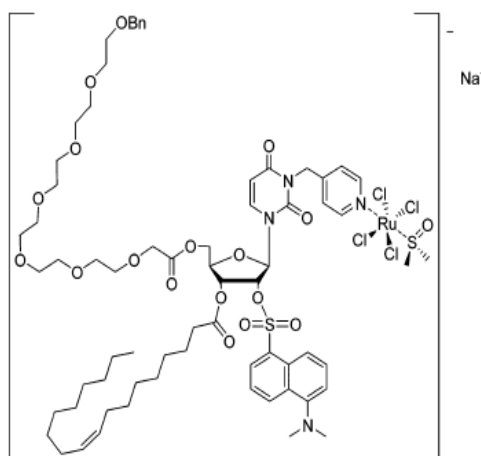


Fig. 23. Molecular structure of HoThyDansRu

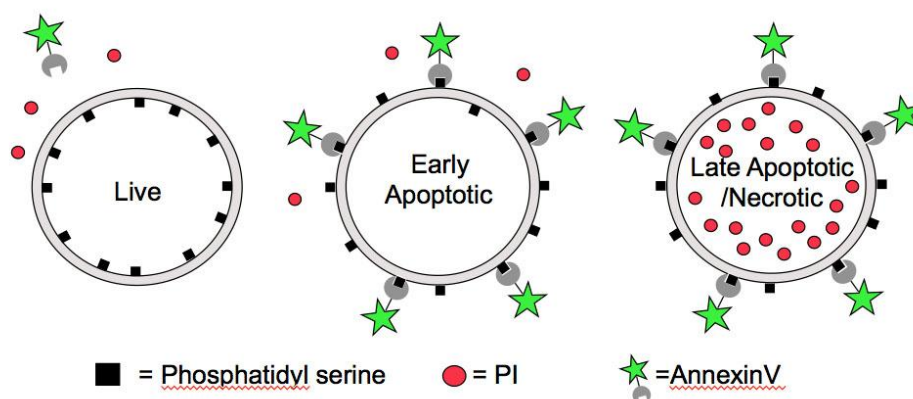
2.3.4 Flow cytometric analysis of autophagosomes formation

To quantify the induction of the autophagic process, MCF-7 cells treated with the various compounds, were stained with the autofluorescent agent monodansylcadaverine (MDC), a selective marker for autophagic vacuoles (AVOs) and especially autolysosomes. Treated cells were incubated with 50 μ M MDC in PBS at 37°C for 15 min. After incubation, cells were washed with PBS, and immediately analyzed by flow cytometry. All fluorescences were analyzed with a FACScalibur flow cytometer (Becton Dickinson). The fluorescent emissions were collected through a 530 nm band pass filter (FL1 channel). At least 10 000 events were acquired in log mode. For the quantitative evaluation of MDC, CellQuest software (Becton Dickinson) was used to calculate mean fluorescence intensities (MFIs). The MFIs were calculated by the formula (MFI treated/MFI control), where MFI treated is the fluorescence intensity of cells treated with the various compounds and MFI control is the fluorescence intensity of untreated and unstained cells. Values reported in the figures are the means \pm S.D.s from three independent experiments.

2.3.5 FACS analysis of apoptosis

Annexin V-FITC (fluorescein isothiocyanate) was used in conjunction with a vital dye, Propidium Iodide (PI). Propidium Iodide is a specific dye for the DNA, excluded by the cells that conserve the integrity of the membranes, whereas it stains DNA in the cells that have damaged membranes. Annexin V/FITC has a high specificity to bind the molecules of phosphatidylserine (PS), a phospholipid of cellular membrane normally exposed on the cytoplasmic side. The externalization of PS is a key event of the first state of apoptosis that lastly allows the recognition by the phagocytes. Thus, by cytofluorimetric analysis of the double fluorescence, it is possible to identify the viable cells (negative to both dyes), the necrotic cells (positive only to PI), the early apoptotic cells (positive only to Annexin V-FITC), and the late apoptosis/necrotic cells (positive to both PI and Annexin V-FITC) [Wlodkowic et al., 2009], as illustrated in Fig. 24. Briefly, cells were incubated with Annexin V-FITC (MedSystems Diagnostics, Vienna, Austria) and propidium iodide (Sigma) in a binding buffer (10 mM Hepes, pH 7.4, 150 mM NaCl, 5 mM KCl, 1 mM MgCl₂, 2.5 mM CaCl₂) for 10 min at room temperature, washed and resuspended in the same buffer. Analysis of apoptotic cells was performed by flow cytometry (FACScan,

Becton 4 Dickinson). For each sample, 2×10^4 events were acquired. Analysis was carried out by triplicate determination on at least three separate experiments.



www.lifesci.dundee.ac.uk

Fig. 24. Double method of PI and Annexin V detection of apoptosis by FACS analysis

2.3.6 DNA fragmentation assay

MCF-7 cells were grown on standard sterile plastic 60 mm culture dishes by plating 5×10^5 cells. After 24 h of growth the cells were treated for 48 h with IC_{50} doses of AziRu, DoHuRu/POPC, DoHuRu/DOTAP. Then, the cells were collected and the pellets were resuspended in lysis buffer (50 mM Tris-HCl, pH 7.5, 5 mM EDTA, 100 mM NaCl, 1% SDS, 0.5 mg/mL Proteinase K) and incubated at 50°C . After 1 h incubation, 10 mg/mL RNase was added to the lysates and incubated for 1 h at 50°C . DNA was precipitated with NaOAc pH 5.2 and ice cold 100% EtOH and centrifuged at $14000 \times g$ for 10 min. Pellets were dissolved in TE buffer (10 mM Tris-HCl, pH 8.0, 1 mM EDTA). A 20 μL aliquot of each DNA sample was analyzed on a 1.5 % agarose gel stained with ethidium bromide and visualized under UV light.

2.3.7 Western blot analysis of caspases expression

MCF-7 cells, treated with the IC₅₀ concentration of ruthenium-based nucleolipids co-aggregated in DOTAP for 48 and 72 h, were lysed at 4 °C in the buffer containing 10 mM Tris-HCl, pH 7.6, 50 mM NaCl, 1% Triton X-100, and protease inhibitor cocktail (Roche Diagnostics, Mannheim, Germany). Cell debris were pelleted by centrifugation at 4 °C for 20 min at 14,000 × g, and protein concentration of cell lysate was determined by the Bio-Rad protein assay (Bio-Rad, Milan, Italy). Samples containing 40 µg of proteins were separated on a 12% SDS-polyacrylamide gel and electrotransferred onto a nitrocellulose membrane (Amersham Biosciences, Little Chalfont, Buckinghamshire, UK) using a Bio-Rad Transblot (Bio-Rad). Proteins were visualized on the filters by reversible staining with Ponceau-S solution and destained in PBS. After blocking for 1 h at room temperature in 5% milk in Tris-Buffered Saline and Tween 20 (TBS-T), membranes were incubated with 1:1,000 dilutions of the primary antibodies to caspase-9, caspase-8 and tubulin (Cell Signaling, Beverly, MA, USA). Membranes were then washed 3 times with TBS-T before being incubated with appropriate horseradish peroxidase conjugated secondary antibodies. The immunocomplexes were visualized by the ECL chemoluminescence method (ECL, Amersham Biosciences) and analyzed by an imaging system (ImageQuant™ 400, GE Healthcare Life Sciences). Densitometric analysis was performed using the GS-800 imaging densitometer (Bio-Rad). Tubulin antibody was used to normalize the results.

2.3.8 Statistical analysis

All data were presented as mean ± SEM. The statistical analysis was performed using Graph-Pad. Prism (Graph-Pad software Inc., San Diego, CA) and ANOVA test for multiple comparisons was performed followed by Bonferroni's test.

2.4 RESULTS

2.4.1 Antiproliferative activity

The cell survival index curves (Fig.25) demonstrate that, as expected, the DOTAP liposome ruthenium-free showed no significant interference with the cell viability and proliferation. Interestingly, the three amphiphilic ruthenium complexes co-aggregated with DOTAP are much more active than the precursor AziRu. In fact, the corresponding IC_{50} values referred at the ruthenium concentration enclosed in the nanovector (50% in moles) are significantly decreased, as highlighted also by the potentiating factors (Tab.1), calculated as the ratio of IC_{50} values of AziRu and the nanovectors in the corresponding cell lines. For example, the nanovectors are about 20 times more effective than AziRu on MCF-7 cells (IC_{50} 15 μ M and 305 μ M, respectively). Presumably, their higher anticancer activity with respect to low molecular weight ruthenium complexes is the result of an enhanced cellular uptake efficiency due to the "nanovectorization", as well as of the capacity of Ru(III) nucleolipidic aggregates themselves in inhibiting cell growth and proliferation. According with the previous results [Mangiapia et al., 2012], Ru(III) derivatives are more active on MCF-7 cells than against other cancer cells. However, the antiproliferative effect observed in rat C6 glioma cells, a current model system useful for the evaluation of new therapies for the treatment of one of the most resistant tumor, the glial neoplasm, [Grobben et al, 2002] is an important indication on the wide spectrum of action of these ruthenium-nanovectors .

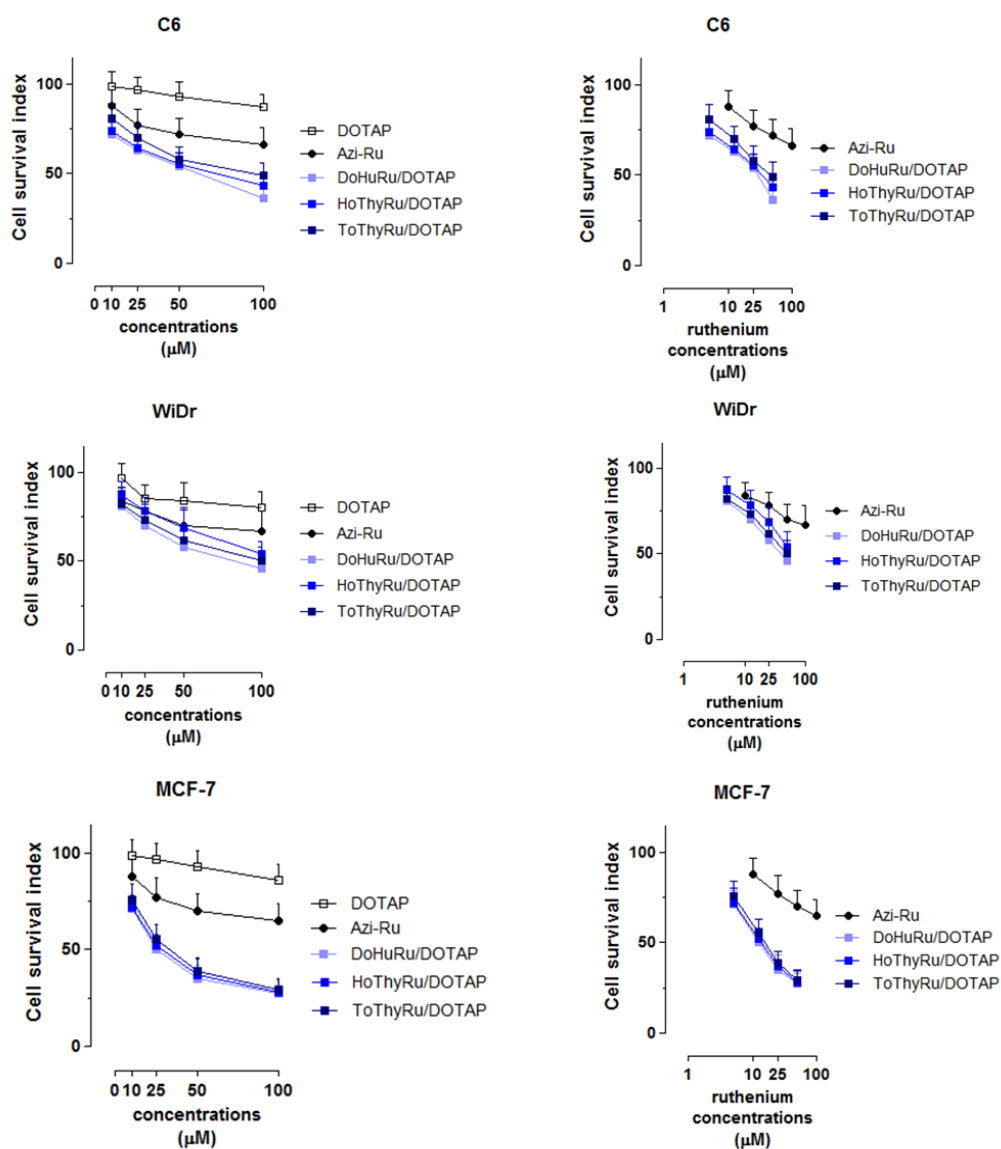


Fig. 25. Cell survival index values, evaluated by MTT assay and total cell count, in C6, WiDr and MCF-7 cell lines incubated for 48 h with DOTAP, with different Ru-containing formulations and with AziRu. On the right, the corresponding concentration-effect curves obtained by normalizing for the actual amount of ruthenium contained in the liposomes.

IC ₅₀ (μM)	MCF-7	WiDr	C6
Azi-Ru	305 ± 16	441 ± 20	318 ± 12
ToThyRu/ DOTAP 50/50	19 ± 8 16	50 ± 11 9	54 ± 8 6
HoThyRu/ DOTAP 50/50	15 ± 7 20	65 ± 8 7	43 ± 11 7
DoHuRu/DOTAP 50/50	13 ± 5 23	41 ± 10 11	34 ± 9 9

Tab.1 IC₅₀ values reported as mean ± SEM. In bold, the Potentiating Factors (PF) of the nucleolipidic ruthenium complexes in DOTAP respect to Azi-Ru are shown, calculated as the ratio of IC₅₀ values of DoHuRu/DOTAP, HoThyRu/DOTAP, and To-ThyRu/DOTAP complexes to the IC₅₀ of AziRu.

2.4.2 Cellular uptake

For both ruthenium and platinum complexes, the cytotoxicity profiles are significantly correlated with the rate of cellular uptake, for which their lipophilicity is a favorable parameter [Tan et al., 2011]. In order to evaluate the kinetics of accumulation of the cationic liposomes ruthenium-based into human MCF-7 cancer cells, the fluorescent probe Rhodamine was inserted in the liposomal bilayer of DoHuRu/DOTAP. These experiments have been also performed by exposing the cells to the rhodamine B adduct alone under the same *in vitro* experimental conditions, like negative control. In the microphotographs reported in Figure 26, the blue areas indicate the cells nuclei stained by DAPI, whereas the green areas represent the rhodamine localization. As shown by time-course experiments starting after 30 min of incubation, DoHuRu/DOTAP liposome seems highly able to cross the cell membranes, through a very fast process of internalization. By merged images (Merge), where the emission of the two fluorophores is overlapped, it is also more clear again that the liposome enters in the cells, and arrives in the proximity of the nuclei too. By means of their lipid properties, it is possible that the Ru complexes/DOTAP nanoaggregates interact with the cells directly via membrane fusion and/or by endocytosis. These processes apparently occur by nonspecific patterns involving multiple molecular mechanisms, probably starting from charge attraction and ultimately leading to close

contact with the membrane [Zabner et al., 1995; Bailey et al., 1997]. Also, at less time of incubation, this liposome shows a more massive uptake than the same system formed by the neutral lipid POPC [Mangiapia, et al., 2012]. This proves that the positive charge of the liposome improves its capacity to interact with the negative charged components of the plasmatic membrane, such as proteoglycans [Wiethoff et al., 2001].

To further investigate cellular uptake, MCF-7 cells were treated with the dansyl-labeled ruthenium complex HoThy- DansRu coaggregated with DOTAP under the same conditions used for HoThyRu, ToThyRu, and DoHuRu. In this way, the fate of the active ruthenium complex can be directly followed, by analyzing its location after nanocarriers application to the cells. According with the above mentioned results, fluorescently labeled HoThyDansRu localizes rapidly within the cells, and the microphotographs in Figure 27 show a growing time-course accumulation. The fluorescence emission analyzed seems also suggest that the complexes loaded in DOTAP liposomes enter the cytoplasm before being predominantly delivered to discrete foci in the perinuclear compartment; moreover, although attenuated by DAPI nuclear staining, dansyl-dependent fluorescence emission is also detectable in the nuclei area. Combining the results of these two kinds of labeling, one for the DOTAP bilayer, and the other for the nucleolipidic component, it is possible to presume a rapid phenomenon of degradation of the whole liposome in the intracellular space and a fast release of the "active agent" in the cytoplasm. This assumption could explain the extensive rhodamine-associated fluorescence and the related generation of discrete dansyl-associated foci. Also, the accumulation of dansyl fluorescence in proximity to the nuclei suggests a possible interaction between the nucleolipid HoThyDansRu and the nuclear membranes by mechanism like adsorption, lipid mixing and lysis, as already described for negative charged vesicles [Lawaczeck et al., 1987]; thus this consideration opens the scenario to the different possible fates of ruthenium-based nucleolipids after liposomes delivery, like the interaction with the nuclear membranes and subsequent accumulation of the metal in the nucleus, but without excluding the binding with targets in other cellular compartments. However, given the wide range of possible modification to which the ruthenium complexes can be subjected in the cellular environments, such as the ligand-exchange reactions or changing of the redox state, further studies will be done to individuate what is/are the effective active specie/species responsible for the antiproliferative effects.

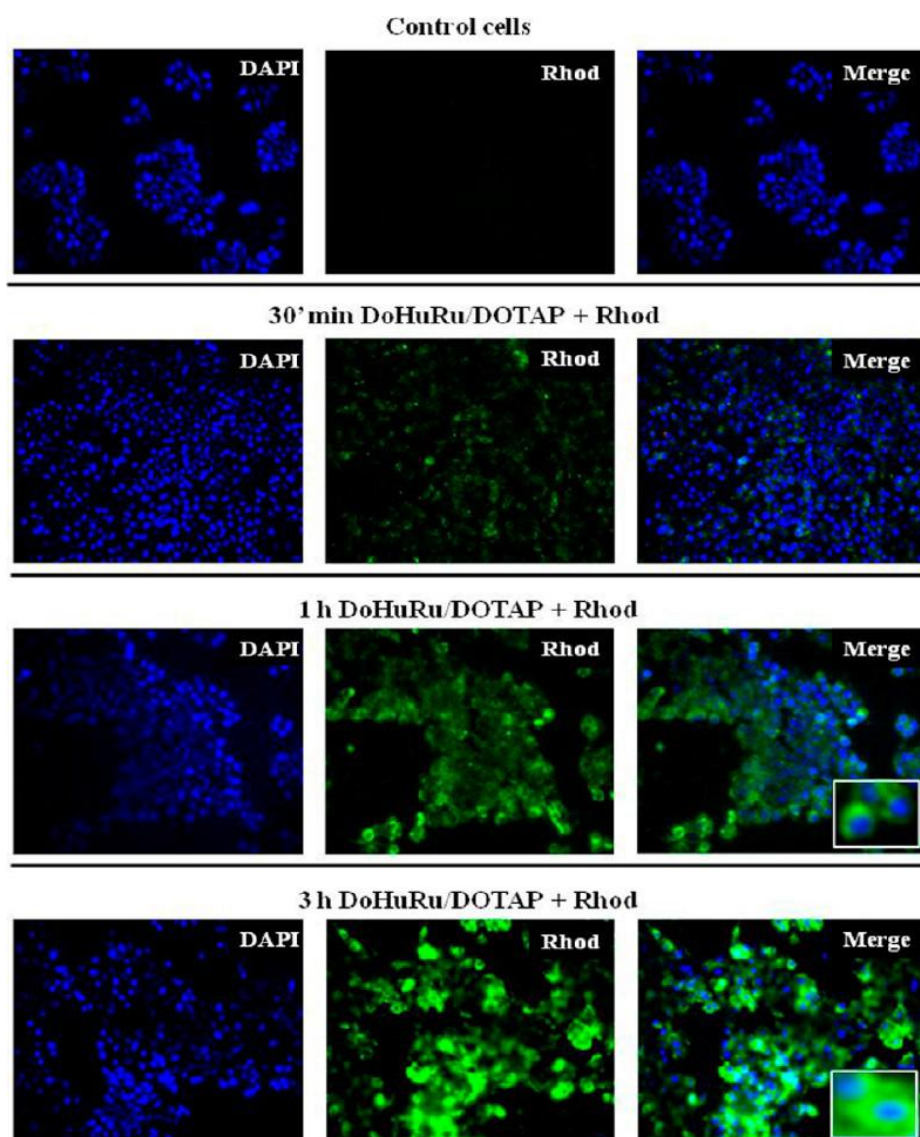


Fig.26. Fluorescent microphotographs of monolayers showing the cellular uptake of liposomes by human MCF-7 breast adenocarcinoma cells. DAPI is used as a nuclear stain (shown in blue). Rhodamine-dependent fluorescence (Rhod) of DoHuRu/DOTAP liposomes is shown in green. In merged images (Merge), the two fluorescent emissions are overlapped.

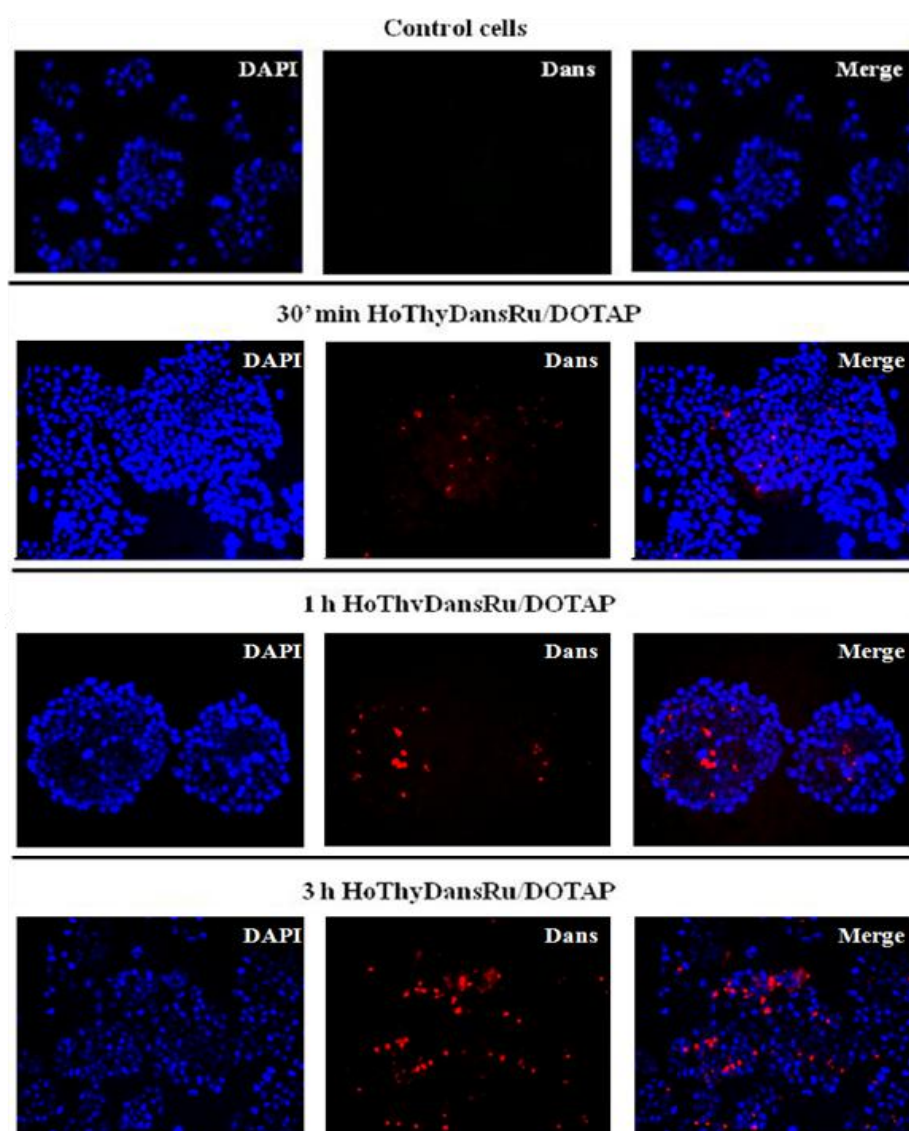


Fig.27. Fluorescent microphotographs of monolayers showing the cellular location of dansylated-HoThyDansRu complex into human MCF-7 breast adenocarcinoma cells subsequent to nanocarriers application. DAPI is used as a nuclear stain (shown in blue). Dansyl-dependent fluorescence (Dans) of HoThyDansRu/DOTAP liposomes is shown in red. In merged images (Merge), the two fluorescent emissions are overlapped.

2.4.3 Apoptosis and autophagy activation

To evaluate the pathways of cell death involved in the antiproliferative effect of the neutral and cationic ruthenium-nanovectors, the MCF-7 cells, which are among the most sensitive to these compounds, were treated for 48 and 72 h with DoHuRu/POPC and DoHuRu/DOTAP with concentrations equal to IC_{50} values. The analysis of the formation of autophagosomes was performed by the Monodansylcadaverine (MDC) staining, an autofluorescent agent specific for the autophagolysosome, and flow cytometric evaluation of the associated fluorescence. The occurrence of autolysosomes, resulting from lysosomes-autophagosomes fusion, exclusively characterizes late steps in the autophagic cell death process. As showed in the Figures 28 and 29, the cationic DoHuRu/DOTAP formulation induces a significant ($p < 0.001$) increase in the Mean Fluorescence Intensity (MFI) that grow over time (4.3 and 5.8-fold at 48 and 72 h, respect to control untreated cells), indicating a strong formation of the MDC-labeled vacuoles. Conversely, no autolysosomes formation was detected after DoHuRu/POPC treatment, at least up to 72 h.

The FACS analysis of apoptosis was carried out by the double staining with Annexin V-FITC and Propidium Iodide. This method has the advantage of discriminating not only between viable, necrotic and apoptotic cells, but also between the early and late stages of apoptosis. Propidium Iodide is a specific dye for the DNA, excluded by the cells that conserve the integrity of their membranes, whereas it stains DNA in the cells that have damaged membranes. Annexin V-FITC has a high specificity to bind the molecules of phosphatidylserine (PS), phospholipid of cellular membrane normally exposed on the cytoplasmic side. The externalization of PS is a key event of the first state of apoptosis that lastly allows the recognition by the phagocyte. Thus, by cytofluorimetric analysis of the double fluorescence, it is possible to identify the healthy cells (negative to both dyes), the necrotic cells (positive only to PI), the cells in early apoptosis (positive only to Annexin V-FITC), the cells in late apoptosis (positive to both PI and Annexin V-FITC). The FACS analysis shows that after 48 h of treatment with the cationic nanovector DoHuRu/DOTAP, a consistent percentage of cells (46.5 %) are already in the phase of late apoptosis (Fig. 30), and that this percentage increases at 72 h of treatment (82.1 %) (Fig. 31). These results confirm that, despite the fast kinetics of uptake, the processes triggered by the active agent persist over time, involving probably different mechanism of cell signaling, which in turn

lead to the induction of cell death. Also, the simultaneous and growing presence of autophagy and apoptosis at long time suggests that no mechanisms of protection are induced by the autophagy that, contrarily, may itself induce apoptosis [Maiuri et al., 2007]. On the other hand, the treatment with neutral liposome DoHuRu/POPC (Fig. 30 and 31) induces early apoptosis (35.8 % at 48 h and 35.2% at 72 h) and just a little percentage of cells arrives in the phase of late apoptosis (13.6 % at 48 h, 37.4% at 72h). The slower kinetics of apoptosis induction as well as the absence of autophagy in the cells treated with the neutral liposomes, indicates that these systems interfere with the cell viability in a different way respect to the cationic nanovectors. Moreover, this result emphasizes the role of the liposomes in the capacity to deliver the drug but also in the explication of the ruthenium mechanism of action. Thus the liposome formulation could be not only *passive* carriers for the ruthenium complexes, but a system that interferes with the affinity of the ruthenium with the molecular targets.

To confirm the apoptosis, DNA was extracted from MCF-7 cells treated with IC_{50} concentrations of nanovectors and AziRu and loaded on agarose gel. The gel in Figure 32 shows that the DNA extracted from cells treated with the cationic liposome is degraded to form fragments called "ladder" of 180 bp and multiples, typical of the late stage of apoptosis. Really, MCF-7 is one of the human breast cancers known to be resistant to some chemotherapeutics due to deletion in the CASP-3 gene that leads to an innate deficiency of caspase-3 [Jänicke et al., 1998]. Caspase-3 cleaves a variety of important cellular proteins and it is ultimately responsible for apoptotic DNA fragmentation. Different patterns of DNA cleavage are involved in the apoptosis process, like the formation of large DNA fragments coupled to single-strand cleavage, of which the specific responsible enzymes are not yet definitively individuated [Bortner et al., 1995]. Also, DNA fragmentation in MFC-7 cells due to cytotoxic agents—may correlate with the activation of different apoptotic pathways and other effector caspases, such as caspases -6 or -7 [Liang et al., 2001]. Moreover, it cannot be excluded that this event is due to a direct effect of the capacity of the ruthenium complex to intercalate the DNA, as occurs in the interaction between a dinuclear Ru(II) polypyridyl complex and a plasmid model [Liu et al., 2016]. Interesting, we can note also a high level of DNA fragmentation with AziRu, but the effective used dose to have the equal concentration/effect (IC_{50}) to the liposomes is very high (305 and 13 μ M respectively). This confirms the efficiency of the liposomes for the drug delivery and

suggests that the mechanism of action that leads to apoptosis induction is explicated inside the cells by binding targets that are not yet known, but that, in consideration of the results obtained at the moment, could be multiples, such as DNA and protein/enzyme. On the other hand, flow cytometric analysis showed that DoHuRu/POPC produces just a bland activation of apoptosis and autophagy pathways. In accordance with these data, DNA fragmentation assay showed that only a little percentage of DNA is fragmented by neutral liposomes. Considering that the rapport of concentration/effect is the same, this means that the liposome formulation and its interaction with the cells influence the mechanism of cell death induced by ruthenium.

Ascertained that the cationic nanovectors cause cell death prevalently by apoptosis, to better characterize this event we started an analysis of caspases expression. This preliminary screening of apoptotic factors was focused on the activation of caspase-8 and -9, the two initiators caspases of the extrinsic and intrinsic pathway of apoptosis, respectively. In this way, we have been able to discriminate between the involvement of these two kinds of apoptosis pathways, evaluating the specific activation of the intrinsic apoptotic pathway (Fig. 33); it is also called mitochondrial pathway because the activation of the caspase-9 depends on the change in the permeability of the mitochondrial membrane, that in turn is due to various stimuli, such as DNA-damaging agents, overload of Ca^{2+} , deprivation of growth factors, oxidants and microtubule-targeted drugs [Baig et al., 2016]. This type of apoptosis could be preferable in the prospective of making a stealth drug delivery system, because it doesn't suppose, unlike the extrinsic apoptosis, a participation of extracellular factors, often involved in the immune responses [Fulda and Debatin, 2006]. However, further investigations on the expression of other apoptotic factors are in progress, in order to obtain a complete view of the apoptotic cascade involved in the activity of ruthenium-based nanovectors.

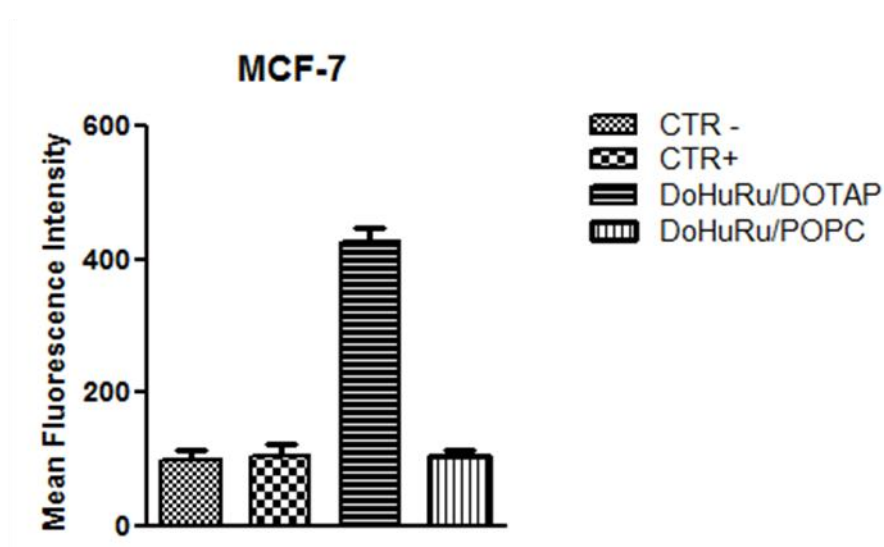
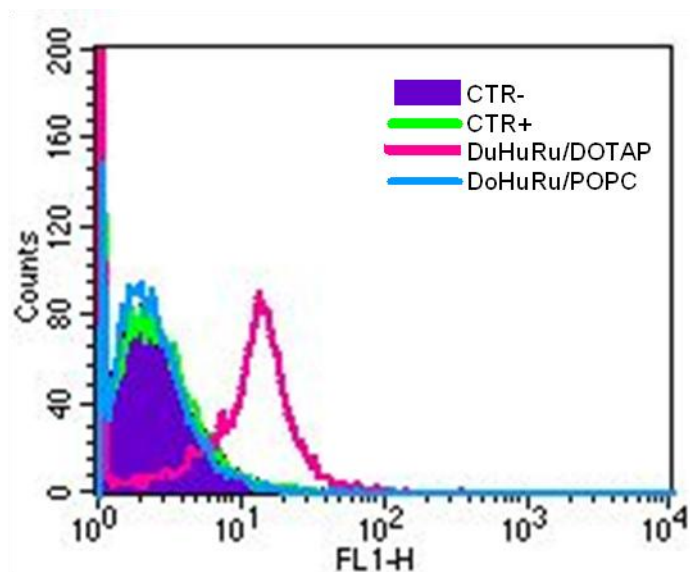


Fig.28. Flow cytometric analysis of autophagosomes formation (MDC incorporation) in MCF-7 treated with IC₅₀ concentrations of DoHuRu/DOTAP or DoHuRu/POPC for 48h. Values are the means of three independent experiments (\pm S.D.).

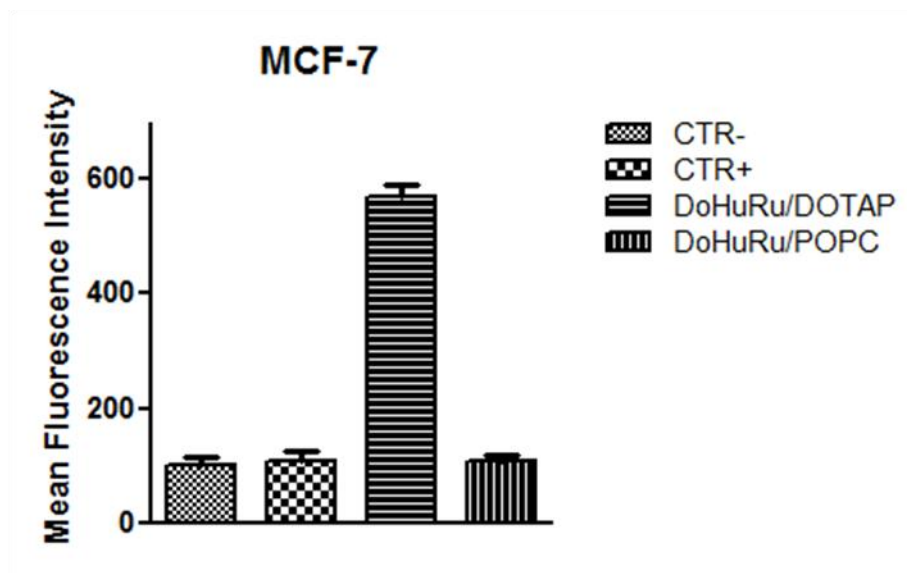
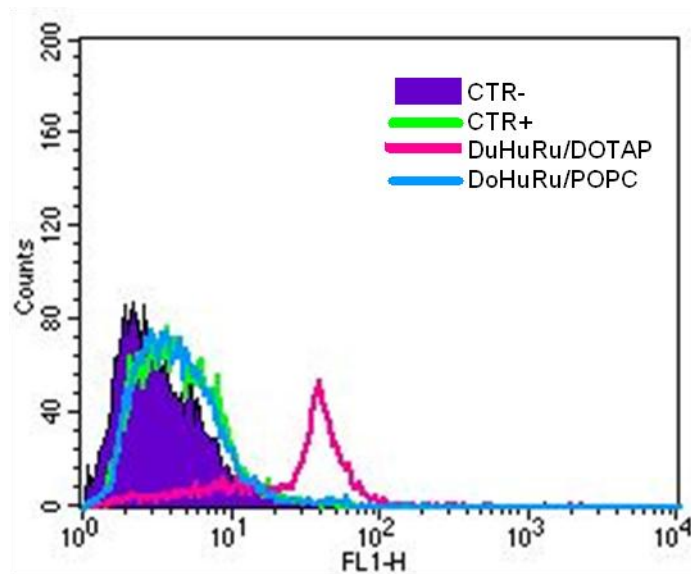


Fig. 29. Flow cytometric analysis of autophagosomes formation (MDC incorporation) in MCF-7 treated with IC₅₀ concentrations of DoHuRu/DOTAP or DoHuRu/POPC for 72h. Values are the means of three independent experiments (\pm S.D.).

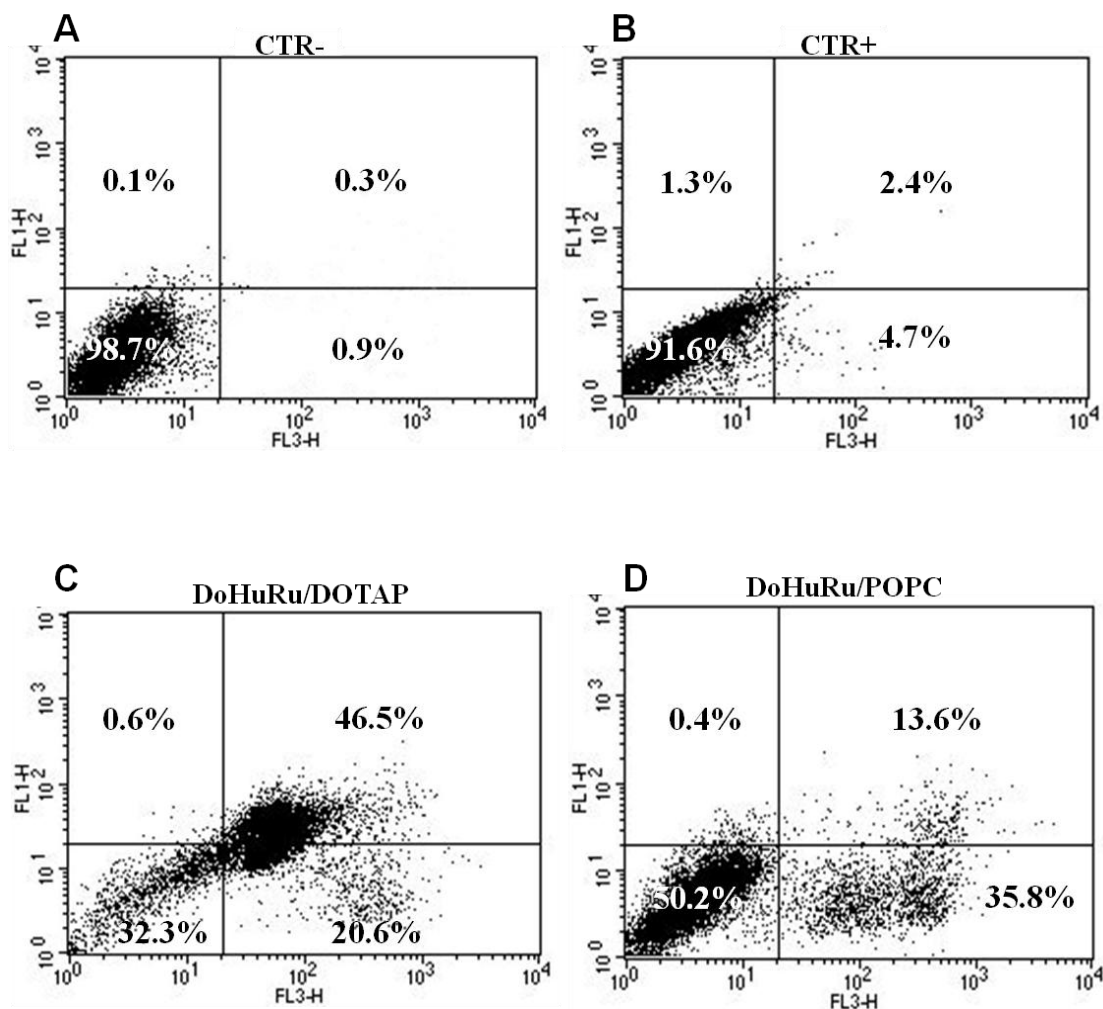


Fig.30. Apoptosis was evaluated by FACS analysis, after cell labeling with PI and FITC-Annexin V. MCF-7 cells were both unlabeled and untreated (A), labeled and not treated (B), treated with IC_{50} concentrations of DoHuRu/DOTAP (C) or DoHuRu/POPC (D) for 48h. The lower left quadrants of each panels show the viable cells, which exclude PI and are negative for FITC-Annexin V binding. The upper left quadrants contain the non-viable, necrotic cells, negative for FITC-Annexin V binding and positive for PI uptake. The lower right quadrants represent the cells in early apoptosis, that are FITC-Annexin V positive and PI negative. The upper right quadrants represent the cells in late apoptosis, positive for both FITC-Annexin V binding and for PI uptake. The experiments were performed at least three times with similar results.

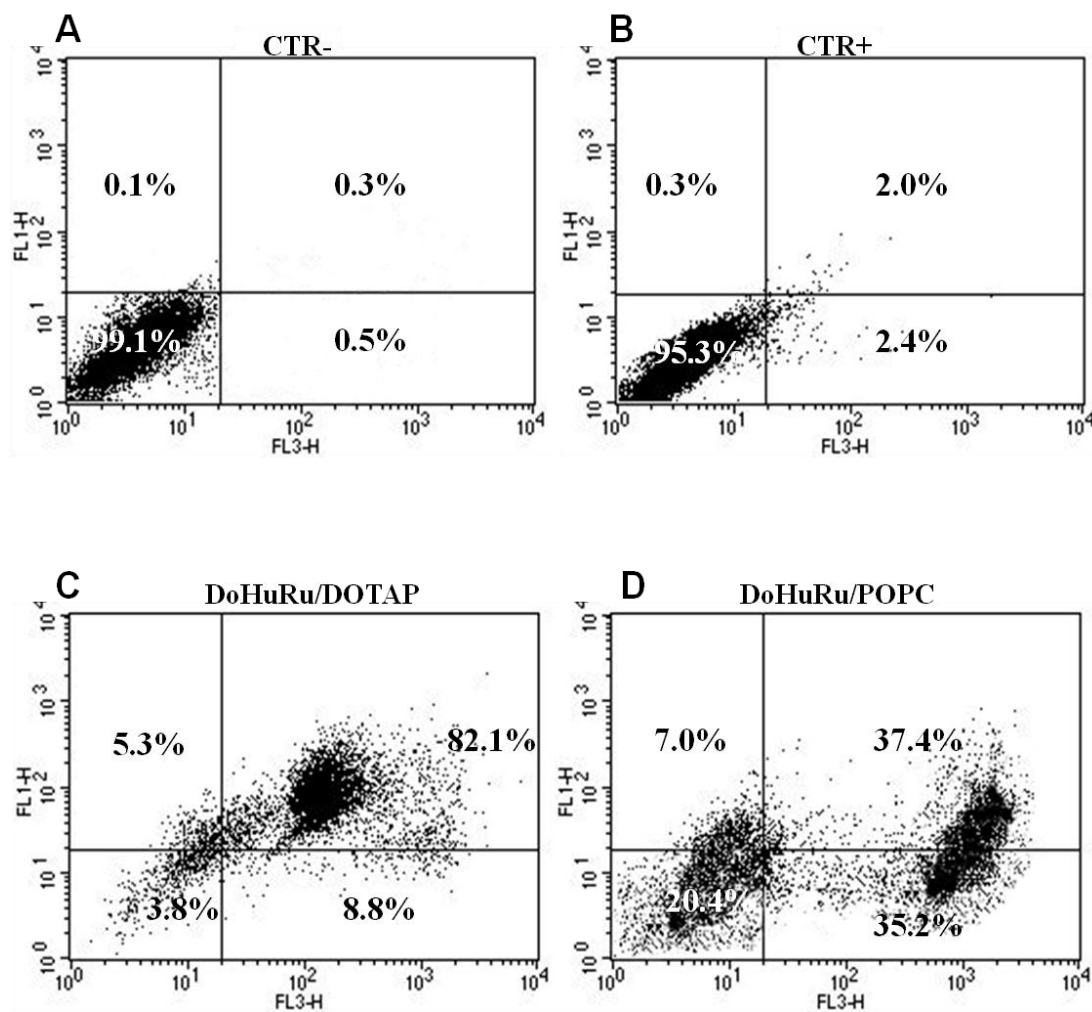


Fig.31. Apoptosis was evaluated by FACS analysis, after cell labeling with PI and FITC-Annexin V. MCF-7 cells were both unlabeled and untreated (A), labeled and not treated (B), treated with IC50 concentrations of DoHuRu/DOTAP (C) or DoHuRu/POPC (D) for 72 h. The lower left quadrants of each panels show the viable cells, which exclude PI and are negative for FITC-Annexin V binding. The upper left quadrants contain the non-viable, necrotic cells, negative for FITC-Annexin V binding and positive for PI uptake. The lower right quadrants represent the cells in early apoptosis, that are FITC-Annexin V positive and PI negative. The upper right quadrants represent the cells in late apoptosis, positive for both FITC-Annexin V binding and for PI uptake. The experiments were performed at least three times with similar results.

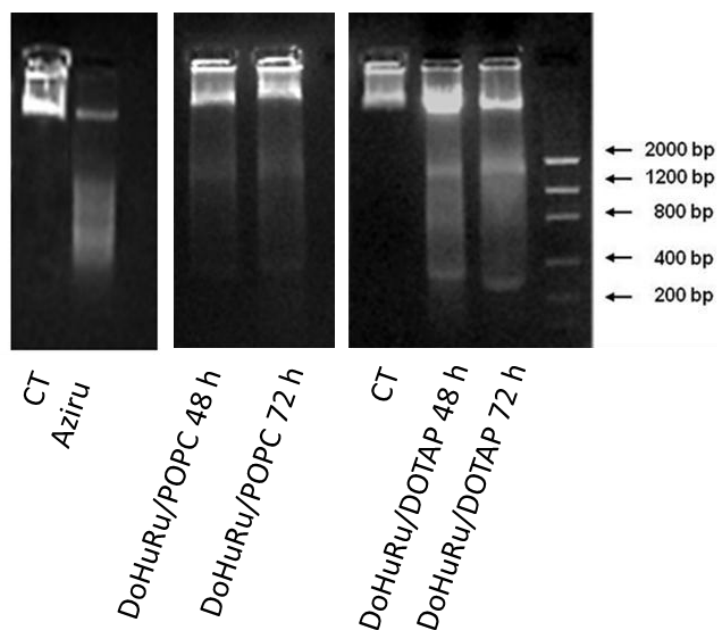


Fig.32. DNA fragmentation assay in MCF-7 cells, treated or not (Ct) for 48 h and 72 h with IC₅₀ doses of DoHuRu/POPC or DoHuRu/DOTAP and AziRu alone.

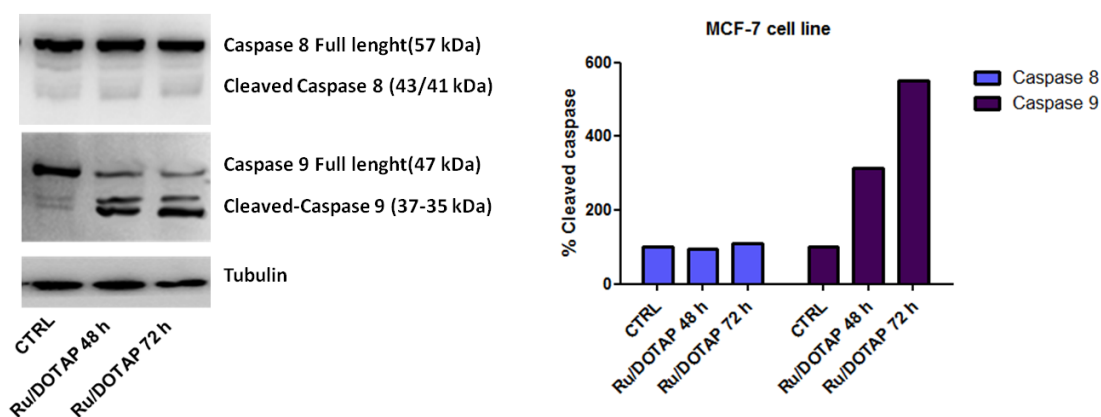


Fig.33. Western Blot Analysis of Caspase-8 and Caspase-9 activation in MCF-7 cells untreated and treated with DoHuRu/DOTAP for 48 and 72 h; In the graph, the quantification of the cleaved/full length caspase-8 and caspase-9, calculated as percent of the control.

2.5 CONCLUSIONS

Previous results obtained on the POPC liposomes, have shown the efficacy of the "nanovectorization" on the activity of the low molecular weight complex AziRu, analog of NAMI-A. NAMI-A showed low cytotoxicity for the primary tumor, but is one of a few antimetastatic drugs. This means that the lack of anticancer activity is due to a poor interaction of the compounds with targets within the cells; when AziRu is vehiculated inside the cells, it can better explicate its antiproliferative effects, as demonstrated for other polymeric system ruthenium-based [Lu et al., 2015; Duan et al., 2015]. Now we demonstrated the efficacy of cationic nanovector, formed by the lipid DOTAP, to carry the ruthenium complexes. Moreover, it induces both autophagy and apoptosis, suggesting the activation of multiple pathways of cell death. The coupled results of viability assay and cellular uptake show that cationic liposomes are a good system to deliver the ruthenium complexes, also in a stronger way respect to neutral liposome, due to the greater interaction between the cationic lipid and the negative component of the cell surface. This is in agreement with a study showing that the fusion of cationic liposomes with the cancer cell membrane, due to the attraction of charges, is easier when the cells expose phosphatidylserine on their surface [Stebelska et al., 2006]. Since DoHuRu/DOTAP has shown to give in the MCF-7 cells a rapid activation of the early state of apoptosis, typically characterized by phosphatidylserine externalization, the hypothesis is that its cellular uptake can increase over time, like a positive feedback mechanism. This event could explain also the poor activation of the late state of apoptosis by the neutral liposome DoHuRu/POPC, as a lack of increment of the cellular uptake, as suggested by the faster kinetics of fluorescent accumulation after treatment of the cells with the rhodamine-labeled cationic liposomes [Mangiapia et al., 2012]. On the other hand, the different profiles of cell death in the cells treated with the neutral and the cationic liposome provides evidences that the nanocarriers, by interfering with the uptake of the ruthenium complex, could change its target-specificity. Thus, the inclusion in the nanocarriers could amplify the scenario of the employment of these complexes, and could represent a strategy to overcome the drug resistance. All together these results demonstrate that the ruthenium-based DOTAP liposomes are a good alternative to the low molecular weight ruthenium complexes. In Figure 34 is illustrated an hypothetical mechanism of cellular interaction suggested for cationic ruthenium-based nanovectors. However, there is still much to investigate about

their mechanism of action and the structure-activity relationship, as well as the physiological implications and the metabolic targets *in vivo* will be tested.

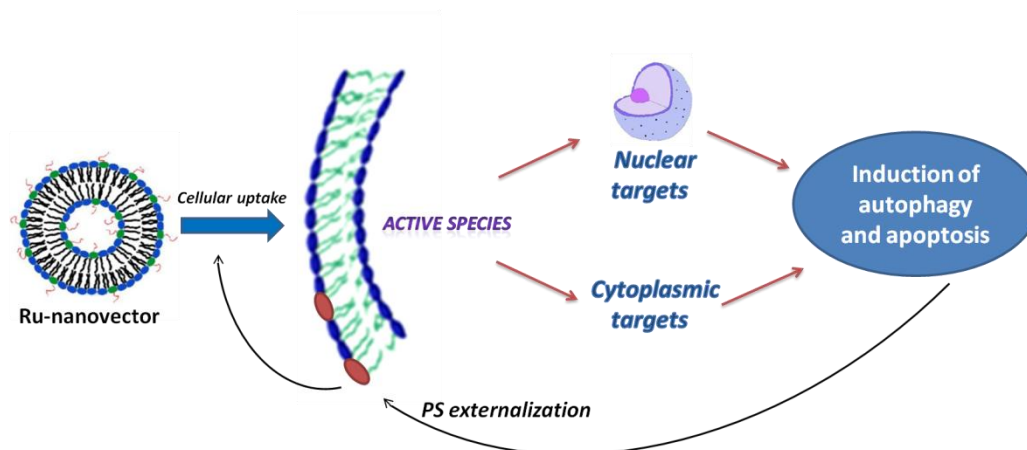


Fig.34. Hypothetical mechanism of cellular interaction proposed for cationic ruthenium-based nanovectors: the liposomes could specifically direct by the passive targeting to the cancer cells, whereas interact with the cell membranes by adsorption and/or endocytosis. Inside the cells, chemical modifications might occur, leading to one or more active species of ruthenium complexes, which can have multiple targets, in the nucleus and/or in the cytoplasm, leading lastly to the induction of autophagy and apoptosis pathways. In addition, the early state of apoptosis is characterized by the exposition of the phosphatidylserine (PS) from the inner membrane to the surface, event that in turn could improve the interaction of the cationic liposome with the cells undergoing apoptosis.

3. DOTAP-TothyCholRu: cholesterol improves the cellular uptake



3.1. INTRODUCTION

3.1.1. The role of cholesterol in natural and biomimetic membranes

Cholesterol is a fundamental constituent of the organism; it is a key component of biological membranes and precursor of bile salts, vitamins and all steroid hormones. Cholesterol has a critic role in keeping the fluidity of the cell membrane: on the one hand reduces the freedom of movement of the chains, on the other hand prevents intermolecular bonds between lipids and thus the rigidity of the membranes [Chapman, 1975]. For this reason many researches are focused on the design of bio-mimetic model membranes system that, exploiting the advantages of the similarity to the biological membranes, could be a new strategy for the drug delivery. Thus the inclusion of cholesterol in membrane models can have different advantages. It increases the rigidity of the lipid bilayer and reduces its instability in the blood, due to the serum protein binding [Mabrey et al., 1978]. Also, it is recognized by receptors of low-density lipoprotein (LDL) facilitating the endocytosis [Krieg et al., 1993], and represents a highly biocompatible system [Lacko et al., 2007]. Some interesting examples of the inclusion of cholesterol in biological systems are already reported in literature: end-modification with a cholesterol motif has been effectively applied to biologically active oligonucleotides [Musumeci and Montesarchio, 2012]; different modifications of lipid architectures introducing cholesterol are reported as good strategy to increase the transfection processes [Bajaj et al., 2008; Bajaj et al., 2007]; DOTAP liposomes including cholesterol as vector for gene transfection, are nowadays in clinical trials for the treatment of lung cancer [Lu et al., 2012]. Some studies concerning liposomes interaction with membrane show also a specific cholesterol/lipid ratio, similar to the one reported for the plasma membrane of animal cells, to obtain the optimal cellular fusion [Hosta-Rigau et al., 2013; Moghaddam et al., 2011]. In the contest of cancer therapy, the use of cholesterol is not only useful for the formation of a biomimetic membrane, but also to make a sort of active targeting. In fact cancer cells need of an excess of cholesterol [Murtola et al., 2012] that have an important impact on tumor development, cell migration and angiogenesis [Cruz et al., 2013; Buchwald, 1992]. Exploiting the altered metabolism of cholesterol in cancer cells, it is possible to make a strategy properly defined by Lacko et al. “Trojan horse” approach [Lacko et al., 2007]; in fact, successful synthetic lipoproteins as drug delivery platform for anti-cancer agents are reported in literature [Sabnis and Lacko, 2012].

3.1.2. ToThyCholRu/DOTAP

As an evolution of the previous work on ruthenium-based cationic liposome (Chapter 2), we here performed the biological characterization of the ruthenium nucleolipid including cholesterol, named ToThyCholRu, co-aggregated with the lipid DOTAP. In particular, the cholesterol is bound with the oxidril 3' of the ribose of the nucleolipid ToThyRu. The so-formed ToThyCholRu (Fig.35), intrinsically negatively charged, is lodged in the cationic DOTAP bilayer (Fig.36). This liposome contains a final concentration of ToThyCholRu equal to 30% in moles and results stable for several months. This system has been characterized using dynamic light scattering (DLS), small angle neutron scattering (SANS), neutron reflectivity (NR) and electron paramagnetic resonance (EPR) techniques. Due to the high affinity of cholesterol with phospholipids, ToThyCholRu could easily interact with the cell membranes, facilitating the ruthenium complex internalization.

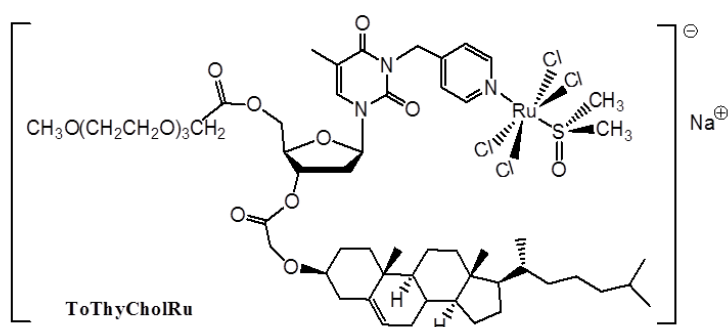


Fig. 35. Molecular structure of the nucleolipid ToThyCholRu

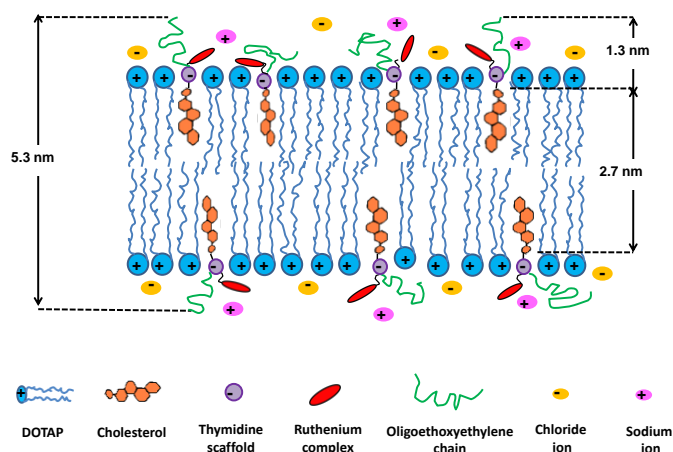


Fig. 36. Graphical representation of how the ruthenium complex anchored to the cholesterol-functionalized nucleolipid is accommodated into the liposome bilayer

3.2 AIM

The aim of this work is the *in vitro* biological characterization of ToThyCholRu/DOTAP, a possible anticancer agent, obtained from the previously tested liposomes ToThyRu/DOTAP, by adding of cholesterol. The goal is thus improving the nanovectorial system by the inclusion of this steroid, that is well known as natural constituent of cell membranes and very important for the integrity of the lipid bilayer; it could ensure not only the stability of the liposomes, but also the biocompatibility and the interaction with cell membranes during the process of internalization. First, we evaluated the effect on the cellular viability both on cancer and healthy cells. Then, the cellular uptake by fluorescent microscope was estimated. Finally, evaluations on the identity of the cell damage caused were provided, by DNA fragmentation assay and the analysis of the cell morphology by light microscopy.

3.3 MATERIALS AND METHODS

3.3.1 Cell cultures

Human WiDr epithelial colorectal adenocarcinoma cells, HeLa cervical adenocarcinoma cells, MCF-7 breast adenocarcinoma cells, and rat L6 skeletal muscle cells were purchased from ATCC (American Type Culture Collection, Manassas, Virginia, USA), while HaCaT keratinocytes were taken from CLS (Cell Lines Service GmbH, Eppelheim, Germany). MCF-7 and WiDr cells were grown in RPMI 1640 medium (Invitrogen, Paisley, UK), whereas HeLa, HaCaT and L6 cells were grown in DMEM (Invitrogen, Paisley, UK). Media were supplemented with 10% fetal bovine serum (FBS, Cambrex, Verviers, Belgium), L-glutamine (2 mM, Sigma, Milan, Italy), penicillin (100 units/ml, Sigma) and streptomycin (100 µg/ml, Sigma), according to ATCC recommendations. The cells were cultured in a humidified 5% carbon dioxide atmosphere at 37 °C.

3.3.2 *In vitro* bioscreening

For the *in vitro* bioscreening, the cells were treated for 48 h with a range of concentrations (10→1000 µM) of AziRu and ToThyCholRu complex lodged in DOTAP liposomes, as

well as with Ruthenium-free ToThyChol/DOTAP liposomes as negative control and with cisplatin (*c*DDP), like positive control for the cytotoxic effects. Cell viability was evaluated with the MTT assay and Trypan Blue Exclusion cell count, as described above (par. 2.3.2).

3.3.3 Fluorescence microscopy and cellular uptake of liposomes

A standardized protocol (par. 2.3.3) based on a rhodamine B fluorescent probe loaded into DOTAP/ToThyCholRu liposomes has been used to evaluate the uptake of ToThyCholRu/DOTAP in human MCF-7 cells and WiDr adenocarcinoma cells; this experiment was carried out at 100 μ M concentration and at incubation times of 30 min, 1, 3 and 6 h.

3.3.4 Light Microscopy

MCF-7, WiDr and HeLa cell lines were grown on standard sterile plastic 60 mm culture dishes by plating 5×10^5 cells. After reaching the subconfluence, cells were incubated for 48 h with 50 μ M concentration of ToThyCholRu/DOTAP liposomes under the same experimental conditions described above. Finally, cells were observed by a contrast-phase light microscope (Labovert microscope, Leitz). Microphotographs at $200 \times$ total magnification ($20 \times$ objective and $10 \times$ eyepiece) were taken with a standard VCR camera (Nikon).

3.3.5 DNA fragmentation assay

MCF-7, WiDr and HeLa cell lines were grown on standard sterile plastic 60 mm culture dishes by plating 5×10^5 cells. After 24 h of growth the cells were treated for 48 h with IC_{50} doses of ToThyCholRu/DOTAP liposomes, as well as with IC_{50} doses of cisplatin (*c*DDP) as positive control for *in vitro* induction of apoptosis. Then, the DNA was extracted and analyzed as previously described (2.3.6).

3.3.6. Statistical Analysis

All data were presented as mean \pm SEM. The statistical analysis was performed using Graph-Pad Prism (Graph-Pad software Inc., San Diego, CA) and ANOVA test for multiple comparisons was performed followed by Bonferroni's test.

3.4. RESULTS

[These data have been published: Vitiello G, Luchini A, D'Errico G, Santamaria R, **Capuozzo A**, Irace C, Montesarchio D, Paduano L. Cationic Liposomes as Efficient Nanocarriers for the Drug Delivery of an Anticancer Cholesterol-based Ruthenium Complex. *J. Mater. Chem. B* 2015, 3:3011-3023]

3.4.1 *In vitro* bioscreening for anticancer activity

The cytotoxic effects of ToThyChol/DOTAP were investigated on a selected panel of cancer and healthy cells. The antiproliferative activity was evaluated through the estimation of a “cell survival index”, arising from the combination of cell viability with cell counting. Data concerning the previously investigated ToThyCholRu/POPC system [Simeone et al., 2012] are included for comparison. The results (Fig. 37 and Table 2) show that ToThyCholRu/DOTAP has an interesting bioactivity pattern characterized by selective cytotoxicity against highly proliferative malignant cells. In fact, different human adenocarcinoma cells, such as MCF-7, WiDr and HeLa, are susceptible to the antiproliferative effects of this nanovector, while no significant cytotoxicity has been detected on normal human HaCaT keratinocytes and rat L6 muscle cells. The poor activity of ToThyCholRu/DOTAP on normal cells could be explained by the Clark's hypothesis of the activation of ruthenium (III) complex only in the reducing environment of cancer cells [Schluga et al. 2006; Clarke et al, 1999; Clarke et al.,1980]. Taking into account that ruthenium is incorporated in 30% in moles in the DOTAP liposomes under investigation, concentration-effects curves related to the actual ruthenium content highlight the antiproliferative activity of the ToThyCholRu/DOTAP system. We can synthesize the antiproliferative results on cancer cells with the following order: ToThyCholRu/DOTAP \geq cisplatin > ToThyCholRu/POPC > AziRu. Indeed in the changeover from ToThyCholRu/POPC to ToThyCholRu/DOTAP the potentiating factor (PF) values (Table 2) for ruthenium vectorization respect to the precursor molecule AziRu in MCF-7 and WiDr cells increases from 4.3 and 3.1 to 23.5 and 22.4, respectively. Thus in MCF-7 cells, the most responsive cells in these *in vitro* models, the same antiproliferative effect of the precursor complex AziRu is achieved in the case of ToThyCholRu in POPC, with a metal concentration 6-fold lower, and in the case of ToThyCholRu in DOTAP, with a metal concentration 10-fold lower. ToThyCholRu/DOTAP is more potent than cisplatin against

two of the three cancer cell lines tested (approximately 1.7 and 1.4-fold more effective on MCF-7 cells and WiDr, respectively), while HeLa cells rest more responsive to cisplatin. In line with the data obtained for ToThyRu/POPC and ToThyRu/DOTAP, discussed in the previous chapter, the calculated IC_{50} for ToThyChol/DOTAP are significantly lower than those related to the same nucleolipidic ruthenium (III) complex lodged in neutral POPC liposomes. This means that, under identical *in vitro* experimental conditions, the use of cationic DOTAP liposomes as nanocarrier for ToThyCholRu enhances its anticancer activity. It is also interesting to confront the IC_{50} values obtained by the cell survival index of ToThyCholRu/DOTAP (Table 2) with those showed in the previous chapter for ToThyRu/DOTAP (Table 1). In fact, we can note an increment of the antiproliferative activity in the transition from cholesterol-free to cholesterol-including cationic liposomes, that is more important again if we take into account that the amount of ruthenium in these liposomes is not the same, but 50% and 30% in moles respectively. The corresponding IC_{50} referring to the ruthenium concentration of ToThyCholRu/DOTAP and ToThyRu/DOTAP are 19 ± 8 (PF 16) versus 13 ± 2 (PF 23.5) on MCF-7 cells, 50 ± 11 (PF 9) versus 23 ± 8 (PF 22.4) on WiDr cells. Therefore, the inclusion of cholesterol improves effectively the antiproliferative effect of the ruthenium-based nanovectors, allowing to reducing the quote of active principle vehiculated to obtain the same activity, and thus minimizing the possible onset of side effects. The observed antiproliferative effects of ToThyCholRu/DOTAP on tumor cells show that the amphiphilic nature of this nanoaggregate, do not perturb, but also helps, the metal-induced biological effects.

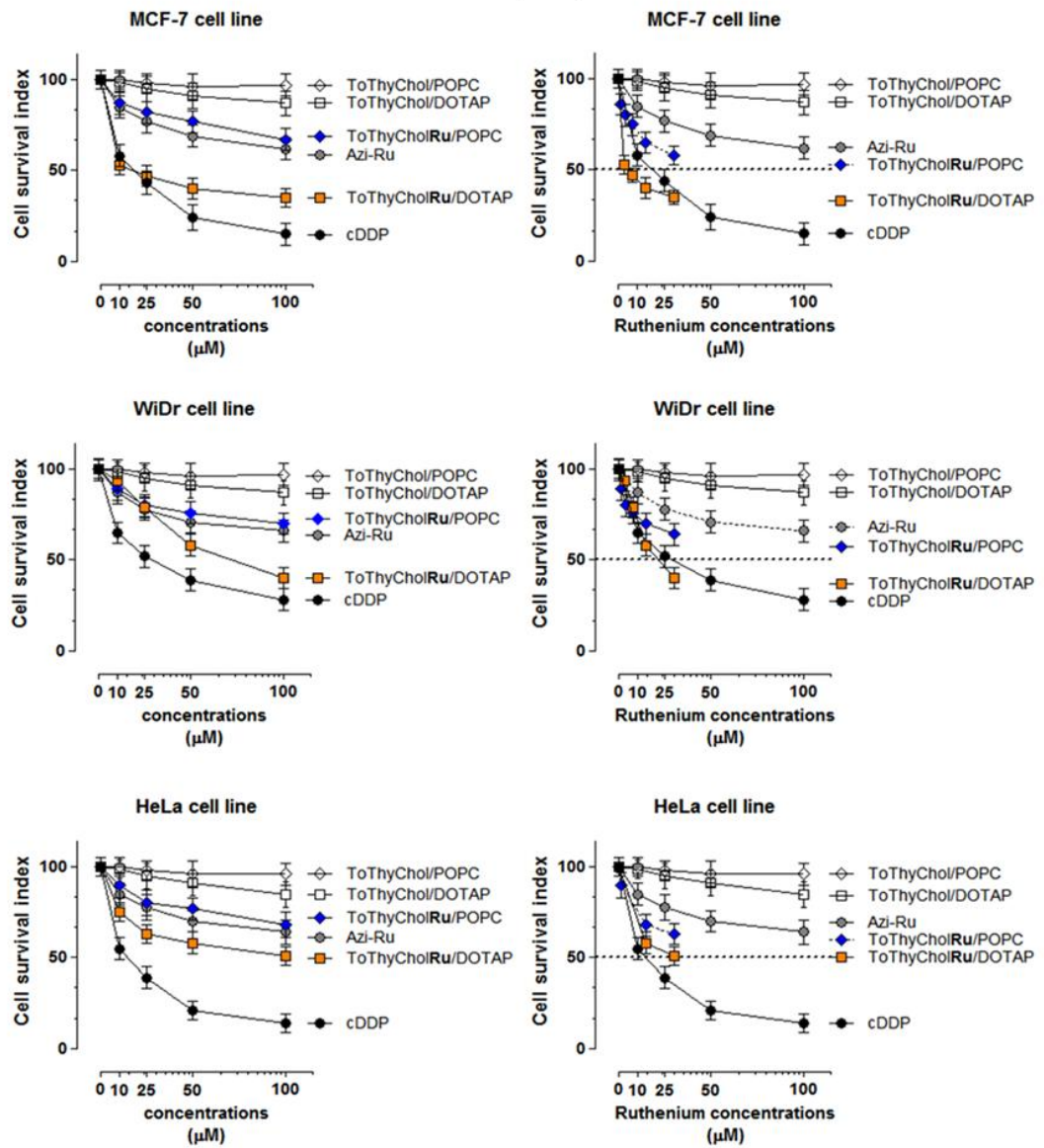


Fig.37. Cell survival index for MCF-7, WiDr, and HeLa cell lines following 48 h of incubation with the indicated concentration of AziRu and of the ruthenium-containing ToThyCholRu/DOTAP and ToThyCholRu/POPC liposomes, cDDP as positive control for cytotoxicity, the ruthenium-free ToThyChol/POPC and ToThyChol/DOTAP liposomes as negative controls. and the corresponding concentration-effect curves by normalizing for the actual ruthenium amount contained within ToThyCholRu/DOTAP and ToThyCholRu/POPC liposomes (on the right). Data are expressed as percentage of untreated control cells and are reported as mean of five independent experiments \pm SEM ($n = 30$).

Cell lines	cDDP	AziRu	ToThyCholRu POPC	ToThyCholRu DOTAP
MCF-7	22 ± 4	305 ± 16	70 ± 12 4.3	13 ± 2 23.5
WiDr	32 ± 5	515 ± 15	165 ± 10 3.1	23 ± 8 22.4
HeLa	12 ± 4	382 ± 19	105 3.6	34 ± 4 11.2
HaCaT	272 ± 7	> 500	> 500	377 ± 2.5
L6	52 ± 6	> 500	> 500	187 ± 1

Tab.2. IC₅₀ values, reported as mean ± SEM (n = 30) of five independent experiments; in bold, the potentiating factor (P.F.), calculated as the ratio of IC₅₀ values of ToThyCholRu/POPC and ToThyCholRu/DOTAP liposomes with respect to the IC₅₀ of AziRu.

3.4.2. Cellular uptake

The internalization and accumulation of the metal-based drugs into cancer cells is crucial for the therapeutic effect against tumors [Groessl et al., 2011]. In view of more detailed investigations on the interactions of the ruthenium-based nanovectors with the cells, we have analyzed their cellular internalization process. A standardized protocol based on a rhodamine B fluorescent probe loaded into DOTAP/ToThyCholRu liposomes has been used to evaluate their uptake in human carcinoma cells. In order to determine the relationship between the incubation times and the ToThyCholRu accumulation within the cells, the experiment was carried for 30 min, 1, 3 and 6 h on human MCF-7 breast and WiDr colorectal adenocarcinoma cells. In the microphotographs (fig. 38 and 39), the blue areas correspond to the cells nuclei specifically stained by DAPI, whereas the rhodamine (RHOD) associated fluorescence within cells is shown in green. Control experiments have been also performed by exposing the cells to the rhodamine B adduct alone, under the same *in vitro* experimental conditions used to evaluate the cellular uptake of ruthenium-containing liposomes. Merged images arise by overlapping fluorophores emission emerging from the same cell monolayers. The cationic ToThyCholRu/DOTAP liposome

rapidly interacts with the cells allowing a massive cellular uptake, even after 30 min. The rhodamine-dependent fluorescence emission is widespread in the cells and merged images show a strong fluorescence accumulation. Interesting, it is possible to identify a different kinetics of action on MCF-7 and WiDr cells; in fact, at 30' of incubation, the accumulated fluorescence seems depend on a high quantity of ToThyCholRu/DOTAP already internalized by the MCF-7 cells, whereas the more diffuse fluorescence at the same time of incubation in WiDr cells is a signal of a more bland interaction, that nevertheless rapidly increase over time. These observations could be correlated with the data about the cell viability, according to which the MCF-7 cells are the more sensitive to the nanovector, suggesting that the selectivity between different types of cancer cells may depend also on the capacity of the liposomes to interact with the cell membranes. In a process of cell internalization that probably occurs *via* membrane fusion and/or by endocytosis, the presence of a cholesterol motif within the amphiphilic structure decorating the ruthenium complex in ToThyCholRu, could further improve the liposome fusion with the plasma membrane, thus promoting nanocarriers accumulation in the cells. In addition to the amphiphilic properties of ToThyCholRu complex, the liposome membranes formed by the cationic lipid DOTAP allow the onset of charge attraction that could play an important role in promoting close contact with the negatively charged target membrane [Xiong et al., 2011].

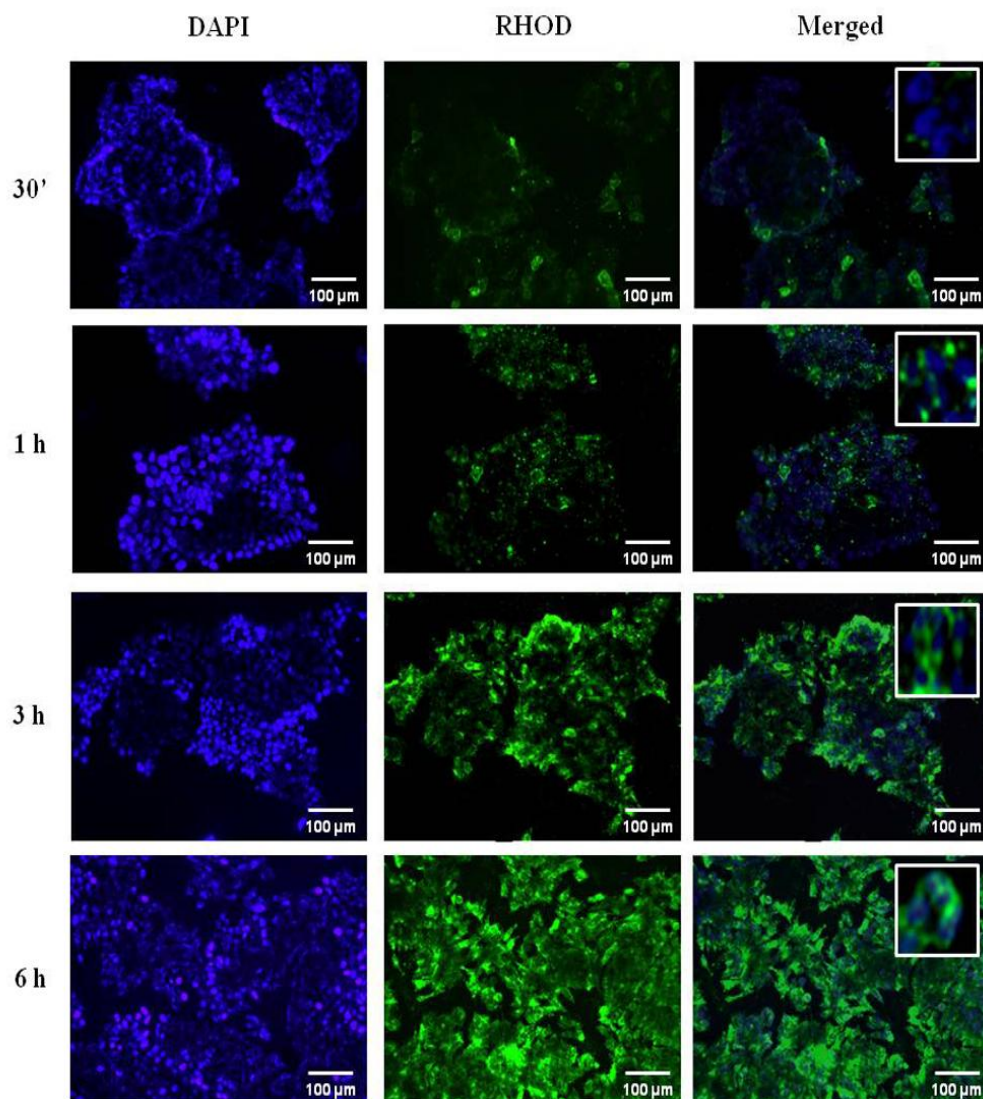


Fig. 38. Uptake of Rhodamine-labeled ToThyCholRu/DOTAP liposomes by human MCF-7 breast adenocarcinoma cells incubated for 30 min, 1, 3 and 6 h. The blue-fluorescent DAPI specifically stains the nuclei. The RHOD fluorescence was shown in green. In merged microphotographs (Merged), the two fluorescent patterns are overlapped. The shown images are representative of three independent experiments. 100× total magnification (10 × objective and a 10 × eyepiece).

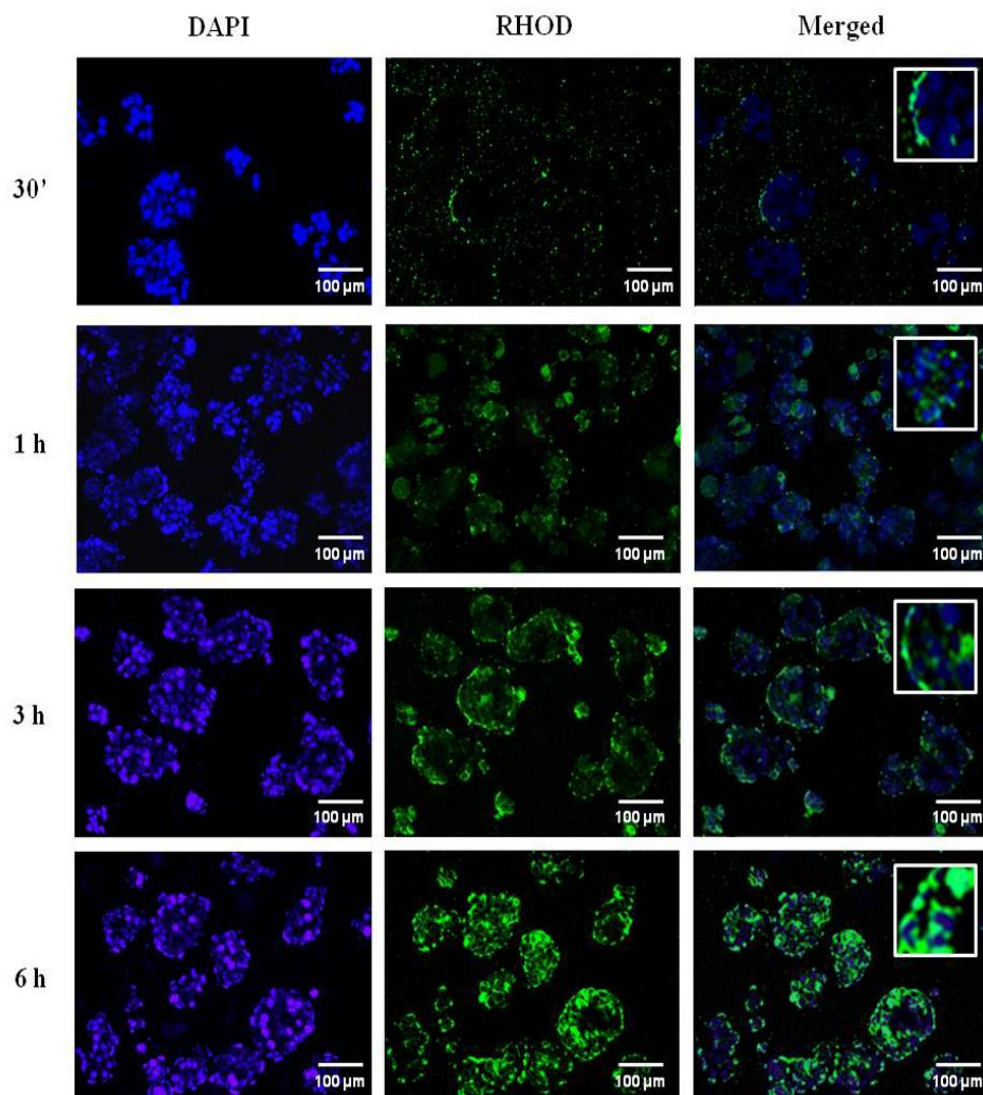


Fig. 39. Uptake of Rhodamine-labeled ToThyCholRu/DOTAP liposomes by human WiDr colorectal adenocarcinoma cells incubated for 30 min, 1, 3 and 6 h. The blue-fluorescent DAPI specifically stains the nuclei. The RHOD fluorescence was shown in green. In merged microphotographs (Merged), the two fluorescent patterns are overlapped. The shown images are representative of three independent experiments. 100× total magnification (10 × objective and a 10 × eyepiece).

3.4.3. Cellular morphological changes and DNA fragmentation

To further support the relationship between cell viability and ruthenium-induced cytotoxicity, subconfluent cultures of MCF-7, WiDr and HeLa cells have been analyzed by phase-contrast light microscopy for monitoring the dynamic morphological changes that occur during cell death induced by the treatment. In fact, following the *in vitro* exposure to ToThyCholRu/DOTAP, the cell monolayers clearly appear perturbed in their morphological architecture. In particular, the microphotographs (Fig. 40) show that the reduction in cell viability by ruthenium-based nanocarriers is associated with well detectable cytotoxic effects and characteristic morphologic hallmarks of apoptosis, such as membrane blebs and cell shrinkage at the start of apoptosis, and the formation of balloon-like structures, due to the loss of plasma membrane integrity, at the late state [Krysko, et al., 2008]. The rounding of the cells visibly increased after 48 h of incubation, with improvement of the surface blebbing and cell contraction. Since late events of apoptosis include nuclear pycnosis and DNA cleavage [Elmore., 2007], we also analyzed the DNA fragmentation by agarose gel electrophoresis. In Fig. 41 untreated cancer cells showed no detectable DNA fragmentation, whereas DNA extracted from cells after 48 h of incubation with IC_{50} doses of both ToThyCholRu/DOTAP and *c*DDP was extensively fragmented. Treatment of the cells with ToThyCholRu/DOTAP resulted in the appearance of the internucleosomal DNA laddering typical of cells undergoing apoptosis. As widely described in the previous chapter, MCF-7 cells not express the CASP-3 [Jänicke, 1998], even if the DNA fragmentation is similar to that induced *in vitro* by IC_{50} doses of *c*DDP, likely *via* caspase-3 activation [Okamura et al., 2004]. We can thus suppose that this fragmentation may correlate with the activation of different effector caspases, such as caspase-6 or -7 [Liang et al., 2001]. Although the implication of different processes of cell death cannot be excluded, these finding provide evidence of an apoptosis-inducing activity.

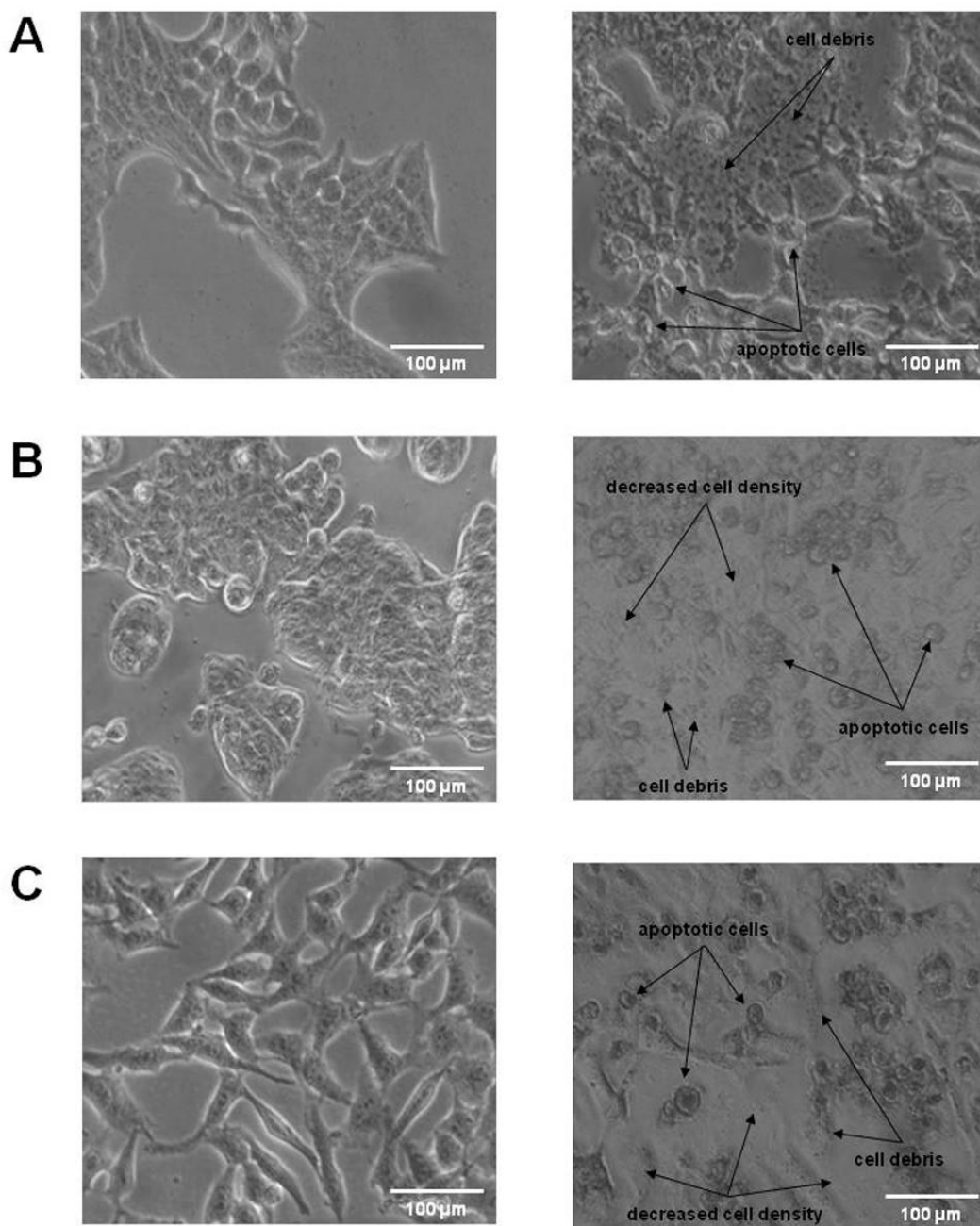


Fig. 40. Representative microphotographs at a $200\times$ magnification ($20\times$ objective and a $10\times$ eyepiece) by phase-contrast light microscopy of MCF-7 (panel A), WiDr (panel B) and HeLa (panel C) cell lines untreated (control cells, left column) or treated for 48 h with $50\ \mu\text{M}$ ToThyCholRu/DOTAP (right column), showing the morphological changes of cells and the cytotoxic effects on cellular monolayers. The shown images are representative of three independent experiments.

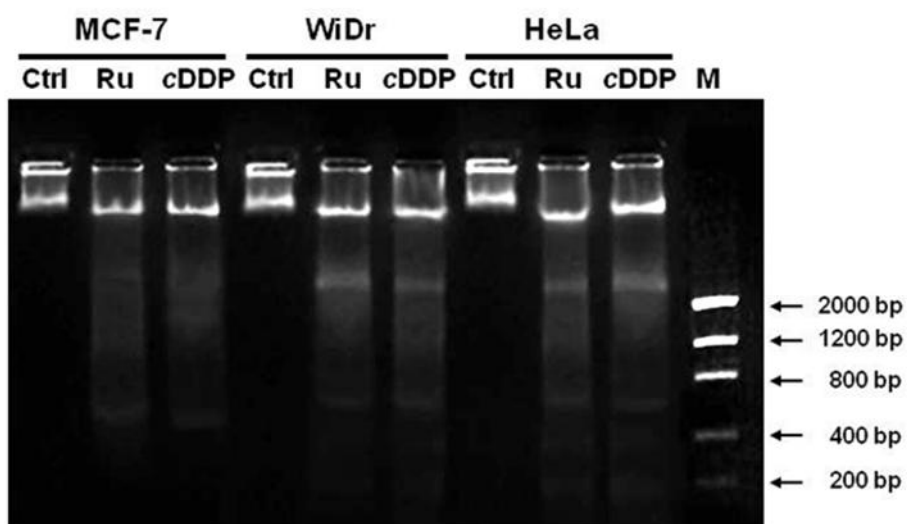


Fig. 41. DNA fragmentation assay on MCF-7, WiDr and HeLa cells, treated or not (Ctrl) for 48 h with IC_{50} doses (13, 23, and 34 μ M, respectively) of ToThyCholRu/DOTAP (Ru) or with IC_{50} doses (22, 32, and 12 μ M, respectively) of cDDP as positive control. Lane M corresponds to molecular weight markers. The agarose gel is representative of three independent experiments.

3.5. CONCLUSIONS

In order to develop stable and long-life anticancer ruthenium agents, the co-aggregation with biocompatible lipids represents an innovative strategy for their *in vivo* delivery. In particular, we tested the cholesterol-containing ruthenium complex, named ToThyCholRu, which is negatively charged and accommodated into the liposome bilayers formed by the cationic lipid DOTAP. Interestingly, ToThyCholRu/DOTAP liposome is stable for several months, ensuring the complete integrity of the active ruthenium complex in physiological environment. Moreover, the antiproliferative activity of ToThyCholRu/DOTAP is comparable to that of cisplatin, whereas this nanovector is less toxic on normal cells. Since most anticancer drugs lack of cancer specificity and cause side effects on normal tissues, ruthenium complexes may provide a more safe and at the same time effective alternative to common chemotherapeutic agents. In addition, in the transition from ToThyCholRu/POPC, as well as from ToThyRu/DOTAP, to ToThyCholRu/DOTAP considerable progresses have been achieved in term of drug delivery, due to the better interaction with the cells. The efficacy of ruthenium is thus improved by the cationic charge of the surface of liposome bilayer, but also specifically by the cholesterol inclusion, as direct consequence of an increased cellular uptake. In confirmation of these results, an efficient and fast liposomes accumulation in the cells has been detected. Thus, in addition to the important role played by the positive superficial charge of the aggregates, the steroid moiety of the nucleolipid complex inserted in the acyl chain region, could play an important role in the improving the nanovector, for its ability to regulate the physico-chemical properties of lipid bilayers, to stabilize liposomes and to modulate membrane trafficking by enhancing the liposome fusion with the plasma membrane. In conclusion, this study shows that the co-aggregation of nucleolipid ruthenium complexes with the cationic lipid DOTAP has a great potential for developing new ruthenium-based anticancer drug candidates. Particularly, ToThyCholRu/DOTAP has exhibited a remarkable cytotoxicity and selectivity toward cancer cells. These findings suggest a relevant specificity in the molecular interactions of ruthenium, in its active form, with the biological targets. Thus, further studies will be done *in vitro* and *in vivo*, in order to investigate the structure–activity relationship and the physiological implications of their antitumor activity.

**4. de-LOS-POPC-TothyRu:
an alternative liposome
inspired to the bacterial wall**



4.1 INTRODUCTION

4.1.1 Long-time circulation strategy for the new generation of liposomes

Many researches are focused on improving the drug delivery activity of the nanovectors, increasing their drug loading, targeting capability, and stability in physiological conditions, minimizing in parallel the toxic effects [Bozzuto and Molinari, 2015]. A common approach to obtain efficient drug delivery systems is based on the introduction of polyethylene glycol (PEG) into liposomal formulations [Vertut-Doi et al., 1996]. This hydrophilic polymer having a flexible chain that occupies the space immediately adjacent to the liposome surface, tends to exclude other macromolecules from this space, such as the serum proteins, and partially covers the aggregates in the blood, bypassing the control of the immune system, thus preventing opsonization and the subsequent macrophage uptake [Immordino et al., 2006]. The result of the use of PEG-vesicles is an increase of the liposomes lifetime under physiological conditions, which makes these systems suitable for *in vivo* applications. However, recent studies have shown several side effects associated with the use of PEGylated systems, including hypersensitivity, formation of toxic products, and accelerated blood clearance after several injections or, in other cases, phenomena of accumulation in the body [Knop et al., 2010]. Consequently, there is a growing interest on the research of alternative substances which, incorporated into liposomes as additives, are able to prolong the life span of the drug, but at the same time making stealth the system and showing less side effects.

4.1.2 The LOS inclusion into the liposome

Aiming at enhancing the efficacy of the second generation of drug delivery systems, we tested a new formulation functionalized with the lipooligosaccharide (LOS) derived from bacteria wall, instead of classical PEG decoration. LOS-liposomes can be produced in large amount by bacterial fermentation thus avoiding long and complicated synthetic procedures, and are bifunctional molecules with a carbohydrate epitope at one side, and the Lipid A moiety at the other, useful to easily incorporate the molecule in the liposome [De Castro et al., 2008; D'Errico et al., 2010; D'Errico et al., 2009]. The LOS and the lipopolysaccharide (LPS) are the principal components of the outer membrane of Gram-negative bacteria, responsible for the integrity and the stability of the bacterial architecture.

LPS consists of the lipid A, the outer and the inner core, and the O-antigen. The O-antigen is exposed on the bacterial surface, allowing the recognition by specific antibody. In this context, the usage of the LOS, lacking of the O-antigen, avoids the acquired immunity. On the other hand, the lipid A moiety, consisting of a glucosamine disaccharide decorated with several long chain fatty acids and two phosphate units is known as a PAMP (Pathogen Associated Molecular Pattern) agent and recognized by receptors of the innate immune system that in response to this binding activate the inflammation process [Molinaro et al., 2015]. However, depending on the bacterial origin, the number and length of the fatty acids of the Lipid A as well as of the kind of sugars forming the core can differ, and can give diverse inflammatory properties. Thus, an appropriate choice of the bacteria species from which the LOS are extracted, joined to a variety of possible chemical modifications to made on the Lipid A structure can significantly reduce, and even eradicate, the response of the immune system. In our case, we tested the LOS extracted by *Rhizobium rubi* (Fig.42), in which the de-*O*-acylation of the lipid A was introduced in order to ensure the liposome stability and to avoid the recognition by the immune system, so that a prolonged circulation in blood can be predict. In addition, this specific LOS presents interesting features: literature data indicate that it has poor inflammatory properties [Vandenplas ML et al., 2002] and it presents within the core region the Lewis B oligosaccharide, a human epitope which should give stealth properties to the liposome, and thus prolonged life span by molecular mimicry of host structures, similarly to the strategy exploited by *Helicobacter pylori* during the infective process [Moran AP,2008].

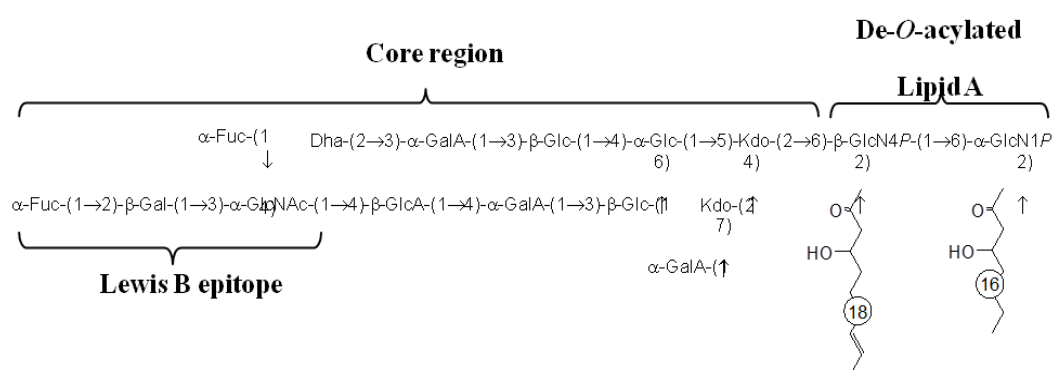


Fig.42. Molecular structure of de-LOS from *Rhizobium rubi*.

This liposome has been prepared by co-formulating the nucleolipid-based Ru (III) complex ToThyRu with the zwitterionic lipid POPC containing *de-O*-acylated LOS (*de*-LOS) in the proportion 10:80:5 (Fig. 43). A detailed physico-chemical characterization has been carried out by means of different experimental techniques, including Dynamic Light Scattering (DLS), Small Angle Neutron Scattering (SANS), and Electron Paramagnetic Resonance (EPR) and has confirmed that insertion of *de*-LOS in the formulation leads to stable multi-layered aggregates.

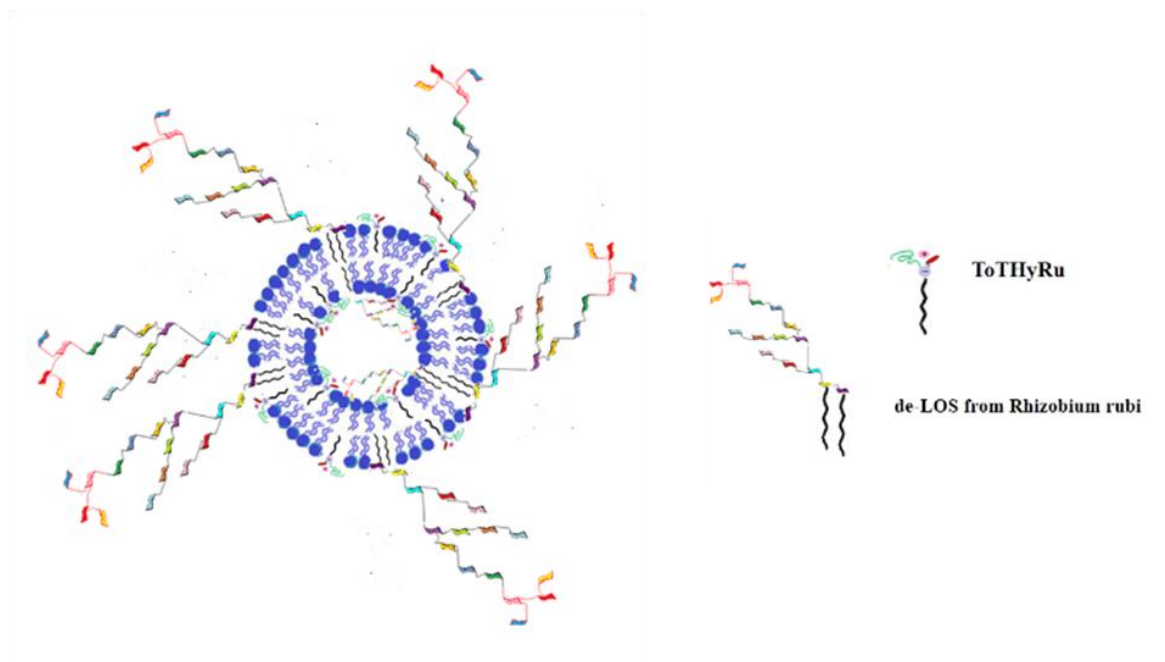


Fig.43. Simplified representation of the *de*-LOS-liposome

4.2 AIM

We tested a neutral liposome functionalized with the lipooligosaccharide extracted from the bacteria *R. rubi*, in order to mimic the bacterial cell wall, and at the same time, by *ad hoc* modification (de-Oacylation), avoiding the activation of inflammatory response. To better elucidate the role played by de-*O*-acylated LOS in the liposome activity, biological investigations were performed, in order to evaluate the effect of ToThyRu/POPC/de-LOS on three different cellular models:

- 1) The human breast adenocarcinoma cell line MCF-7, to assess its anticancer efficacy
- 2) The normal cell line of human keratinocytes HaCaT, to investigate the cytotoxic effect
- 3) The murine monocyte/macrophages J774 to predict the immune innate response and thus verify their capacity to be a stealth system

Thus the first goal was to verify the effective biocompatibility of *de*-LOS-containing nanovectors, ensuring the theoretical safety of these nanoaggregates towards biostructures, as important prerequisite for their possible *in vivo* use, as well as the efficacy of ToThyRu/*de*-LOS on the cancer cells. Then, to investigate the cellular uptake, experiments of fluorescence microscopy were performed. Finally the absence of immune responses was ascertained by determination of nitric oxide production and Western Blot analysis of the inducible form of nitric oxide synthase (iNOS).

4.3. MATERIALS AND METHODS

4.3.1. Cell cultures

Experiments were carried out on human HaCaT keratinocytes cells (CLS service), human MCF-7 breast adenocarcinoma cells and murine J774 monocyte/macrophage cell line (ATCC). HaCaT and J774 cells were grown in Dulbecco's modified Eagle's medium (DMEM, Invitrogen, Paisley, UK) containing high glucose (4.5 g/l), while MCF-7 cells were grown in RPMI 1640 medium (Invitrogen, Paisley, UK). Media were supplemented with 10% fetal bovine serum (FBS, Cambrex, Verviers, Belgium), L-glutamine (2 mM, Sigma), penicillin (100 units/ml, Sigma) and streptomycin (100 mg/ml, Sigma). All the cells were cultured in a humidified 5% carbon dioxide atmosphere at 37 °C.

4.3.2. *In vitro* bioscreens for cell survival

Each cell line was treated with a range of concentrations (10→100 μM) of AziRu and ToThyRu lodged in POPC liposomes functionalized or not with *de*-LOS (ToThyRu/POPC and ToThyRu/POPC/*de*-LOS, respectively). Using the same experimental procedure, cell cultures were also incubated with the ruthenium-free ToThy/POPC and ToThy/POPC/*de*-LOS liposomes as negative controls, as well as with cisplatin (*c*DDP) like positive control for cytotoxic effects. The bioactivity was investigated by the cell viability evaluation and the cell counting, as described above (par. 2.3.2).

4.3.3. Cellular uptake by fluorescence microscopy

The cells were treated for 3 and 6 h with 100 μM of *de*-LOS liposomes containing a fluorescent rhodamine B derivative. The procedure for the fluorescent microscopy experiment is illustrated in the chapter 2 (par. 2.3.3).

4.3.4. Macrophage activation and nitric oxide production

J774 monocyte/macrophage cells were plated in 96-well cell culture microplate at density of 10^4 cells/well and allowed to adhere for 24 h at 37 °C. The medium was replaced with fresh medium and cells were treated for 24 h with a range of concentrations (10-100 μM) of POPC/*de*-LOS liposomes and of ToThyRu/POPC/*de*-LOS, as well as with 1 and 10 $\mu\text{g/ml}$ of LPS from *Salmonella typhosa* used as positive control for macrophage activation and nitric oxide production. *In vitro* integrated nitric oxide production was estimated by determining the concentration of nitrite and nitrate end-products. The measurement of nitrate/nitrite concentration or of total nitrate and nitrite concentration (NO_x) is routinely used as an index of NO production. In particular, to evaluate the total nitrite release in the culture medium, 100 μl of Griess reagent (0.1% naphthylethylenediamide dihydrochloride in H₂O and 1% sulphanilamide in 5% concentrated H₂PO₄) were added to 100 μl medium of each sample. Nitrite concentration was calculated by comparison of OD₅₅₀ samples with sodium nitrite standard solution OD₅₅₀. The optical density at 550 nm (OD₅₅₀) was measured using a microplate reader (iMark microplate reader, Bio-Rad).

4.3.5. Western blot analysis of iNOS expression

After 24 h of treatment with (10-100 μ M) of ToThy/POPC-de-LOS and ToThyRu/POPC-de-LOS, J774 cells were collected, washed, and resuspended in the buffer containing 10 mM Tris-HCl, pH 7.6, 50 mM NaCl, 1% Triton X-100, and protease inhibitor cocktail (Roche Diagnostics, Mannheim, Germany). Cell debris were pelleted by centrifugation at 4 °C for 20 min at 14,000 \times g, and protein concentration of cell lysate was determined by the Bio-Rad protein assay (Bio-Rad). 50 μ g of proteins were separated on a 8% SDS-polyacrylamide gel and electrotransferred onto a nitrocellulose membrane (Amersham Biosciences) using a Bio-Rad Transblot (Bio-Rad). Immunodetection was performed using a primary rabbit antibody iNOS (Calbiochem, San Diego, CA) with appropriate secondary antibody and detected by chemiluminescence. Tubulin antibody was used to normalize the results.

4.3.6. Statistical Analysis

All data were presented as mean \pm SEM. The statistical analysis was performed using Graph-Pad Prism (Graph-Pad software Inc., San Diego, CA) and ANOVA test for multiple comparisons was performed followed by Bonferroni's test.

4.4. RESULTS

4.4.1. Anticancer activity

As showed in figure 44A, *in vitro* bioscreens were performed in order to explore the bioactivity of zwitterionic POPC liposomes incorporating both ToThyRu and *de*-LOS. Notably, the related IC₅₀ values (Table 3) for the LOS derivative ruthenium-free are higher than 10³ μM for all the examined cell populations, suggestive of the absence of antiproliferative effects and of virtually null cytotoxicity; this result make possible the potential use of this nanovector as biocompatible system for the drug delivery. On the other hand, ToThyRu/POPC/*de*-LOS has shown cytotoxicity against highly proliferative malignant cells. Human MCF-7 adenocarcinoma cells undergo remarkable antiproliferative effects following incubation with POPC liposomes incorporating both the ruthenium-based nucleolipidic complex ToThyRu and *de*-LOS. Taking into account that the actual ruthenium concentration in this nanosystem is only the 10 %, these results indicate an *in vitro* cytotoxic activity similar to that of cisplatin, but at the same time the nanovectorial system can significantly contribute to reduce the side effects associated with chemotherapy. Aiming at investigating the cellular internalization processes, a standardized protocol, based on a rhodamine B fluorescent probe loaded into ToThyRu/POPC/*de*-LOS liposomes at 2% mol, was used. The microphotographs (Fig. 44B) show a strong fluorescence accumulation following the treatment with the liposomes in the cancer cells, confirming the ability of this system to act as nanocarrier for ToThyRu.

4.4.2. Effect on healthy cells

Very interestingly, no significant cytotoxicity has been detected on the human HaCaT keratinocytes treated with ToThyRu/POPC/*de*-LOS, showing approximately the same cell survival index of the liposomes ruthenium-free (Fig. 45A and Table 3). On the other hand, its uptake in these cells should not be overlooked. In fact, the microphotographs in figure 45B demonstrate that a discrete quote of fluorescence is accumulated inside the cells, in a similar way to that showed for the cancer cellular uptake, suggesting that the nanovector, by mechanism of adsorption and/or fusion with the cell membranes, is internalized in the keratinocytes. Therefore, the comparison between the cellular uptake and the lack of bioactivity, gives important information about the *in vitro* pharmacodynamics of the

ruthenium complex; in fact, although delivered in the normal cells as in the cancer cells, it doesn't explicate the same cytotoxic effect. This result provides further evidences of an *in situ* activation mechanism for Ru-complexes, specifically operative in the cancer cells microenvironment, in accordance with the assumption that Ru (II) complexes are generally more reactive than Ru (III) complexes, which substantially act as inactive pro-drug, and that exclusively the chemically reducing environment of cancerous cells would allow the ruthenium reduction [Schluga et al. 2006; Clarke et al, 1999; Clarke et al.,1980]. However, the evaluation of ruthenium-based complexes effects on healthy control cell cultures needs further study, focusing mainly on the understanding the molecular basis of this different response to the drug.

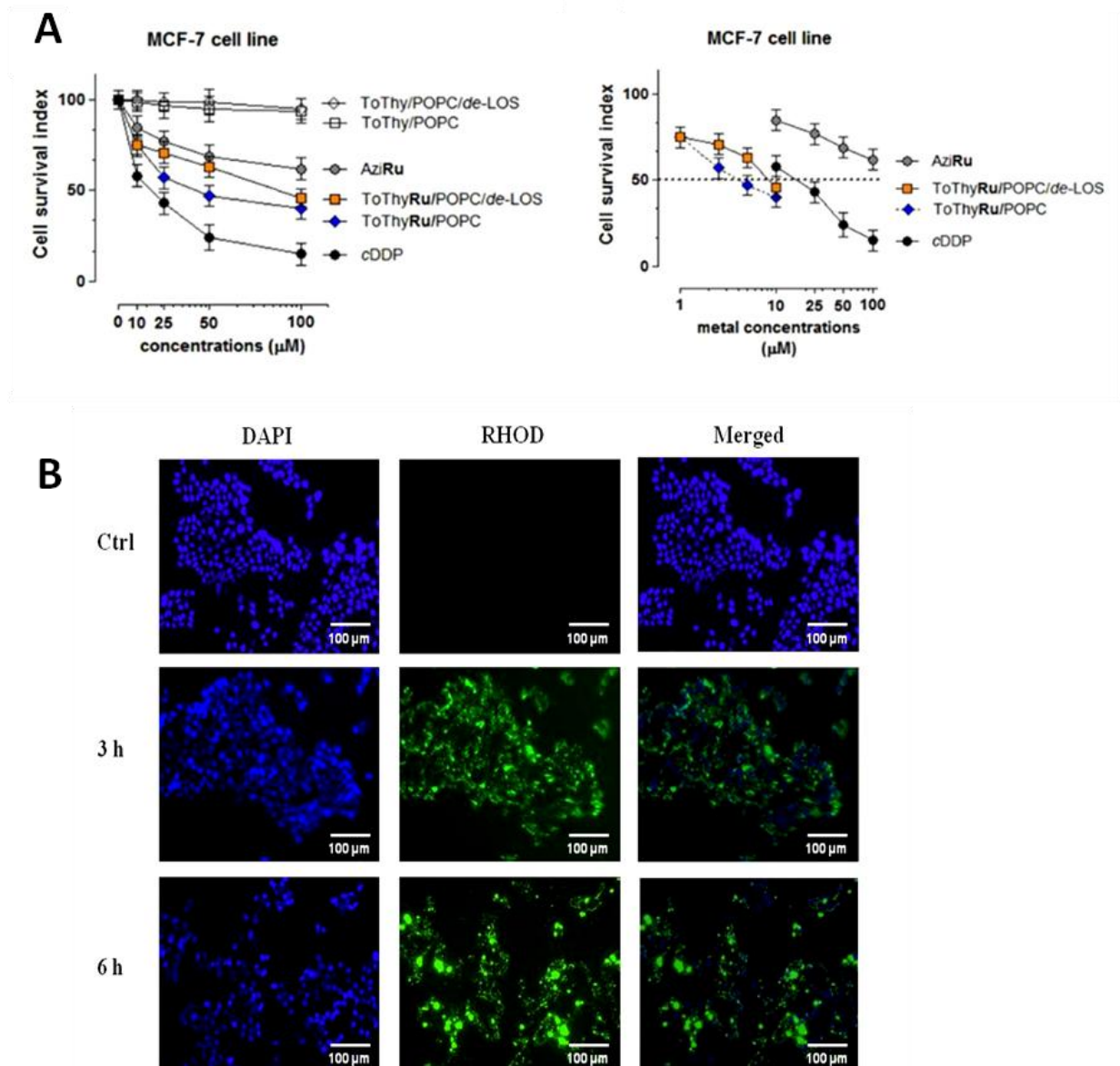


Fig. 44. MCF-7 cell lines. **A.** Cell survival index following 48 h of incubation with the indicated concentration of AziRu, Cisplatin (cDDP), the ruthenium-free (ToThy/POPC, ToThy/POPC/de-LOS) and ruthenium-containing (ToThyRu/POPC, ToThyRu/POPC/de-LOS) liposomes. On the right, the corresponding concentration-effect curves by normalizing for the actual ruthenium amount (in logarithmic scale) contained within the liposomes. **B.** Uptake of the Rhodamine B-labeled ToThyRu/POPC/de-LOS liposomes (shown in green) after 3 and 6 h of treatment. The blue fluorescence of DAPI specifically stains the nuclei. In merged microphotographs the two fluorescent patterns are overlapped. The images are representative of three independent experiments.

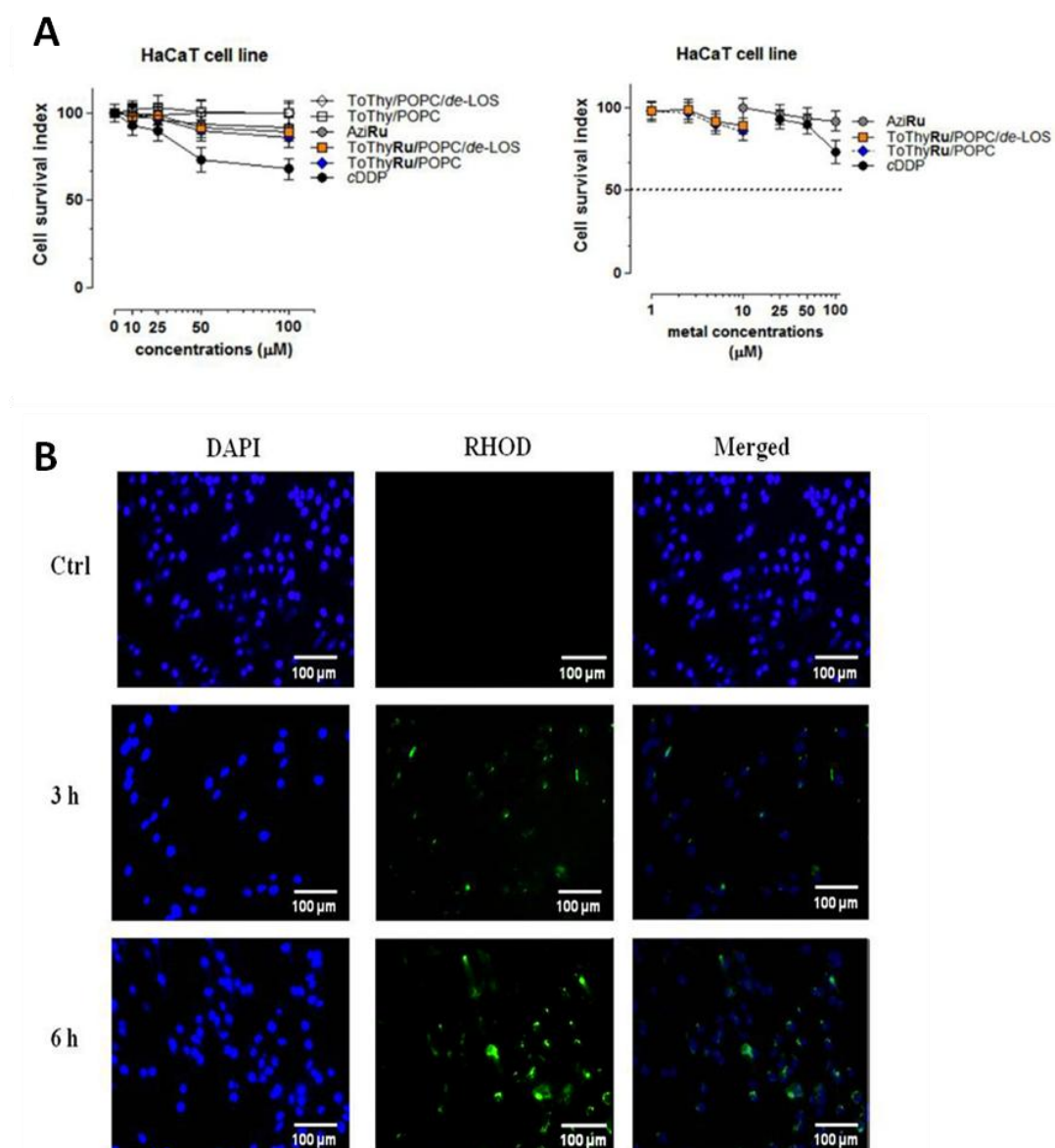


Fig. 45. HaCaT cell lines. **A.** Cell survival index following 48 h of incubation with the indicated concentration of AziRu, Cisplatin (cDDP), the ruthenium-free (ToThy/POPC, ToThy/POPC/de-LOS) and ruthenium-containing (ToThyRu/POPC, ToThyRu/POPC/de-LOS) liposomes. On the right, the corresponding concentration-effect curves by normalizing for the actual ruthenium amount (in logarithmic scale) contained within the liposomes. **B.** Uptake of the Rhodamine B-labeled ToThyRu/POPC/de-LOS liposomes (shown in green) after 3 and 6 h of treatment. The blue fluorescence of DAPI specifically stains the nuclei. In merged microphotographs the two fluorescent patterns are overlapped. The images are representative of three independent experiments.

4.4.3. Macrophage response to de-LOS liposomes

Macrophages, involved at all stages of immune response, are a central component of the host defence system and the detection of nitric oxide (NO \cdot) produced by activated phagocytes *in vitro* represents a good method to estimate the antigenic ability of functionalized liposomes [Bogdan et al., 2015]. In the biological environment, the nitric oxide is rapidly oxidized to nitrite and/or nitrate by oxygen, so that nitric oxide production can be estimated by determining the concentration of nitrite or nitrate end-products [Pacher et al., 2007]. Due to their multitasking aptitude, the murine J774 macrophage-like cell lines are a well-established *in vitro* model system in cell biology and immunology [Lam et al., 2009]. As shown in Figure 46A, the stimulation of J774 macrophages by bacterial lipopolysaccharide (LPS from *Salmonella typhosa*, 1 and 10 $\mu\text{g/ml}$ for 24 h) visibly results in a marked increase of NO production (6.5 ± 1.3 and $9.7 \pm 1.03 \mu\text{M}/10^4$ cells, respectively), compared with control cultures ($0.02 \pm 0.3 \mu\text{M}/10^4$ cells). In the same experimental conditions, *in vitro* macrophages treatment with POPC/*de*-LOS liposomes, and with ToThyRu/POPC/*de*-LOS liposomes does not induce significant NO production at all the tested concentrations. Activated murine macrophages produce large amounts of NO from L-arginine *via* induction of the inducible form of nitric oxide synthase (iNOS), a highly regulated enzyme [Hillaireau et al., 2009]. According to nitrite determination, Western blot analysis of iNOS (Fig. 46B) shows that LPS stimulation significantly induces iNOS expression, whereas no protein induction following macrophages exposure to LOS-decorated liposomes is detected. It is interesting to highlight that the experiments on the cellular uptake, showed in Figure 47B, reveal a low level of internalized *de*-LOS-decorated liposomes in this cell line, although no evidence of macrophages activation response effects were observed. Therefore, it is likely that *de*-LOS-containing liposomes interact with macrophages by a passive process, such as cell fusion and/or adsorption as well as for the other cell lines, without stimulating the surface receptors involved in macrophages activation. This scenario does not change in the presence of the liposome-entrapped ruthenium complex. The cell survival index (Fig. 47A) demonstrates that this "passive uptake" doesn't lead to a cytotoxic effect, according with the absence of significant bioactivity by Ru (III) complexes in the keratinocytes and thus remarking the possibility of the ruthenium activation specifically in cancer cells. Therefore, the tested

ToThyRu/POPC/de-LOS does not interfere with *in vitro* macrophages activation as well as with the cell viability.

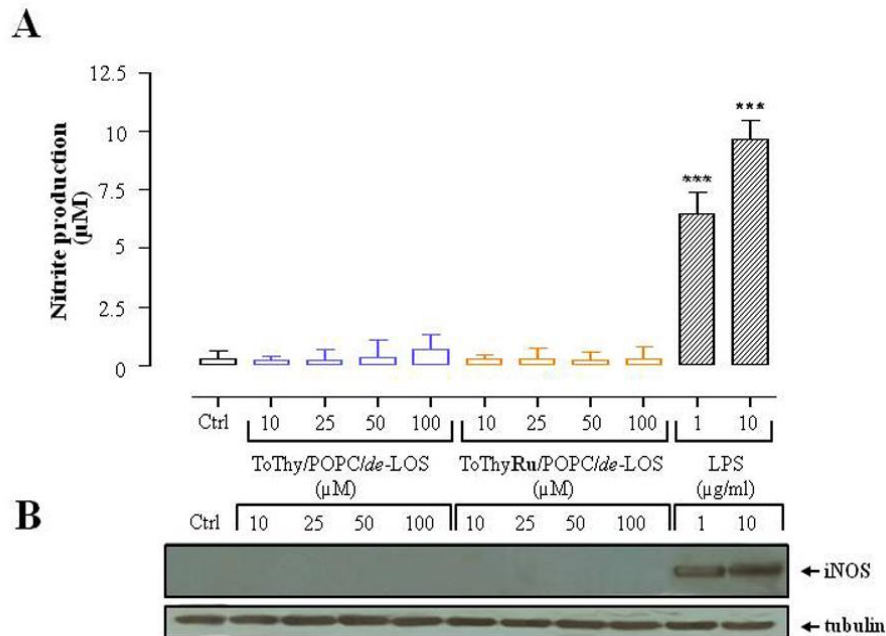


Fig.46. (A) Effect of the indicated concentrations of ToThy/POPC/de-LOS and of ToThyRu/POPC/de-LOS functionalized liposomes on nitric oxide production in J774 cells evaluated by means of nitrite determination following 24 h of exposition to liposomes. J774 cells were stimulated for 24 h with LPS (1 and 10 µg/ml) as positive controls. Data are expressed as µM of nitrite/million viable cells and are plotted in a bar graph as mean ± SEM (n = 15) of three independent experiments. *** p<0.001 vs unstimulated macrophages. (B) Effect of the indicated concentrations of ToThy/POPC/de-LOS and of ToThyRu/POPC/de-LOS functionalized liposomes on iNOS protein expression in J774 macrophages evaluated by Western blot analysis. Data normalization was provided by LPS-stimulation (1 and 10 µg/ml for 24 h) and tubulin levels.

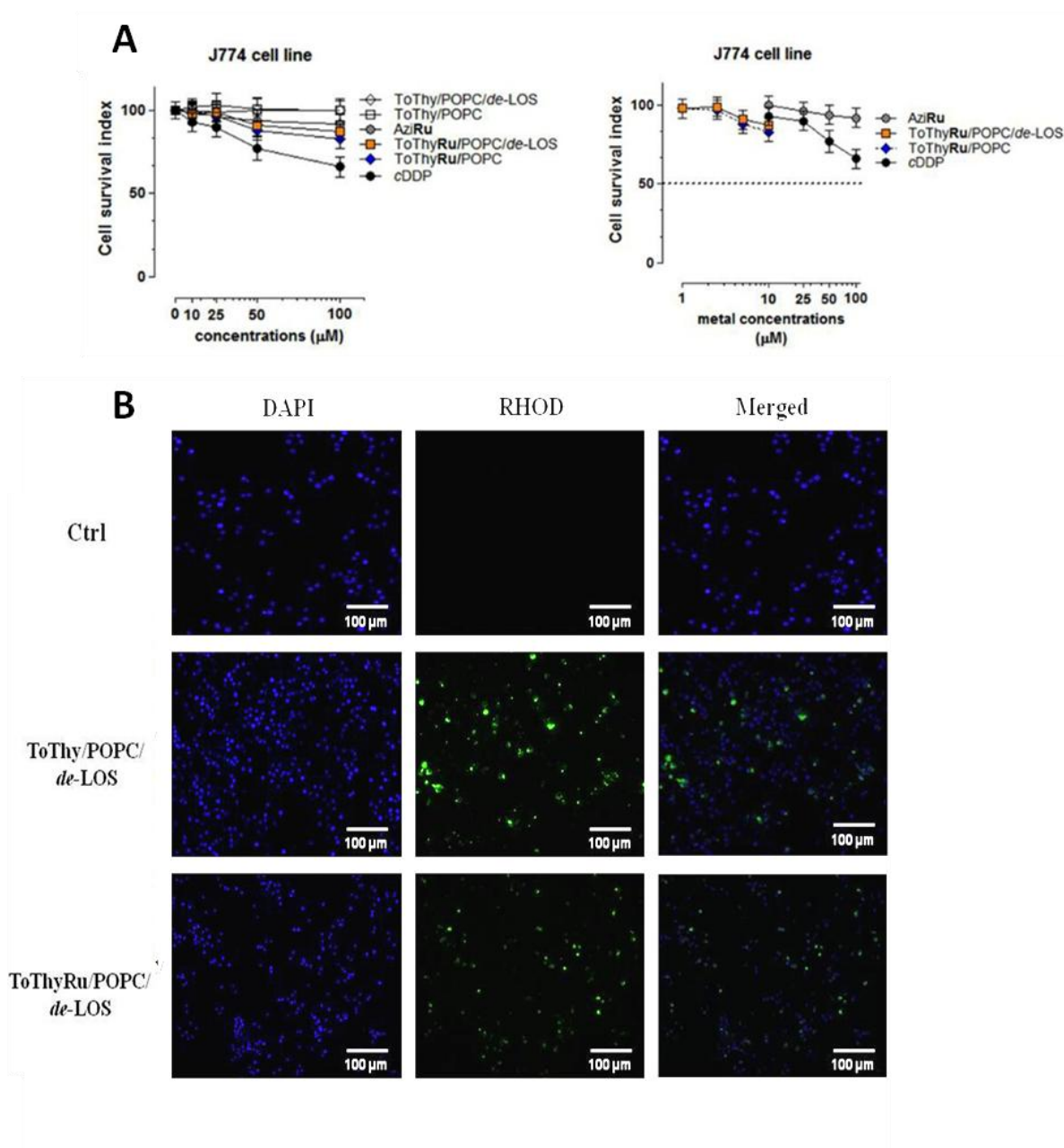


Fig. 47. J774 cell lines. **A.** Cell survival index following 48 h of incubation with the indicated concentration of AziRu, Cisplatin (cDDP), the ruthenium-free (ToThy/POPC, ToThy/POPC/de-LOS) and ruthenium-containing (ToThyRu/POPC, ToThyRu/POPC/de-LOS) liposomes. On the right, the corresponding concentration-effect curves by normalizing for the actual ruthenium amount (in logarithmic scale) contained within the liposomes. **B.** Uptake of the Rhodamine B-labeled ToThyRu/POPC/de-LOS liposomes (shown in green) after 3 and 6 h of treatment. The blue fluorescence of DAPI specifically stains the nuclei. In merged microphotographs the two fluorescent patterns are overlapped. The images are representative of three independent experiments.

4.5. CONCLUSIONS

In vitro bioscreenings to test the effect of ruthenium-based de-LOS liposome, have shown its selective cytotoxicity against human adenocarcinoma cells as well as extremely low toxicity for healthy cells. Also, the induction of cell stress in monocytes/macrophages and the subsequent analysis of NO production revealed the absence of significant NO production for both ToThyRu/POPC/*de*-LOS and ToThy/POPC/*de*-LOS formulations, indicating that no *in vitro* immune response is activated by this treatment, despite a cellular uptake process.

Thus, we have demonstrated that the combination of the anticancer agent ToThyRu with a mixture of POPC and *de*-LOS lead to a liposomal formulation provided with:

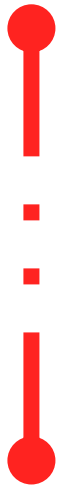
- i) marked and selective anticancer activity, due to the presence of a properly functionalized amphiphilic Ru(III) complex
- ii) affinity for the human lipid cell membrane, due to the POPC self-assembly
- iii) no immune system stimulation, due to the capacity to act as a stealth system

Taken together, these results demonstrate that, in the development of efficient nanocarriers for drug delivery, the here described supramolecular system, is a functional and biocompatible nanovector, efficient in the transport of an amphiphilic anticancer Ru(III) complex, but in principle useful for the *in vivo* delivery of a large variety of lipophilic drugs, that could enhance their life span in the blood.

	cDDP	AziRu	ToThyRu/POPC	ToThy/POPC/ de-LOS	ToThyRu/POPC/ de-LOS
MCF-7	22 ± 4	305 ± 16	9 ± 4	>10 ³	15 ± 6
HaCaT	272 ± 7	>500	>500	>10 ³	>500
J774	240 ± 8	>500	>500	>10 ³	>500

Table 3. Summary table of all the IC₅₀ values (μM) arising from the cell survival index of MCF-7, HaCaT and J774 cells, following 48 h-incubation of treatments. The effective metal concentrations within the ruthenium-containing aggregates were considered. IC₅₀ values are reported as mean ± SEM (n = 30) of five independent experiments.

**5. RDCs and ODCs: the role of
epigenetic changes in their
mechanism of action**



5.1. INTRODUCTION

5.1.1. Ruthenium derived compounds (RDCs): state of the art

RDC constitutes a family of cycloruthenated compounds, of which RDC11 ([ruthenium[phenanthroline][κ -C,N-[2-phenyl-pyridine][NCMe]₂]PF₆) is one of the best exponents, proving to be a good alternative to platinum compounds (Fig.48). In fact, it showed high antiproliferative effect (IC₅₀ between 1-5 μ M) on multiple cancer cell lines, including also cells and human primary ovarian tumors that are resistant to Cisplatin [Gaiddon et al., 2005]. It inhibits also the growth of various tumors implanted in mice, including mouse syngeneic models (melanoma, lung cancer) and human xenografted models (glioma and ovarian cancer). In addition, unlike platinum compounds, RDCs do not cause severe side effects to the liver, kidneys, the neuronal sensory system or blood cells [Meng et al., 2009]. RDCs accumulate in nucleus, endoplasmic reticulum and mitochondria. Studies using drugs that block the active transport or various types of carriers indicate that a portion of RDCs enter the cells through an active mechanisms, in a concentration-dependent way and using several types of transporters [Klajner et al., 2014]. However, each component of RDC family showed a specific cytotoxic profile and different mechanism of action, suggesting that changes on the ligands in their structure modify their anticancer spectra of activity, because of different redox potential and ability to interact with DNA and other different macromolecules [Bergamo et al., 2012]. In the case of RDC11, only a bland interaction with DNA was found [Klajner et al., 2010], indicating that alternative targets are involved in their anti-tumor activity. Interestingly, RDC11 induces p53-independent apoptosis [Gaiddon et al., 2005] but exerts its cytotoxicity through Endoplasmic Reticulum (ER) stress pathways. In particular, previous studies showed the activation of some gene-keys in the ER stress, like Bip, XBP1, PDI, and CHOP [Meng et al., 2009]. Activation of the transcription factor CHOP leads to the expression of several target genes, among which also the pro-apoptotic gene CHAC1 (Fig.49). However, both pathways, p53-independent apoptosis and ER stress, could not enough to explain all the biological effects of RDC11. Finally, structure-activity studies have indicated that RDCs' cytotoxicity is at least partially associated with their redox potential and the production of reactive oxygen species [Vidimar et al., 2012].

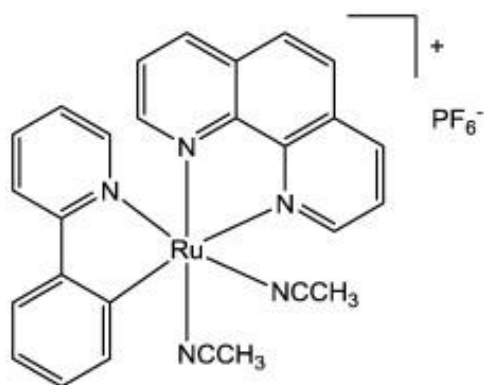
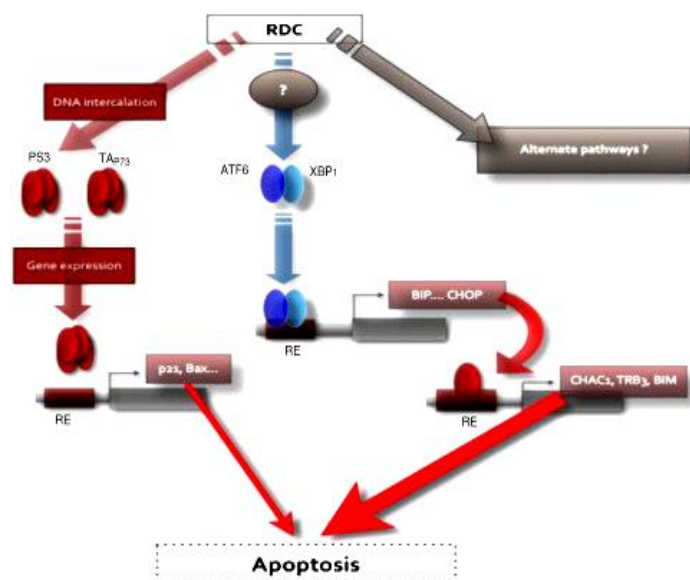


Fig. 48. Chemical structure of RDC11



Bergamo et al., Journal of Inorganic Biochemistry, 2012 106:90–99

Fig. 49. Proposed hypothesis on the mode of action of RDC11 on cancer cells. Abbreviations: ATF6 = Activating Transcription Factor 6; BiP: = binding immunoglobulin protein; BIM: = BH-3 (Bcl-2 homology domain-3) only protein; CHAC1 = cation transport regulator-like protein 1; CHOP = C/EBP homologous protein; RE = Response Element; TAp73 = transactivating p73; Trb3 = mammalian homolog of *Drosophila* tribbles; XBP1 = X-box binding protein 1.

5.1.2 Osmium derived compounds (ODCs)

Recently, on the model of RDCs, a library of Cyclometalated Osmium (II) compounds were designed [Ryabov et al., 2003; Boff et al., 2013]. In figure 50, the structure of some of these ODC compounds of particular interest are reported; i) ODC2 that has the structure identical of RDC11 (the only difference is the metal change) serves as a model along with RDC11 at addressing the role of the metal in the cytotoxic activity; ii) ODC16 and ODC20 that present a particular high cytotoxicity on the 60 cancer cell line of the National Cancer Institute and represent the second generation of ODC distinguished by having tri-dentate ligands, that could significantly change the scenario of interaction with macromolecules and cellular targets, as well as their uptake. ODCs have shown good *in vitro* cytotoxic profile, also in a cellular line of glioblastoma [Boff et al., 2013], that represents nowadays one of the most refractory tumors [Theeler et al., 2015]. As in the case of the cycloruthenate derivatives, these compounds showed a different activity in relation to the structure and the relative redox potential; in particular, it seems that the compounds which are more reactive to substitution reactions of a ligand, are less cytotoxic, suggesting that the most probable active species are those in which the coordination area of the metal is not modified before entering in the cells [Boff et al., 2013]. However, at the present there is no information about ODCs mechanism of action, even if the importance of their redox potential suggests that the mechanism involved in the tumor cell death could be, as reported for RDCs [Vidimar et al., 2012], a strong modification of the cellular metabolism, trough several interaction with different oxido-reductase enzymes.

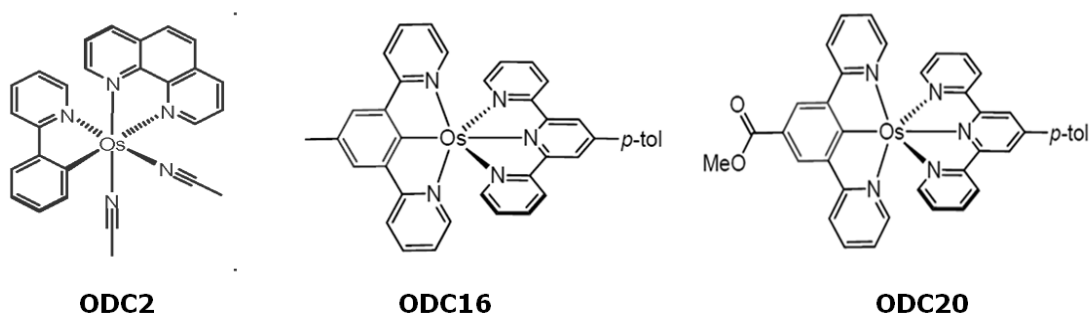


Fig. 50 Structure of some compounds of the ODC series (ODC2, ODC16, ODC20)

5.1.3. Epigenetic role in the mechanism of action of metal-based compounds

Since there is a lack in the comprehension of the metal-based complexes' mechanism of action, many efforts have been done in attempting to identify possible direct targets. In fact, several of these compounds, among which also RDC11, are not as good as platinum drugs to form stable DNA adducts [Klajner et al., 2010]. Nevertheless, they showed high cytotoxicity, suggesting the possibility of other targets as key players in the implementation of their antiproliferative effects. Also, the evaluation of the naked DNA binding "*in vitro*" would exclude all the physiological implications, like the ligand-exchange kinetics and the binding with other molecules, as well as the interactions with the protein forming the chromatin, such as the histones [Davey GE and CA., 2008]. For example, the ruthenium containing drug RAPTA-C has been shown to interact with nucleosome core particle (NCP) by making adducts with the histones [Wu et al., 2011]. Interesting, it was found that RAPTA-C is more able to form adducts with histones than with the naked DNA, unlike another ruthenium-cymene compound, RAED-C, for which the binding balance is shifted toward the DNA, proving how the ligand substitutions are crucial for the ruthenium compounds interactions [Adhireksan et al., 2014]. Moreover, the ruthenium complex KP1019 showed a specific binding to the histone H3 [Singh et al., 2014], that would evict histones from chromatin and provoke its destabilization. These events could finally promote a secondary binding with the DNA, making it more accessible, as hypothesized for oxaliplatin [Soori, 2015]. H3 is the unique histone that contains one or two cysteine (Cys) residues, highly conserved in the evolution; this aminoacid containing sulphhydryl group, could make H3 as a "sensor" of redox state, very susceptible to oxidation [Garrard et al., 1977; Wood et al., 2006]. In the contest of metal-based agents having different redox potentials and that explicate their mechanism of action partially by ROS production, H3 could represent the weakest link of chromatin, leading to chromatin disorganization.

The possibility of ruthenium binding with histones is also supported by the identification of their specific sequences that can bind transition metals (Fig.51), such as Ni(II), Cu(II), Zn(II), Co(II). These sequences are the "C-tails" of H2A and H2B [Bal et al., 2000; Nunes et al., 2010], probably followed by their hydrolysis [Bal et al., 2000], the "N-Tail" of H4 [Midorikawa et al., 2005; Zoroddu et al., 2010] in which the sites of acetylation are clustered, and in the cys-including motif of the H3 core [Bal et al., 1995].

<p>Histone H2A.1</p> <p>10 20 30 40 50 MSGRGKGGK ARAKAKTRSS RAGLQFPVGR VHRLLRKGNY AERVGAGAPV 60 70 80 90 100 YLAAVLEYLT AEILELAGNA ARDNKKTRII PRHLQLAIRN DEELNLLGK 110 120 130 VTIAQGGVLP NIQAVLLPKK / TESHKAKGK</p>	<p>Histone H3.1</p> <p>10 20 30 40 50 MARTKQTARK STGGKAPRKQ LATKAARKSA PATGGVKKPH RYRPGTVALR 60 70 80 90 100 EIRRYQKSTE LLIRKLPFQR LVREIAQDFK TDLRFQSSAV MALQEACEAY 110 120 130 LVGLFEDTNL CAIH AKRVTI MPKDIQLARR IRGERA</p>
<p>Histone H2B.1A</p> <p>10 20 30 40 50 MPEVSSKGAT ISKGGFKKAV VKTQKKEGKK RKRTKESYS IYIYKVLKQV 60 70 80 90 100 HPDTGISSKA MSIMNSFVTD IFERIASEAS RLAHYSKRST ISSREQTAV 110 120 RLLLPGELAK HAVSEGTAV TKYTSSK</p>	<p>Histone H4</p> <p>10 20 30 40 50 MSGRGKGGK LGKGGAKRHR KVLRDNIQGI TKPAIRRLAR RGGVKRISGL 60 70 80 90 100 IYEETRGVLK VFLENVIRDA VTYTEHAKRK TVTAMDVVYA LKRQGRTLYG FGG</p>

Fig. 51. H2A.1, H2B.1A, H3.1, H4 sequences, in which the putative metal binding sites are highlighted. For H2A.1, the more probable point of hydrolysis subsequent to the binding is signed.

As widely described above (par. 1.1.3.2.), the role of epigenetic changes in drug response is often attributed to their post-translational modifications, whose the most known are methylation, phosphorylation and acetylation [Kouzarides, 2007]. Also, the use of HDAC inhibitor has a synergic effect with platinum chemotherapy [Zhang et al., 2015] and can overcome the chemoresistance [Kumar et al., 2015]. All together, these evidences provide convincing considerations about the implication of the complex epigenetic machinery in the transition metals mechanism of action.

5.2 AIM

While it is well established that the principal mechanism of platinum compounds is the DNA damage due to its direct binding and subsequent activation of apoptosis [Siddik, 2003], it's not yet clear the activity of the complexes based on other transition metals. Some evidences showed a bland binding of RDC11 with DNA, which is not enough to explain its antiproliferative effects *in vitro* and *in vivo*, also higher than cisplatin. Moreover, the chromatin binding could involve not only the DNA, but also the protein components, such as the histones, that are very important for the chromatin organization and for the regulation of gene expression [Zhang et al., 2015]. Also, histones epigenetic modifications have proved essential for the mechanism of action of some anticancer drugs. In view of giving new information about the mode of action of metal-based compounds, our objective is to elucidate the role of histones as possible targets, and more in general of the epigenetic changes involved in their activity. In particular, this study is focused on the evaluation of:

- i) early DNA damage
- ii) direct interaction with histones
- iii) changes in histones expression and/or in their localization, due to the direct binding or to secondary processes subsequent i.e. to the oxidative stress
- iv) histones post-translational modifications

Thus, Comet Assay was performed to analyze the DNA breaks, while electrophoresis of the purified histones treated with the compounds was carried out to see the difference on the migration of the monomers and their multiples, as well as to detect the presence of fragments. Western blot analysis were performed to investigate the histones expression and H3 acetylation, as well as to evaluate their different localization by means of two kinds of protein extraction buffer (NP-40, RIPA). Also, the analysis of caspase-3 activated fragments were conducted in order to considerate the results in the light of apoptotic cell levels. In addition, to correlate the data with the oxidative stress induced by the metal compounds, some experiments were carried out using the pre-treatment with the antioxidant agent N-acetylcystein.

5.3 MATERIALS AND METHODS

5.3.1 Cell viability

The antiproliferative effects of metal-based compounds were investigated by MTT assay on two cancer cell lines: the colorectal carcinoma HCT116 and gastric adenocarcinoma MKN45 cells. The cells were washed with PBS buffer solution (Sigma), collected by trypsin (Sigma) and then inoculated in a 96-microwell culture plates at density of 10^4 cells/well. Cells were allowed to grow for 24 h, then the medium was replaced with fresh medium and cells were treated for further 48 h with a range of concentrations (0.25→50 μ M) of cisplatin, oxaliplatin, RDC11, ODC2, ODC16 and ODC20. The MTT assay was performed as described above (par. 2.3.2) and the absorbance was monitored at 560 nm by using TriStar² LB 942 Multimode Microplate reader (Berthold Technologies GmbH & Co. KG Bad Wildbad, Germany). The calculation of the concentration required to inhibit the cell viability by 50% and 75% (IC_{50} and IC_{75}) is based on plots of data carried (eight points per concentration, repeated three times). IC_{50} and IC_{75} values were obtained using a dose-response curve by nonlinear regression using a curve fitting program, GraphPad Prism 5.0, and are expressed as mean \pm SEM.

5.3.2. Comet Assay

The comet assay is a simple way for detecting DNA breaks. Cells are embedded in agarose, lysed, and subjected to electrophoresis; DNA containing breaks is attracted to the anode, forming a comet like image when viewed by fluorescence microscopy. Briefly, HCT116 cells were plated in 6 well plates (300.000 cells/well) one day before exposure. Semi-confluent cultures were exposed for 1 h with 10 and 25 μ M of metal-based compounds. To detect the role of the oxidative stress induced by metal-based compounds in the DNA damage, cells were pre-treated with 2 mM solution of the antioxidant N-acetylcysteine (NAC) for 30 min. Hydrogen peroxide (H_2O_2) at 1 mM of concentration for 10 minutes, is used as positive control of the oxidative DNA damage. The Comet assay was performed under neutral conditions [Boutet-Robinet et al., 2013]. Briefly, the cells were collected in 1x PBS and 500 μ L of each sample is mixed with 500 μ L of 1% low-melting-point agarose gel. The agarose was pipetted onto slides previously coated with 1% agarose. Slides were stored in the dark for 10 min before adding in pre-chilled lysis buffer

(2.5M NaCl, 100 mM EDTA, 10 mM Tris-HCl, 1% N-lauroylsarcosine) for 1 h. The slides were washed three times for five minutes with the electrophoresis buffer (300 mM NaOAc, 100 mM Tris HCl, pH 8.3). Gel electrophoresis was performed at 20 V and 65 mA for 25 min. The Comet slides were washed three times for 5 minutes with 0.4 M Tris-HCl solution (pH 7.5) and air-dried over night at room temperature. 1 mL of a solution 2 µg/mL of ethidium bromide was placed to each slide. The slides were then analyzed with a fluorescence microscope (Zeiss fluorescence microscope with ApoTome attachment-Axio Zoom V.16, ZEISS, Germany). A total of 45 cells/sample were scored to determine the average percentage of DNA damaged.

5.3.3. Peptides binding

Solutions containing 3.5 µM of human recombinant H2A, H2B and H3.1 proteins (New England Biolabs, UK) and 0.05, 0.1, or 0.25 mM RDC11, ODC2, ODC16 and ODC20 in PBS, were incubated at 37°C for 1, 6, 24, 48 h in the dark. The aliquots were then resolved in non-reducing 14% sodium dodecyl sulfate-polyacrylamide gels, for 90 min at constant voltage (125 V) and visualized by Silver staining (Silver Stain PLus Kit, Bio-Rad, Marnes-la-Coquette, France).

5.3.4. Western Blot analysis

MKN45 cells were treated with the IC₅₀ and IC₇₅ concentration of metal-based compounds for 6, 24, 48, 72 h. In some experiments, the pre-treatment with NAC (2 mM for 30') was carried out in order to detect the impact of the oxidative stress inducted by the compounds in the histones expression. To extract the proteins, RIPA buffer (150 mM sodium chloride, 1.0% NP-40, 0.5% sodium deoxycholate, 0.1% SDS 50 mM Tris, pH 8.0, 1x protease inhibitor cocktail-Roche Diagnostics, Mannheim, Germany) was preferred for the nuclear fraction, whereas for the whole extract NP40 buffer (150 mM sodium chloride, 1.0% NP-40, 50 mM Tris, pH 8.0, 1x protease inhibitor cocktail-Roche Diagnostics, Mannheim, Germany) was used. Debris was pelleted by centrifugation for 20 min at 14,000 x g at 4 °C, and protein concentration of cell lysate was determined using Bio-Rad D_c Protein Reagents. Aliquots of 40 µg of each sample were electrophoretically separated by non-

reducing sodium dodecyl sulfate-polyacrylamide gel (SDS-PAGE) 12 % and transferred to the nitrocellulose membrane. After blocking for 1 h at room temperature in 5% milk in Tris-Buffered Saline and Tween 20 (TBS-T), membranes were incubated with the antibody for H2A and H2B histones (Santa Cruz Biotechnology Inc., Texas, USA.), acetyl-K9-H3 (Abcam, Paris, France), H3 histone and cleaved caspase-3 (Asp175) (Cell Signaling, Beverly, MA, USA). Membranes were then washed 3x with TBS-T before being incubated with appropriate horseradish peroxidase conjugated secondary antibodies.

5.3.5. Protein immunoprecipitation

For the immunoprecipitation, 100 µg of protein extracts were diluted in RIPA buffer and incubated at 4 °C overnight with 2 µg/ml of H2A or H2B antibody (Santa Cruz Biotechnology Inc., Texas, USA). After incubation, 30 µl of protein A-Agarose (Sigma) were added to the reaction mixture and rotated for 1 h at 4 °C. Moreover, as negative control, purified rabbit IgG (Sigma) was mixed with the protein A. Immunoprecipitates were collected, by centrifuging at 500 x g for 5 min, and washed with the RIPA buffer three times. All proteins that adhered to the protein A beads were separated by mixing with 30 µL of Laemmli buffer 2X and boiling the beads for 5 min. Samples were then centrifuged at 5000 x g for 1 min to pellet the agarose beads, and supernatants were analyzed by 12 % SDS-polyacrylamide gel electrophoresis and electrophoretically transferred to the nitrocellulose membrane. After blocking for 1 h at room temperature in 5% milk in Tris-Buffered Saline and Tween 20 (TBS-T), membranes were incubated with the antibody corresponding to the histones H2A and H2B immunoprecipitated.

5.3.6. Statistical analysis

All data were presented as mean \pm SEM. The statistical analysis was performed using Graph-Pad Prism (Graph-Pad software Inc., San Diego, CA) and ANOVA test for multiple comparisons was performed followed by Bonferroni's test.

5.4 RESULTS

5.4.1. Impact of organometallic compounds on cell viability

The cytotoxic effect of metal-based compounds was investigated on the colorectal carcinoma HCT116 and the gastric adenocarcinoma MKN45 cell lines. The gastric cancer is the fourth most common cancer and the second most common cause of cancer death worldwide and more than 90% of gastric cancers are adenocarcinomas [Correa et al., 2004]. It is considered one of the most difficult tumours to treat because of their frequency to show an innate or acquire multidrug resistance [Zhang et al., 2010; Hutchinson, 2012]. Since the tumours with low grade of differentiation are more aggressive [Jögi et al., 2012], the poorly differentiated MKN45 cells [Izuishi et al., 2000] can represent a good *in vitro* model to test the efficacy of organometallic compounds. The analysis of the dose-response curve obtained by MTT assay and the corresponding IC₅₀ and IC₇₅ values, showed remarkable antiproliferative effects with RDC11 and ODC2, also greater than that induced by platinum-based compounds (Fig.52 and table 4). In particular, cisplatin showed highest concentrations to inhibit the cell populations of 50% or 75%. As expected, MKN45 are in general less sensitive, but mostly on platinum compounds, whereas the effect produced by organometallics is noteworthy. The different structure of ODC16-ODC20 is responsible of a very high toxicity on both cell lines, so that the concentrations to inhibit of 50% the cell populations is in the nanomolar range; this pronounced difference in the cell viability confirms the importance of the structure-relationships in the activity of metal based complexes.

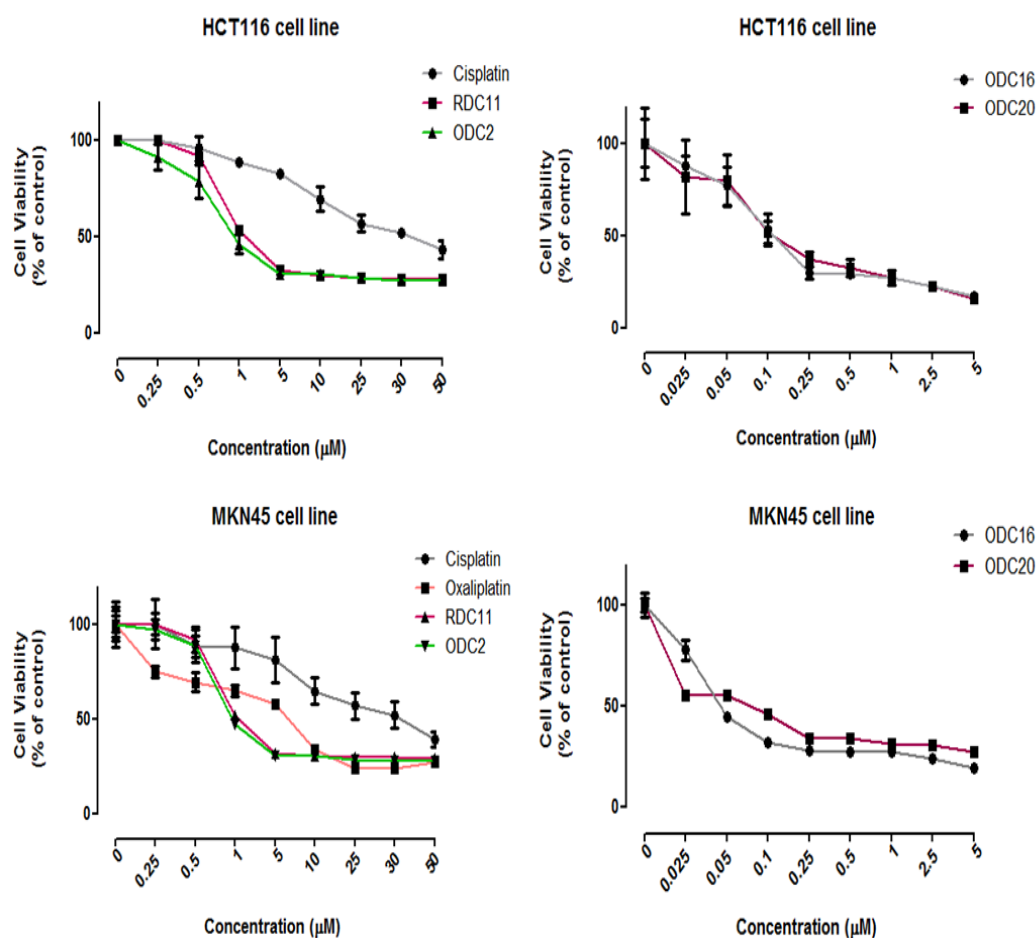


Fig. 52. Cell viability assay. Dose-response curves of HCT116 and MKN45 cell lines treated for 48 h with Cisplatin, Oxaliplatin, RDC11, ODC2, ODC16 and ODC20 at the indicated concentrations

IC50 IC75(µM)	Cisplatin	Oxaliplatin	RDC11	ODC2	ODC16	ODC20
HCT116	33.25 ± 0.06	—	1.0 ± 0.1	1.3 ± 0.05	0.16 ± 0.1	0.2 ± 0.07
	56.82 ± 0.06		2.8 ± 0.1	3.6 ± 0.05	0.8 ± 0.1	1.2 ± 0.07
MKN45	31.2 ± 0.7	4.6 ± 0.8	3.8 ± 0.7	1.8 ± 0.8	0.07 ± 0.04	0.09 ± 0.1
	164.6 ± 0.07	41.03 ± 0.08	23.5 ± 0.7	20.77 ± 0.8	0.8 ± 0.04	4.2 ± 0.1

Tab. 4. IC₅₀ and IC₇₅ values (µM ± SEM) in the indicated cell lines following 48 h of treatment with metal-based compounds

5.4.2. DNA damage induced by organometallic compounds

To better elucidate the effect of metal complexes on DNA damage, we analyzed its degradation by Comet Assay. This test, based on the higher electrophoretic mobility of the negatively charged DNA breaks [Olive and Banáth, 2006], allows detecting the immediate and direct impact on DNA *in vivo*, before the fragmentation due to the activation of apoptosis pathways. Thus, HCT116 colorectal carcinoma cells were treated for 1 h with 10 or 25 μM of RDC11, ODC2, ODC16, ODC20. As shown in the microphotographs (Fig.53), a significant dose-dependent increment of DNA breaks occurs after treatment with RDC11 and ODC2. Interesting, when the cells are pre-treated with the antioxidant NAC, the damage is partially reverted. This means that in the early events leading to the DNA damage during treatment with organometallics the induction of oxidative stress is also involved, even if only in part. In particular, it can be estimated that the oxidative DNA damage represents about the 40% for RDC11 and 30% for ODC2 of the total DNA damage. On the other hand, ODC16 induces no significant DNA damage, whereas ODC20 provokes just a little percentage of fragmentation. The lack of DNA damage, found also changing the parameters of the treatment, such as the time of incubation and/or the concentrations, seems to be in contrast with the high cytotoxicity that these compounds have proved by the viability assay. Nevertheless, the atypical activity of the ODC16 and ODC20 may depend mainly on a different profile of ligand-substitution reaction, cellular uptake and macromolecules affinity; for this reason, they need further investigation to individuate the basis of their high antiproliferative effect.

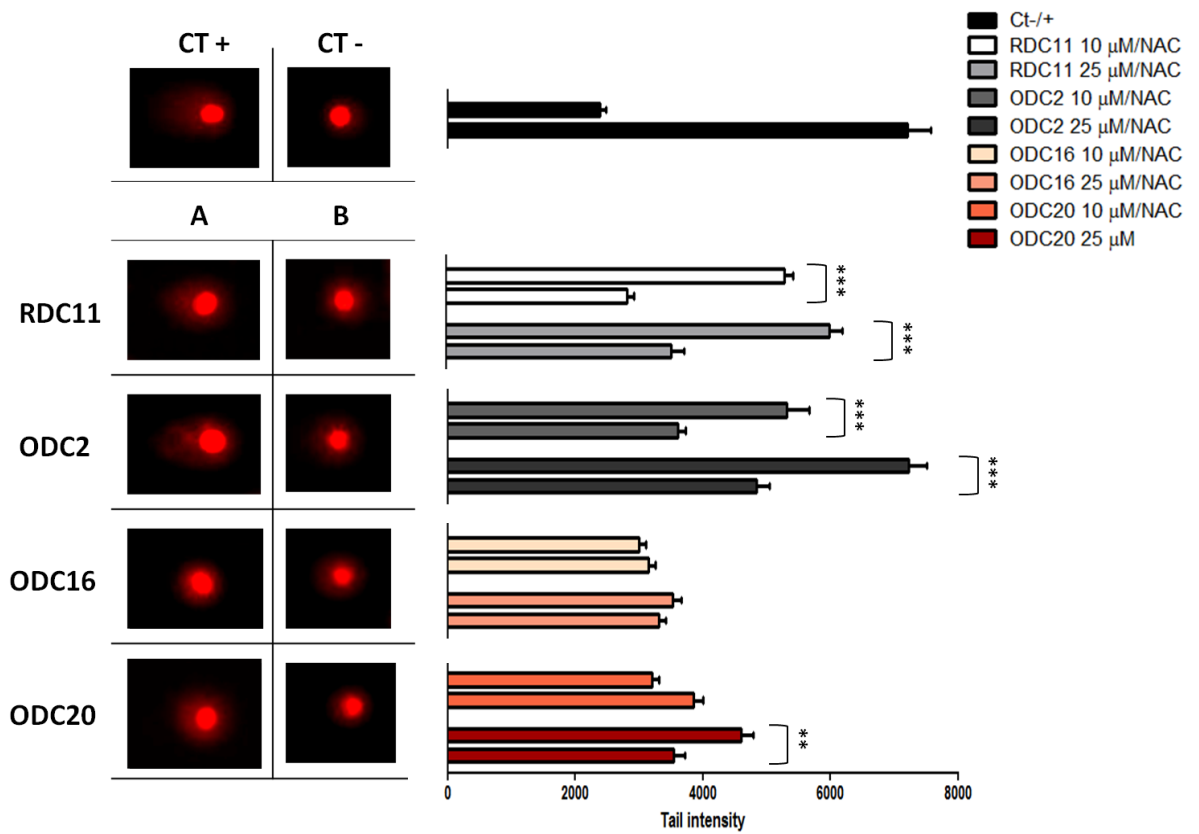


Fig. 53. Comet assay on HCT116 cells. Representative microphotographs of cells untreated (CT-), treated with positive control H₂O₂ (CT+), treated with RDC11, ODC2, ODC16, ODC20 without (A) or with (B) NAC and statistical analysis referred to an average of 40 cells per conditions.

5.4.3. Binding of organometallic compounds to histones

Data in literature showed the importance of chromatin reorganization in the drug response activation [Jiang and Pugh, 2009], as well as the possibility of protein targets in the chromatin [Wu et al., 2011; Singh et al., 2014]. In addition, it is reported that there is specific sequence in the histones capable of binding the metals [Nunes et al., 2010; Bal et al., 2000; Midorikawa et al., 2005; Zoroddu et al., 2010; Bal et al., 1995].

Here we reported the *in vitro* binding of the peptides H2A, H2B and H3 with different concentration (0.05, 0.1, 0.25 mM) of RDC11, ODC2, ODC16, ODC20 for 1, 6, 24 or 48 h. In general, the treated histones migrate slower and with a more diffuse pattern, suggesting the presence of higher molecular weight proteins, due to the interaction with the organometallics. Also a shift in the height of monomers is visible, suggesting that the excess of histones remaining in monomeric form is bound to the metals. At 48 h of treatment of H2A with RDC11, it is clear the formation of dimers and trimers, while with ODC2, the trimers are less (Fig.54). Moreover, if on one hand the polymerization of H2A increases in a dose-dependent way, on the other hand the polymerization of H2B decreases with the higher concentration of treatments, especially with RDC11, proving a faster kinetics of action that finally could lead in histone degradations (Fig.54). In fact, by performing a time-course RDC11 treatment of H2B at shorter time (1, 6, 24 h), this histone showed a linear increase of polymerization over time and dose-dependent (Fig.55).

In the case of H3, the time-course showed a shift in the migrations of the treated monomers, the fastest kinetics of polymerization with a presumably subsequent massive degradation and, unlike H2A and H2B, a marked polymerization in the control (Fig.55). Being H3 the only histone with sulphhydryl groups that could form disulfide bonds, it's plausible that, in accordance with the data present in literature [Wood, 2006; Garrard et al., 1977], it auto-assembles in non reducing conditions and that is more susceptible to the oxidation. Therefore the oxidation-reduction potential of these compounds may be the basis of their ability to induce phenomena of co-protein aggregation, and also explain the fact that, at the same dose and times of treatment with RDC11 and ODC2, which differ only in the metal center, they cause different degrees of aggregation.

Conversely ODC16 and ODC20 time-course showed a very bland binding to H2B and H3 (Fig.56), which remain in prevalent form of monomer, except for the treatment with the

higher concentrations of ODC20 after 24 h. At the same time, the H3 degradation is not present. These results can be correlated with those obtained in comet assay. For instance, it is interesting to see that the compounds that induce more DNA damages (RDC11, ODC2) are the ones that interact the best with histones, while the compounds interacting less with histones (ODC16 and ODC20) induces also less DNA damages although showing high cytotoxicity. Hence, it is tempting to hypothesize that part of the DNA damage seen *in vivo* could be caused by the interaction between the compounds and histone through a destabilization of the nucleo-DNA complexes. In addition it also indicates that ODC16 and ODC20 that are the most cytotoxic do not have the same mode of action, which remains to be identified.

The atypical behavior of these compounds depends clearly on the ligand functions, and their analysis could help to clarify the structure-activity relationship also of other components of this class of metal compounds. All together, these data showed a great and diversified kinetics of histones interaction that requires a deepening in cell models, to investigate their implication in a physiological and biochemical environment.

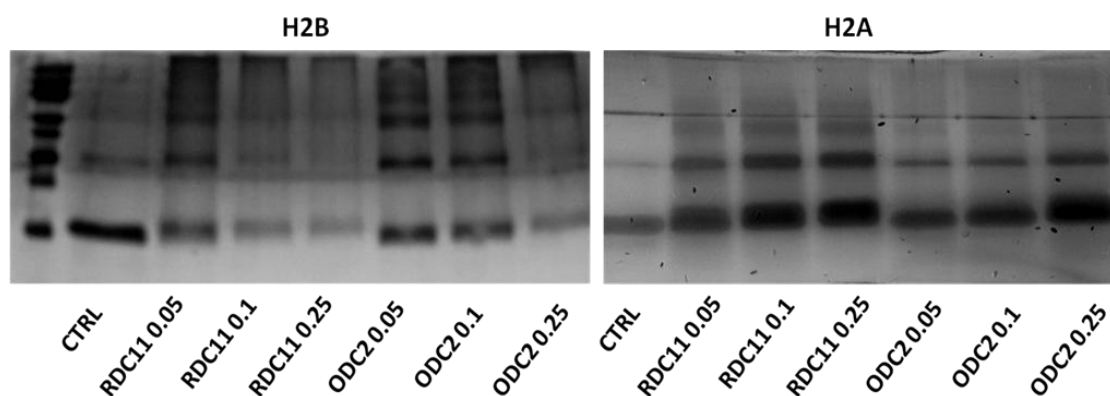


Fig.54. H2B and H2A binding. SDS-PAGE of H2B and H2A histones incubated for 48 with different concentrations (0.05, 0.1, 0.25 mM) of RDC11 and ODC2 compounds.

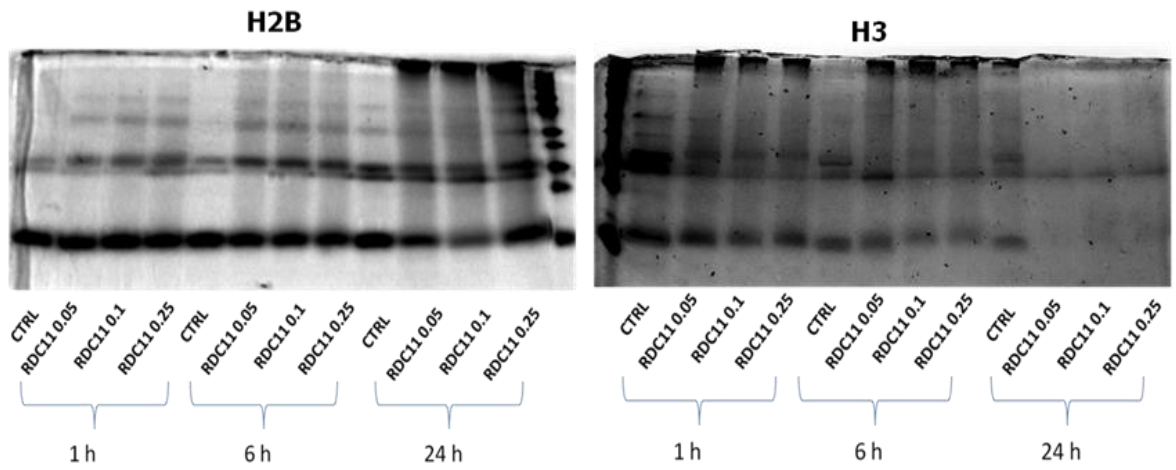


Fig.55. Time course of H2B and H3 binding. SDS-PAGE of H2B and H3 histones incubated for 1, 6, 24 h with different concentrations (0.05, 0.1, 0.25 mM) of RDC11.

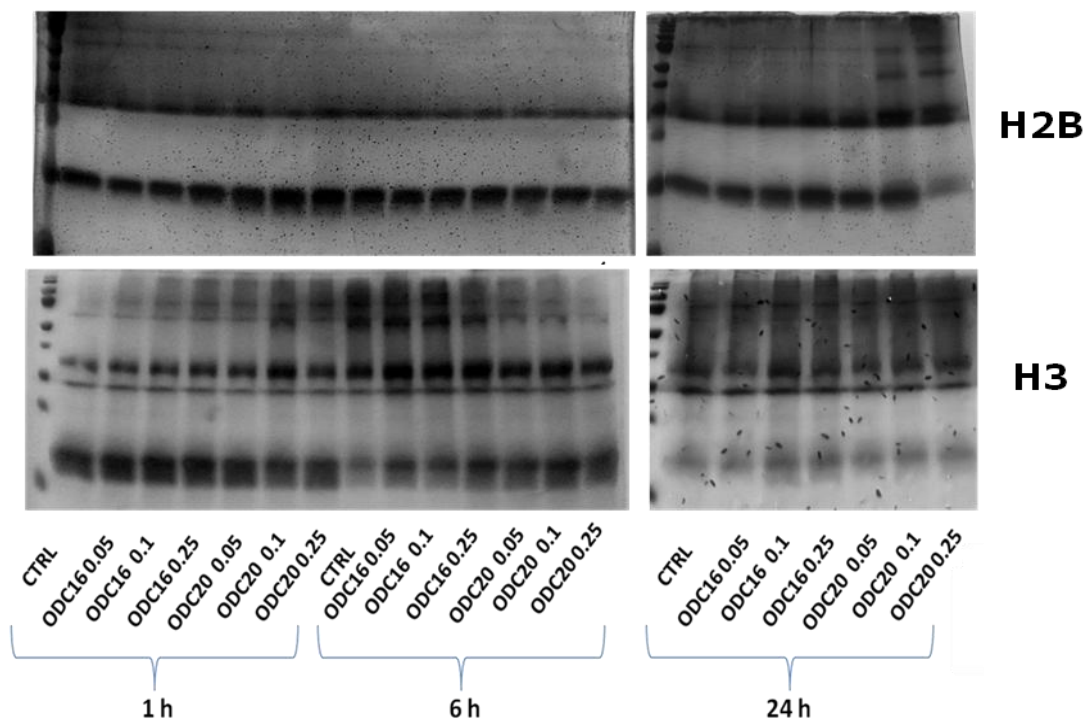


Fig.56. Time course of H2B and H3 binding. SDS-PAGE of H2B and H3 histones incubated for 1, 6, 24 h with different concentrations (0.05, 0.1, 0.25 mM) of ODC16 and ODC20 compounds.

5.4.4. Modification of H2A and H2B expression patterns in cells treated with organometallic compounds

To assess whether the aggregation of histones H2A and H2B evaluated in the experiments with purified histones also occurred in cellular models, western blot analysis of H2A and H2B expression was performed in non reducing conditions. Since more bands were detected, the cellular extracts were subjected to immunoprecipitation, in order to reduce the background. It was possible to estimate an increment of aggregation in a similar way to the "*in vitro*" binding experiments; however, in this case it is possible that the bands are homo-multiples or hetero-multiples, due to the binding with other histones forming the octamer. In addition, it is likely that in the complex intracellular environment the compounds interact also with other targets and it is difficult to assess in such complexity what would be the contribution of the interaction with histones. Also, additional mechanisms of histone modifications occurring *in vivo* are likely to impact on their expression level, polymerization status, post-translational modifications, and therefore altering their migration pattern.

In particular, H2B showed just a little increase of polymerization (Fig. 58), whereas for H2A both monomers and its multiple resulted increased (Fig.57), except for the higher treatment of RDC11 and ODC2, for which the significant decrease of monomers is contextual with the relevant augment of their multiples. Thus it seems that the histones can be regulated in two different ways, leading to the general increase of expression, or to an induction of aggregation by a not yet known specific reaction. Moreover, in general the rapport polymerization/monomer is higher for RDC11 and ODC2 than for the platinum compounds. Interesting, unlike the experiments with purified histones, these results showed a stronger alteration of H2A migration pattern, meaning that, in the presence of all the histones forming the octamer, H2A is a favorite target or is more susceptible to the redox activity of the organometallics. Also, the presence of another band of H2B slightly higher than the monomers is relievable; it may represent presumably a post-translational modification, like acetylation, that of course, needs to be confirmed by using a specific antibody to detect this form. These results showed that also in the cancer cells the interaction between histones and metal-based compounds occurs, but with different profiles, that reflects the effect of the physical and biochemical microenvironment on the different ligand substitution reactions and redox potential.

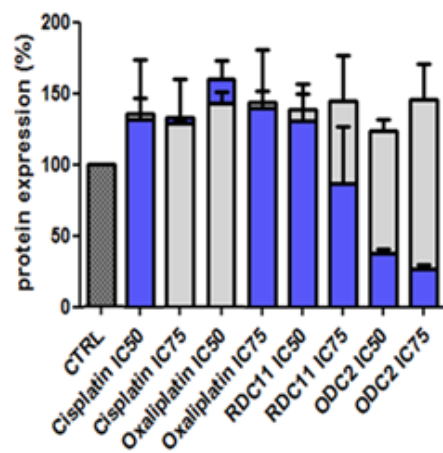
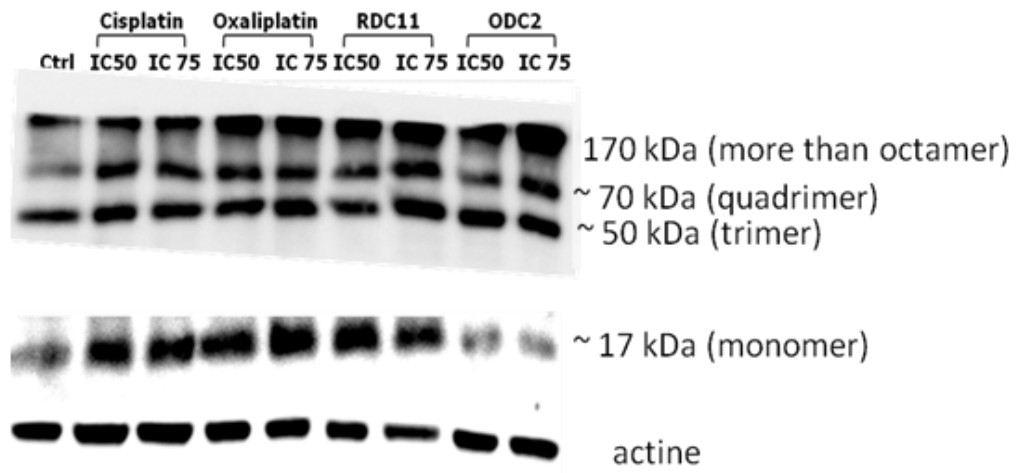


Fig.57. H2A immunoprecipitation. H2A expression in MKN45 cells, after treatment with IC₅₀ and IC₇₅ of cisplatin, oxaliplatin, RDC11 and ODC2 for 24 h.

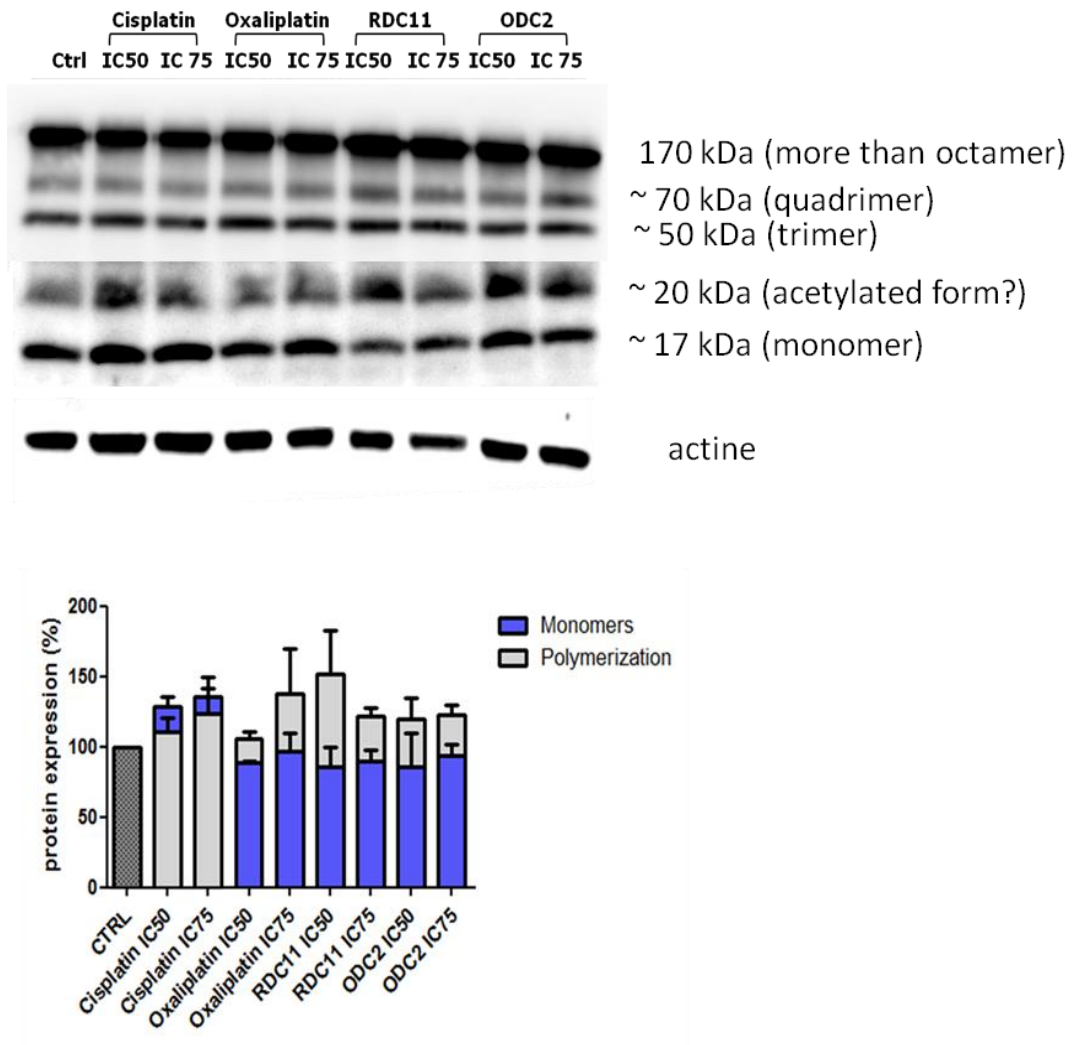


Fig.58. H2B immunoprecipitation. H2B expression in MKN45 cells, after treatment with IC₅₀ and IC₇₅ of cisplatin, oxaliplatin, RDC11 and ODC2 for 24 h.

5.4.5. Modification of H3 expression pattern in cells treated with organometallic compounds

In the cells the histones are the subject to multiple modifications that modulate their association with DNA, DNA compaction and also their translocation into the cytoplasm [Chen et al., 2014]. To evaluate how the organometallic interaction with histones impacts in the cells, the analysis of H3 expression by Western Blot was performed. MKN45 cells were treated for 24 h with IC₅₀ and IC₇₅ concentrations of RDC11 and ODC2, and also with cisplatin and oxaliplatin. Two kinds of buffer of protein extraction were used: the blander NP40 buffer, and RIPA buffer, more specific to extract the histones tightly attached to DNA (the nuclear fraction of H3) [Holden and Horton, 2009]. In these conditions, we found two different patterns of H3 histones, suggesting of a soluble fraction in the first case, and of a less soluble fraction, bound to the DNA, in the second case. While the less soluble fraction is uniformly and highly expressed in each sample, the soluble fraction of H3 is present prevalently in the treatments, and increases with the concentrations of these (Fig.59A). Interesting, when the cells are pre-treated with the antioxidant N-acetylcysteine, the increment of soluble H3 is completely reverted (Fig.59B). It therefore tempting to hypothesize that, as well as it happens in "*in vitro*" binding experiments, the oxidation of H3 by metal compounds occurs, provoking a massive detachment of this histone from the DNA, and its possible translocation in the cytoplasm.

In this context, recent discoveries about the role of "free" histones are remarkable. It is believed in fact that when histones translocate from the nucleus to the cytoplasm and then to extracellular space, can act as signals for different pathological conditions, among which the apoptosis [Chen, 2014]. In particular, after a damaging on DNA, H3 can translocate and bind the mitochondria, influencing its function and ultrastructure, thus inducing a rapid and extensive release of the pro-apoptotic proteins cytochrome c and Smac/DIABLO [Cascone et al., 2012]. Thus it may serve as an amplifier of the apoptotic response. Also, the response to the antioxidant is stronger with organometallic compounds than with the classical platinum compounds, suggesting that while the redox activity, probably responsible for the direct oxidation of H3, is essential for the activity of organometallics, it is not the only component in the platinum compounds mechanism that leads to the separation of H3 also in an indirect way, perhaps due to the DNA binding.

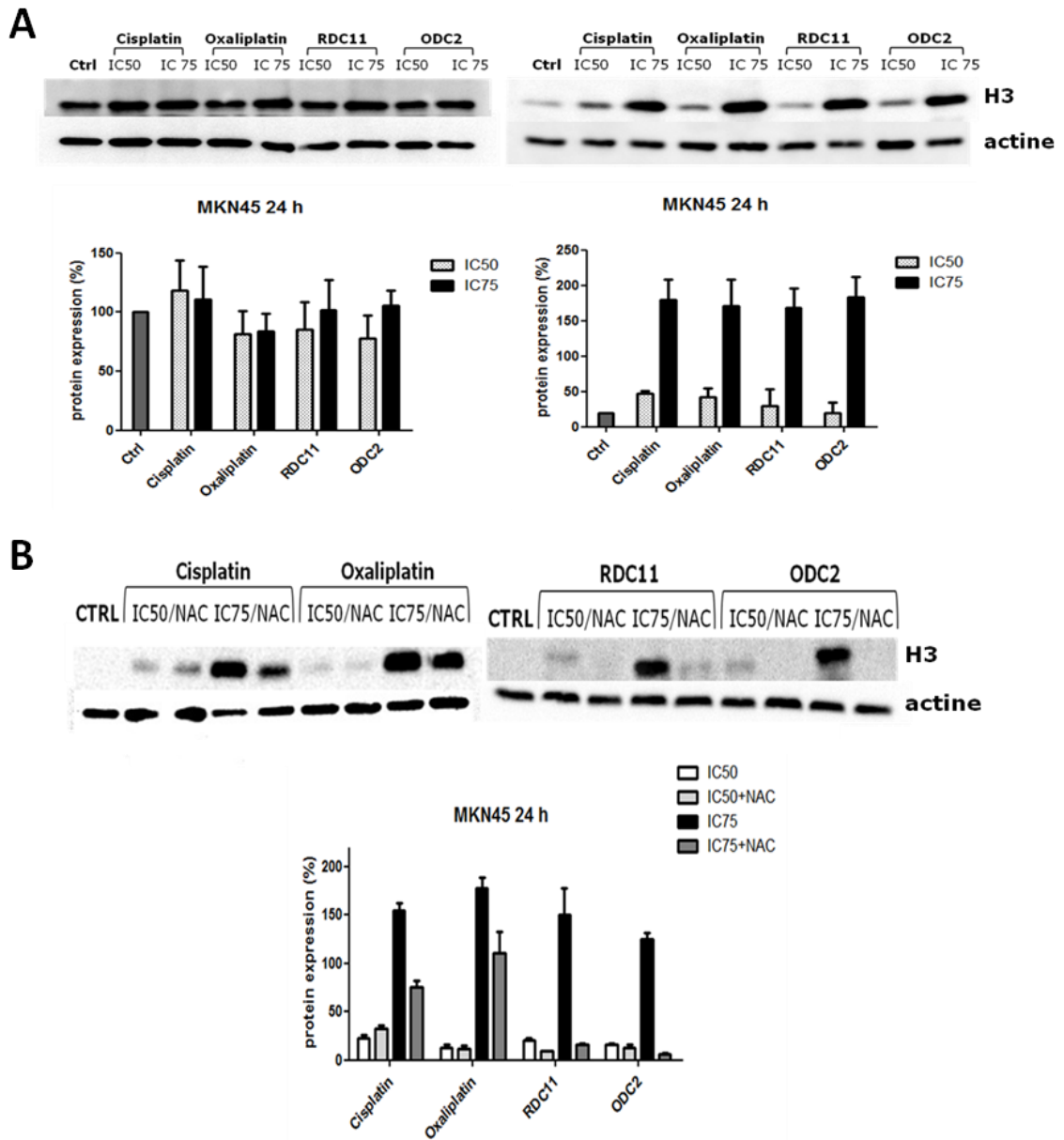


Fig.59. H3 expression. Western blot analysis of H3 histone in MKN45 cells after treatment with IC₅₀ and IC₇₅ of cisplatin, oxaliplatin, RDC11 and ODC2 without (A) or with (B) pretreatment with NAC.

5.4.6. Caspase-3 activation

Stressing factor, such as ROS production, viral infection and chemotherapeutic agents, can lead to cell death by apoptosis. This process, starting with the amplification of signaling pathways, culminates with the DNA fragmentations and the formation of apoptotic bodies, rapidly removed by phagocytic cells [Savill and Fadok, 2000; Kurosaka et al., 2003]. In the scenario of the late state of apoptosis the reversion of nuclear components in the cytoplasm could occur. To evaluate the conditions in which the histone H3 translocation is detected, we thus analyzed the caspase-3 activated fragments as a marker of apoptosis.

Surprisingly, the patterns of caspase 3 fragments induced by ODC2, RDC11 and platinum-based compounds were different, highlighting again a different mode of action. As showed in Figure 60, for RDC11 and ODC2, high fragments of caspase 3 (about 25 kDa respect to 17 kDa of the main activated form), that are presumably forms of a bland activation of caspase-3, were clearly observed at 24 h, but surprisingly, not latter. Inversely and more in line with the literature, high and lower fragments were progressively observed after treatment with cisplatin and oxaliplatin starting weakly at 24 hours. This result indicated a lack of correlation between the ability of the compounds to induce caspase 3 cleavage and the presence of more soluble H3. It also questioned the ability of RDC11 and ODC2 to induce completely apoptosis in these cells. Anyhow, it suggests that the cause of an increase of soluble fraction after treatment with the cytotoxic compounds is likely to be independent from the apoptosis process.

A study on different cancer cell lines supports the idea [Wu et al., 2002] by describing that apoptotic cell lines showed release of histones from nuclei, but this event not necessarily coincides with the presence of fragmentations. In fact, not all cell lines release histones from nucleosomes during DNA fragmentation and apoptosis, and histones release and DNA fragmentation can be clearly separated into two independent processes. Thus it is plausible that the H3 translocation observed in our conditions is an early event preceding the cytotoxic process, apoptotic or not. This hypothesis is in accordance with the evidences about the destabilization of the outer and inner mitochondrial membranes (with subsequent release of pro-apoptotic proteins) due to the DNA damage-mediate histones release [Cascone et al., 2012]. Moreover, some studies showed the detection of histones in lymphoblasts lysates in a premature state of apoptosis, before also the exposition of PS on their cellular membranes [Gabler et al., 2004 and 2003].

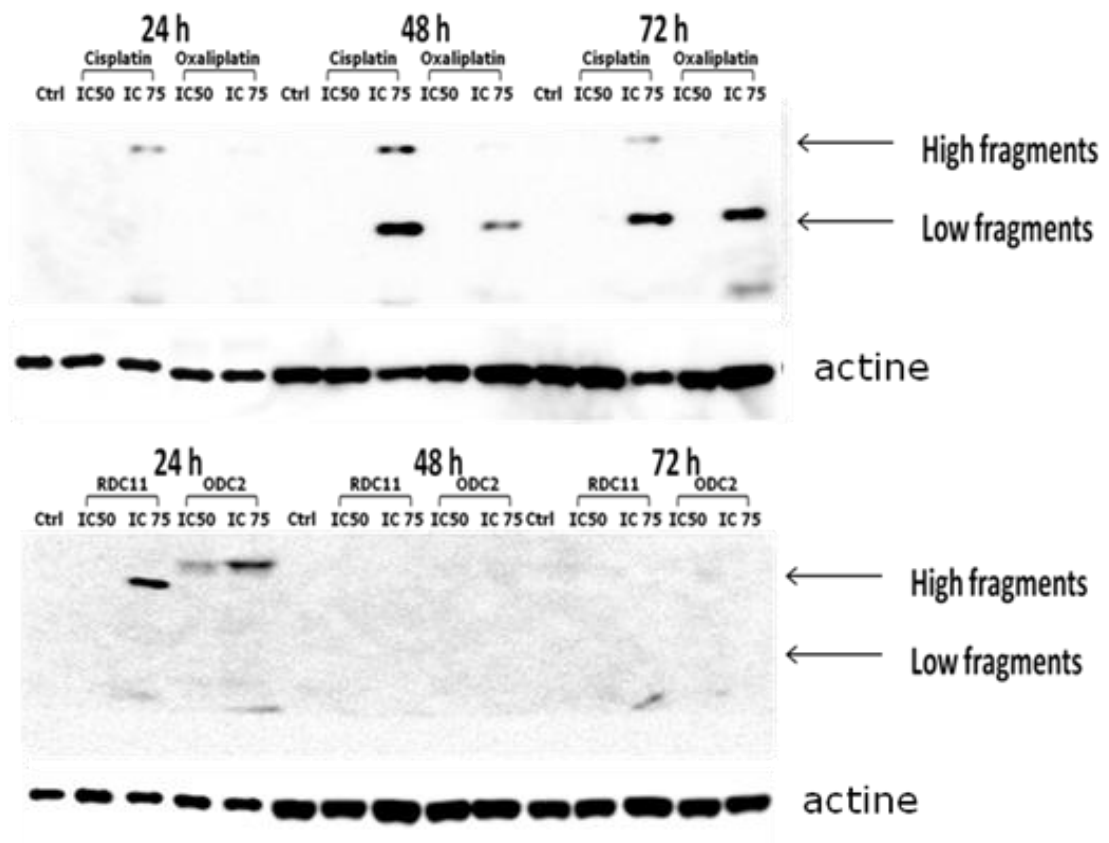


Fig.60. Caspase-3 activation. Western Blot Analysis of cleaved-caspase-3 in MKN45 cells untreated and treated with IC₅₀ and IC₇₅ of cisplatin, oxaliplatin, RDC11, ODC2 for 24, 48 and 72 h.

5.4.7. H3-acetylation

As widely discussed above (par.1.1.3.), the term epigenetic is referred to the protein modifications that lead to changes in gene expression; this process has a central role to control the cell proliferation and metabolism and could be a crucial point of regulation in the anticancer therapy. In this field, there is a wide report in literature about the important role of H3 histone acetylation in the gene regulation [Ganesan et al., 2009], that can lead to the expression of pro-apoptotic factors [Glozak and Seto, 2007]. In order to understand if RDC and ODC compounds impact the histones only by a direct binding, or also indirectly by induction of post-translational modifications, the acetylated form of H3 was detected by Western Blot analysis.

As showed in Figure 61, an increment of acetylation both at fast time of incubation (6 h) and more (24 h) was found, even if with different kinetics for each compound. Generally, while at 6 h the acetylation is more with IC_{75} concentration of cisplatin, oxaliplatin and ODC2, at 24 h it increases with the IC_{50} treatment; this difference is especially strong with ODC2 treatment, showing an important dose/time/stimulus correlation; in fact, it seems an early process inducted by the compounds at right stimulus-concentration (IC_{50} conc. at 6h), not present in the extreme condition (IC_{75} conc. at 24 h), whereas the downstream activation of gene expression could occur. Conversely, induction of acetylation by RDC11 rises over time with the higher concentration of the compound. However, these findings need further investigations to understand the relevance of this post-translational modification on the induction of specific gene expression. These considerations assume more relevance again in view of the extensive literature data about the epigenetic alterations present in gastric cancer type, among which a strong decrease of acetyl-H3, leading to an inhibition of gene expression [Muratani et al., 2014; Kang et al., 2014; Yang et al., 2014].

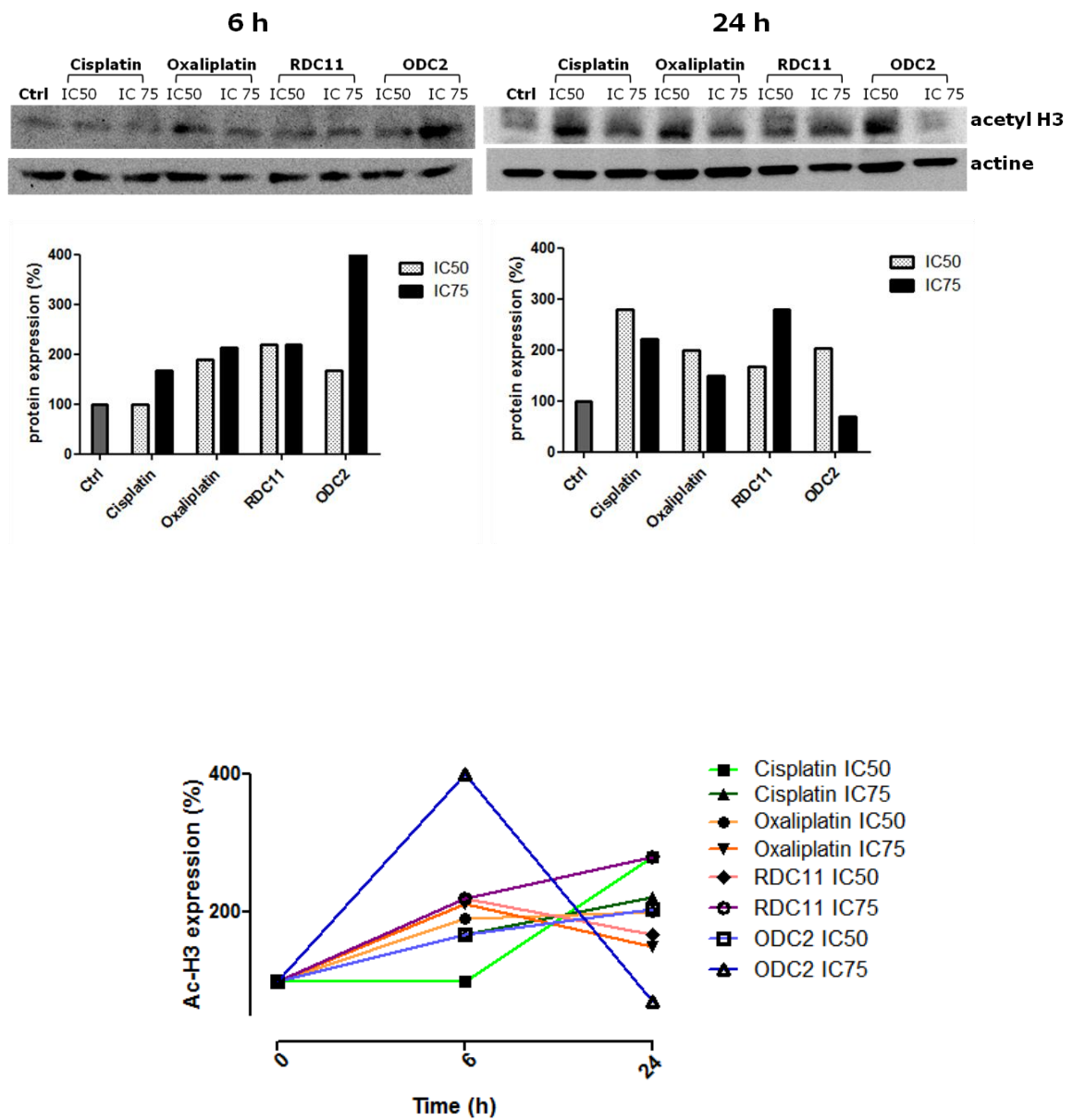


Fig.61. Acetyl-H3 expression. Western blot analysis of acetylated form of H3 histone in MKN45 cells after 6 and 24 h of treatment with IC₅₀ and IC₇₅ of cisplatin, oxaliplatin, RDC11 and ODC2.

5.5. CONCLUSIONS

Recently, anticancer agents based on alternative transition metals to platinum have emerged for their good cytotoxic profiles joined with fewer side effects and no resistance phenomena. On the other hand, the drawback of these new candidates is the lack of information on their mechanism of action, which is strictly correlated with the chemical characteristic of the structure and thus typical for each compound. Generally, ruthenium derivatives, among which RDC11, have shown a weak interaction with DNA, suggesting that other macromolecules can be preferentially their targets. Among these, the histones have emerged; they, allowing the different chromatin condensation states, have a crucial role in the DNA replication, transcription and repair. For these reasons, epigenetic modifications on histones are object of studies to elucidate their role in the activity of anticancer drugs. We have thus investigated if histones represent targets of the ruthenium derivate RDC11 and in the osmium derivates ODC2, ODC16, ODC20. All together, the data have shown a direct binding of organometallics with the histones, joined with a peculiar ability to provoke protein polymerization, events that could strengthen the chromatin perturbation. The hypothesis that the interaction with the histones could participate in causes of the DNA damage is tempting and might be supported by the different behavior of ODC16 and ODC20, for which the lack of histones binding corresponds with a poor induction of the DNA damage (Table 5). However, they showed high antiproliferative activity and need more investigations to understand their activity.

	IC ₅₀ (μ M)	DNA damage	Histones interactions
RDC11	~ 1	+++	++++
ODC2	~ 1	++++	+++
ODC16	~ 0.2	+	+
ODC20	~ 0.2	++	++

Tab.5. Comparison between the IC₅₀, the DNA damage induction and the histones interactions of RDC11, ODC2, ODC16 and ODC20.

On the other hand, the DNA damage inducted by RDC11 and ODC2 is marked and depends partially on the oxidative stress inducted; thus is probable that also the histones interaction is due to their redox potential, as demonstrated by the different capacity to

interact with the histones of RDC11 and ODC2, compounds that share the same organic structure. Therefore these results are in accordance with the previous showed for RDC11, about the crucial role of the oxidative stress and ROS production in its mechanism of action [Vidimar et al., 2012]. The oxidative stress seems to have an impact also on the oxidation of the histone H3, that not only could lead to the chromatin stress and thus to the DNA damage, but also in H3 translocation, event that recently was found to be crucial in several stress signaling pathways. Also, the treatment with organometallics induces H3 acetylation, which is a key-event in the regulation of gene expression, for example inducing the transcription of pro-apoptotic genes [Glozak and Seto, 2007] (Fig.62). These promising results need thus further investigations to evaluate the impact of the organometallic interaction with histones on the chromatin, as well as to individuate the specific genes that are regulated by H3 acetylation.

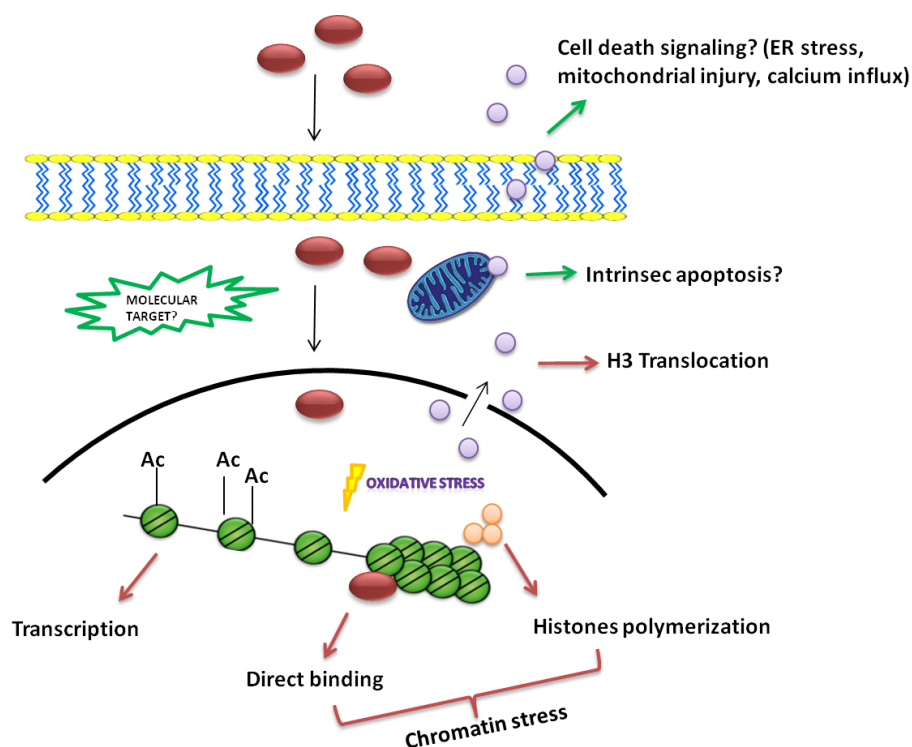


Fig.62. Mechanism proposed for the role of epigenetic targets in the RDC11 and ODC2 mechanism of action: the compound (in red) can impact on the chromatin (in green) structure by direct binding, induction of histones polymerization (in pink), induction of acetylation (Ac) and H3 translocation. The extranuclear H3 could induce intrinsic apoptosis, as well as act as extracellular signal of cell death.

6. DISCUSSION



Cancer is the second leading cause of death. Although it is already validated the use of techniques such as radiotherapy, immunotherapy and chemotherapy, in the last decade the medical community has focused on the research of less invasive drugs, through the identification of new anticancer agents, as well as by the design of innovative systems for the drug delivery, like the liposomes, that allow the protection of the active principle until the achievement of molecular targets, reducing the toxic effects. Among the new anticancer agents currently in clinical trials, there are the ruthenium-based compounds, NAMI-A and KP1019 [Sava et al., 1998; Kersten et al., 1998], which have emerged as promising alternatives to platinum compounds, because of their great anticancer and/or antimetastatic activity, associated with fewer side effects. The difference between the derivatives of ruthenium and platinum is probably due to their different pharmacodynamics that, if is well known for cisplatin and its analogs, it is not yet completely clarified for the other metal complexes. Also, chemical characteristics like the redox potential, the charges and the lipophilicity are very different among the various classes of metal-based compounds, reflecting their different biological effects. In fact, while KP1019 is considered prevalently an anticancer agent, NAMI-A is prevalently an anti-metastatic compound, probably because it interacts more with extracellular components [Brescacin et al., 2015; Pelillo et al., 2015]. The low molecular weight AziRu [Mangiapia et al., 2012], is an analog of NAMI-A, in which, instead of the imidazole, there is the pyridine. This substitution gives more lipophilicity to the complex, which thus should more easily interact with the cell membranes; in fact, the IC₅₀ values relative to AziRu are lower than those calculated for NAMI-A. However, the values are still too high to be considered an anticancer agent. Also, this generation of low molecular weight ruthenium complexes, is not stable in physiological solution.

In this context, my Ph.D. was aimed to the *in vitro* characterization of different classes of new metal-based compounds. First of all the interest of this work was to evaluate their anticancer activity as well as their safety. Subsequently, the study was focused on the identification of the kind of cell death pathway induced by these compounds and their specific targets, in order to clarify their mechanism of action. The first tested class belongs to a new nanotechnological platform in which different kinds of liposomes contain AziRu. These drug delivery systems represent thus an innovative evolution of the ruthenium complexes, improving both chemical and biological profiles. In particular, AziRu is bound

to a nucleolipid acting as central scaffold, in which different substituents can be inserted, among these the lipophilic chains allowing the self-assembly. These nucleolipids based-Ru are prepared in co-aggregation with neutral (POPC) or cationic (DOTAP) lipids, in order to improve the stability of the aggregates. In fact, the ruthenium-based liposomes have shown good stability both in water and physiological solutions, as well as an important reduction of the IC₅₀ values (whereas the free-ruthenium liposomes are not cytotoxic), proving the efficacy of the "nanovectorization" on the explication of the anticancer effect of ruthenium-based compound AziRu. In particular, the cationic formulations with the lipid DOTAP have shown more efficacy than the previous investigated neutral liposomes [Mangiapia et al., 2012], both in term of antiproliferative effect, than in term of cellular uptake. Thus, the coupled results of the cell viability and of the cellular uptake showed that the cationic liposomes are a good system to deliver the ruthenium complexes, probably due to the greater interaction between the cationic lipid and the negative component of the cell surface, such as proteoglycans [Wiethoff et al., 2001]. Moreover, we demonstrated that the cationic liposomes induce both autophagy and apoptosis, suggesting the activation of multiple pathways of cell death, perhaps due to the binding of targets in different cellular compartments.

Subsequent modifications of neutral and cationic nanovectors have led to: *i*)ToThyCholRu/DOTAP, in which the liposome is functionalized with the cholesterol able to regulate the physico-chemical properties of lipid bilayers, in order to stabilize liposomes and to improve their cellular uptake; *ii*)ToThyRu/POPC/de-LOS, in which a modified lipooligosaccharide derived by the bacteria *Rhizobium rubi* is inserted into the liposomal bilayer to mimic the bacteria walls, thus exploiting its quality of resistance and stability, and at the same time the *de-O-acylation* avoids the recognition by the immune system and thus making it a good stealth system. These two formulations have been tested also on healthy cells, whereas either showed no significant activity. These results give support to the hypothesis of the ruthenium activation by reduction in cancer cells [Clarke et al., 1999]. Since most anticancer drugs lack of cancer specificity and cause side effects on normal tissues, ruthenium complexes may provide a less toxic and more effective alternative to common chemotherapeutic agents.

Overall, this tested mini-library of nanovectors demonstrated how it is possible, by *ad hoc* modifications of their structure, to modulate their chemical and biological characteristic

and thus make them appropriate for different applications. Also, these systems effectively improve the anticancer activity of ruthenium, as direct effect of the "nanovectorization", that in principle, could be applied also to to deliver *in vivo* a a large variety of lipophilic drugs, enhancing their long-life in the blood. Therefore, as well as these screenings have led to some important conclusions in the context of the characterization of a new nanotechnological platform of ruthenium-based compounds, these results lay the groundwork for further deeps both on the usability of these nanovectors as possible drug carriers and for the understanding the wide spectra of actions of the ruthenium-based complexes.

Thus, the next goals of this study will be testing the specific targets involved in their mechanism of action that, as widely discussed, differ substantially for each compound, in a manner strictly related to their chemical and physical characteristics. In the last decade, a large number of chemical and biological investigations have been carried out in order to individuate the targets of metal compounds, showing that, beside the DNA [Bergamo and Sava, 2007; Brabec and Novakova, 2006], nuclear and cytosolic proteins could have a central role in the mechanism of action of ruthenium-based complexes [Mendes et al., 2011; Casini et al., 2010]. Among these, the proteins binding DNA, the histones, have emerged [Davey GE and CA, 2008; Wu et al., 2011; Adhireksan et al., 2014; Singh et al., 2014; Soori H., 2015]. These proteins, allowing the different chromatin condensation state, have a crucial role in the DNA replication, transcription and repair. In an attempt to elucidate this possible mechanism of action, the present Ph.D. research was then focused on the role of histones, and more in general of the epigenetics, on the class of N-C ruthenium and osmium heterocyclic compounds, named RDC11, ODC2, ODC16, ODC20 [Gaiddon et al., 2005; Ryabov et al., 2003; Boff et al., 2013]. These compounds, in particular RDC11, are already chemically and biologically well characterized, showing a remarkable cytotoxicity *in vivo* and *in vitro*, whereas the activation of different pathways of cell death, as well as the induction of oxidative stress, were found [Gaiddon et al., 2005; Meng et al., 2009; Vidimar et al., 2012]. We found a different pattern of activity for the ruthenium- and osmium-derived compounds RDC11 and ODC2 respect to the second generation of osmium-derived compounds ODC16 and ODC20; in fact, these last complexes didn't induce a marked DNA damage, as well as didn't seem to strongly interact with the histones, despite their high cytotoxicity. Conversely, RDC11 and ODC2 showed

both to induce DNA damage (partially mediated by oxidative phenomena) and to interact with the histones. These results support the hypothesis that the DNA damage could be mediated by the direct interaction with the histones, as well as the different profile of ODC16 and ODC20 demonstrates the importance of the structure-activity relationship. In addition, some differences prevalently in term of kinetics of action, occur also between RDC11 and ODC2, compounds that share the same structures, and thus highlighting how the response to the metal drugs is correlated with the metal redox potential. Moreover, we found both the histone H3 translocation, an event that recently has been correlated with the stress signaling pathways [Chen et al., 2014], and the H3 acetylation, an important post-translational modification, leading to the induction of specific gene expression, such as the pro-apoptotic genes [Glozak and Seto, 2007]. Since the different redox potential of the metals modulate the kinetics of histones binding, and the induction of oxidative stress is important for the DNA damage and the H3 translocation, we can hypothesize that the interaction of organometallic compounds with the histones is strictly correlated with their potential to induce oxidative stress. All together these data demonstrated that the histones could be crucial targets to mediate the cellular response to the organometallic compounds, and confirm also an important role of the epigenetics changes in their mechanism of action.

Overall, this doctoral study, focused on the characterization of different class of metal-based compounds, demonstrated that ruthenium and osmium complexes could be promising alternative to platinum compounds, as well as it has shown how the chemical modifications in their structure are responsible for different pharmacodynamics, remarking thus the advantage of their wide spectrum of action due to the important role of the oxidation/reduction state and the possibility of functionalization with different ligands.

BIBLIOGRAPHY

A

- Adams JM, Cory S. Apoptosomes: engines for caspase activation. *Curr Opin Cell Biol.* 2002; 14(6):715-20.
- Adhireksan Z., Davey GE Campomanes P., Groessl M., Clavel CM, Yu H., Nazarov AA, Yeo CH, Ang WH, Dröge P, Rothlisberger U, Dayson PJ, Davey CA. Ligand substitutions between ruthenium cymene compounds can control protein versus DNA targeting and anticancer activity. *Nat Commun.* 2014; 5:3462.
- Akbarzadeh A., Rezaei-Sadabady R., Davaran S., Joo SW, Zarghami N., Hanifehpour Y, Samiei M, Kouhi M, Nejati-Koshki K. Liposome: classification, preparation, and applications. *Nanoscale Res Lett* 2013; 8(1):102.
- Alcindor T, Beauger N. Oxaliplatin: a review in the era of molecularly targeted therapy. *Curr Oncol.* 2011; 18(1):18-25.
- Alemdaroglu FE, Herrmann A. DNA meets synthetic polymers highly versatile hybrid materials. *Org Biomol Chem.* 2007; 5(9):1311-20
- Allardyce CS, Dyson PJ. Ruthenium in Medicine: Current Clinical Uses and Future Prospects. *Platinum Metals Rev.* 2001; 45(2): 62-69
- Andrews AJ, Luger K. Nucleosome structure(s) and stability: variations on a theme. *Annu Rev Biophys* 2011; 40:99–117.
- Apps MG, Choi EH, Wheate NJ. The state-of-play and future of platinum drugs. *Endocr Relat Cancer.* 2015; 22(4):R219-33.
- Arents G, Burlingame RW, Wang BC, Love WE, Moudrianakis EN, The nucleosomal core octamer at 3.1 Å resolution: a tripartite protein assembly and a left-handed superhelix, *Proc. Natl. Acad. Sci. U. S. A.* 1991; 88(22): 10148–10152.
- Arents G, Moudrianakis EN. The histone fold: A ubiquitous architectural motif utilized in DNA compaction and protein dimerization. *Proc Natl Acad Sci U S A* 1995; 92(24):11170–11174.
- Arigon J., Prata CA, Grinstaff MW, Barthelemy P. Nucleic acid complexing glycosyl nucleoside-based amphiphile. *Bioconjugate Chem.*, 2005; 16(4): 864–872

B

- Baehrecke, EH. Autophagy: dual roles in life and death? *Nature Rev. Mol. Cell Biol.* 2005; 6(6): 505–510.
- Baig S, Seevasant I, Mohamad J, Mukheem A, Huri HZ, Kamarul T. Potential of apoptotic pathway-targeted

- cancer therapeutic research: Where do we stand? *Cell Death Dis.* 2016 ; 7:e2058.
- Bailey AL, Cullis PR. Membrane fusion with cationic liposomes: effects of target membrane lipid composition. *Biochemistry.* 1997; 36(7):1628-34
 - Bajaj A., Kondaiah P, Bhattacharya S. Synthesis and gene transfer activities of novel serum compatible cholesterol-based gemini lipids possessing oxyethylene-type spacers. *Bioconjug Chem.* 2007; 18(5):1537-46.
 - Bajaj A, Mishra SK, Kondaiah P, Bhattacharya S. Effect of the headgroup variation on the gene transfer properties of cholesterol based cationic lipids possessing ether linkage. *Biochim Biophys Acta.* 2008; 1778(5):1222-36.
 - Bal W, Liang R, Lukszo J, Lee SH, Dizdaroglu M, Kasprzak KS. Ni(II) specifically cleaves the C-terminal tail of the major variant of histone H2A and forms an oxidative damage-mediating complex with the cleaved-off octapeptide. *Chem Res Toxicol.* 2000; 13(7):616-24.
 - Bal W, Lukszo J, Jezowska-Bojczuk M, Kasprzak KS. Interactions of nickel(II) with histones. Stability and solution structure of complexes with CH₃CO-Cys-Ala-Ile-His-NH₂, a putative metal binding sequence of histone H3. *Chem Res Toxicol.* 1995; 8(5):683-92
 - Bangham AD, Standish MM, Miller N. Cation permeability of phospholipid model membranes: effect of narcotics. *Nature.* 1965; 208(5017):1295-7.
 - Bartel DP. MicroRNAs: genomics, biogenesis, mechanism, and function. *Cell.* 2004; 116(2):281-97.
 - Barthelemy P., Prata CA, Filocamo SF, Immoos CE, Maynor BW, Hashmi SA, Leeand S. J., Grinstaff, MW. Supramolecular assemblies of DNA with neutral nucleoside amphiphiles. *Chem.Commun.* 2005; (10):1261-1263
 - Bergamo A., Gaiddon C., Schellens J.H.M., Beijnen J.H., Sava G. Approaching tumour therapy beyond platinum drugs: Status of the art and perspectives of ruthenium drug candidates. *J Inorg Biochem* 2012; 116 (1): 90–99
 - Bergamo A., Masi A., Jakupec M.A., Keppler B.K., Sava G. “Inhibitory Effects of the Ruthenium Complex KP1019 in Models of Mammary Cancer Cell Migration and Invasion” *Met Based Drugs.* 2009; 2009: 681270.
 - Bergamo A., Sava G. Ruthenium anticancer compounds: myths and realities of the emerging metal-based drugs *Dalton Trans.*, 2011; 40(31): 7817-23.
 - Bergamo A., Sava G., Linking the future of anticancer metal-complexes to the therapy of tumour metastases, *Chem. Soc. Rev.*, 2015; 44(24):8818-35.
 - Bergamo A, Sava G. Ruthenium complexes can target determinants of tumour malignancy. *Dalton Trans.* 2007; (13):1267-72.

- Bernges F, Holler E. The reaction of platinum(II) complexes with DNA. Kinetics of intrastrand crosslink formation in vitro. *Nucleic Acids Res.* 1991; 19(7):1483-9.
- Besker N, Coletti C, Marrone A, Re N. Binding of antitumor ruthenium complexes to DNA and proteins: a theoretical approach *J Phys Chem B.* 2007; 111(33):9955-64.
- Bird A. DNA methylation patterns and epigenetic memory. *Genes Dev.* 2002; 16(1):6-21
- Blunden BM, Lu H, Stenzel MH. Enhanced delivery of the RAPTA-C macromolecular chemotherapeutic by conjugation to degradable polymeric micelles. *Biomacromolecules.* 2013; 14(12):4177-88.
- Boff B, Gaiddon C, Pfeffer M. Cancer cell cytotoxicity of cyclometalated compounds obtained with osmium(II) complexes. *Inorg Chem.* 2013; 52(5):2705-15.
- Bogdan C. Nitric oxide synthase in innate and adaptive immunity: an update. *Trends Immunol.* 2015; 36(3):161-78
- Bortner CD, Oldenburg NB, Cidlowski JA. The role of DNA fragmentation in apoptosis. *Trends Cell Biol.* 1995; 5(1):21-6.
- Botrugno OA, Robert T, Vanoli F, Foiani M, Minucci S. Molecular pathways: old drugs define new pathways: non-histone acetylation at the crossroads of the DNA damage response and autophagy. *Clin Cancer Res* 2012; 18: 2436–2442
- Boutet-Robinet E., Trouche D., Canitrot Y. Neutral Comet Assay. *Bio-protocol* 2013; 3(18): e915.
- Bozzuto G, Molinari A. Liposomes as nanomedical devices. *Int J Nanomedicine.* 2015; 10:975-99.
- Brabec V, Nováková O. DNA binding mode of ruthenium complexes and relationship to tumor cell toxicity. *Drug Resist Updat.* 2006; 9(3):111-22.
- Brescacin L, Masi A, Sava G, Bergamo A. Effects of the ruthenium-based drug NAMI-A on the roles played by TGF- β 1 in the metastatic process. *Biol Inorg Chem.* 2015; 20(7):1163-73.
- Brinkmann V, Reichard U, Goosmann C, Fauler B, Uhlemann Y, Weiss DS, Weinrauch Y., Zychlinsky A. Neutrophil extracellular traps kill bacteria. *Science.* 2004; 303(5663):1532-5.
- Brown JM, Attardi LD. The role of apoptosis in cancer development and treatment response. *Nat Rev Cancer.* 2005; 5(3):231-7.
- Buchwald H. Cholesterol inhibition, cancer, and chemotherapy. *Lancet.* 1992; 339(8802):1154-6.

C

- Cascone A, Bruelle C, Lindholm D, Bernardi P, Eriksson O. Destabilization of the Outer and Inner Mitochondrial Membranes by Core and

- Linker Histones. *PLoS One*. 2012; 7(4): e35357.
- Casini A. Exploring the mechanisms of metal-based pharmacological agents via an integrated approach. *J Inorg Biochem*. 2012; 109:97-106.
 - Casini A, Gabbiani C, Michelucci E, Pieraccini G, Moneti G, Dyson PJ, Messori L. Exploring metallodrug-protein interactions by mass spectrometry: comparisons between platinum coordination complexes and an organometallic ruthenium compound. *J Biol Inorg Chem*. 2009; 14(5):761-70.
 - Casini A., Diawara MC, Scopelliti R., Zakeeruddin SM, Gratzel M., Dyson PJ. Synthesis, characterisation and biological properties of gold(III) compounds with modified bipyridine and bipyridylamine ligands. *Dalton Trans*. 2010; 39 (9): 2239-2245.
 - Castedo M., Perfettini JL, Roumier T., Andreau K., Medema R., Kroemer G. Cell death by mitotic catastrophe: a molecular definition. *Oncogene*. 2004; 23:2825–2837.
 - Cattel L, Ceruti M, Dosio F. From conventional to stealth liposomes: a new frontier in cancer chemotherapy. *Tumori*. 2003; 89(3):237-49.
 - Cecconi F, Levine B. The role of autophagy in mammalian development: cell makeover rather than cell death. *Dev Cell* 2008; 15: 344–57.
 - Chapman D. Fluidity and phase transitions of cell membranes. *Biomembranes*. 1975; 7:1-9.
 - Chen R, Kang R, Fan XG, Tang D. Release and activity of histone in diseases. *Cell Death Dis*. 2014; 5:e1370.
 - Chen T., Mei WJ, Wong YS, Liu J., Liu Y., Xie HS, Zheng WJ. Chiral ruthenium polypyridyl complexes as mitochondria-targeted apoptosis inducers. *Med. Chem. Commun.*, 2010; 1: 73–75.
 - Chidambaram M, Manavalan R, Kathiresan K. Nanotherapeutics to overcome conventional cancer chemotherapy limitations. *J Pharm Pharm Sci*. 2011; 14(1):67-77.
 - Choudhuri S. From Waddington's epigenetic landscape to small noncoding RNA: some important milestones in the history of epigenetics research. *Toxicol Mech Methods*. 2011; 21(4):252-74.
 - Christofferson D., Yuan J. Necroptosis as an alternative form of programmed cell death *Curr Opin Cell Biol*. 2010; 22(2): 263–268.
 - Ciuffreda L, Di Sanza C, Incani UC, Milella M. The mTOR pathway: a new target in cancer therapy. *Curr Cancer Drug Targets* 2010; 10: 484–495.
 - Clarke M.J. Zhu F, Frasca DR. Non-platinum chemotherapeutic metallopharmaceuticals *Chem. Rev.*, 1999; 99(9): 2511–2533
 - Clarke MJ, Bitler S, Rennert D, Buchbinder M, Kelman AD. Reduction and subsequent binding of ruthenium ions

- catalyzed by subcellular components. *J Inorg Biochem.* 1980; 12(1):79-87.
- Corcé V, Gouin SG, Renaud S, Gaboriau F, Deniaud D. Recent advances in cancer treatment by iron chelators. *Bioorg Med Chem Lett.* 2016; 26(2):251-6.
 - Correa P, Piazzuelo MB, Camargo MC. The future of gastric cancer prevention. *Gastric Cancer.* 2004; 7(1):9-16.
 - Corrin ML, Harkins WD. Determination of the critical concentration for micelle formation in solutions of colloidal electrolytes by the spectral change of a dye. *J Am Chem Soc.* 1947; 69(3):679-83.
 - Cosse JP, Rommelaere G, Ninane N, Arnould T, Michiels C. BNIP3 protects HepG2 cells against etoposide-induced cell death under hypoxia by an autophagy-independent pathway. *Biochem Pharmacol* 2010; 80(8):1160–9
 - Cowling V, Downward J. Caspase-6 is the direct activator of caspase-8 in the cytochrome c-induced apoptosis pathway: absolute requirement for removal of caspase-6 prodomain. *Cell Death Differ.* 2002; 9(10):1046-56.
 - Cruz PM, Mo H, McConathy WJ, Sabnis N, Lacko AG. The role of cholesterol metabolism and cholesterol transport in carcinogenesis: a review of scientific findings, relevant to future cancer therapeutics. *Front Pharmacol.* 2013; 4:119.
- D**
- Danial NN, Korsmeyer SJ. Cell death: critical control points. *Cell.* 2004; 116:205–219.
 - Davey GE, Davey CA. Chromatin - a new, old drug target? *Chem Biol Drug Des.* 2008; 72(3):165-70.
 - De Castro C., Molinaro A., Lanzetta R., Silipo A., Parrilli M., Lipopolysaccharide structures from *Agrobacterium* and *Rhizobiaceae* species, *Carbohydr Res.* 2008; 343(12): 1924-1933.
 - De Smet C, Lurquin C, Lethé B, Martelange V, Boon T. DNA methylation is the primary silencing mechanism for a set of germ line- and tumor-specific genes with a CpG-rich promoter. *Mol Cell Biol.* 1999; 19(11):7327-35.
 - Degterev A, Boyce M, Yuan J. A decade of caspases. *Oncogene.* 2003; 22(53):8543-67.
 - Dekker F.J., H.J.Haisma, Histoneacetyl transferases as emerging drug targets, *Drug Discov.Today* 2009; 14(19–20):942–48.
 - D'Errico G, Silipo A, Mangiapia G, Molinaro A, Paduano L, Lanzetta R. Mesoscopic and microstructural characterization of liposomes formed by the lipooligosaccharide from *Salmonella minnesota* strain 595 (Re mutant). *Phys Chem Chem Phys.* 2009; 11(13):2314-22.
 - D'Errico G, Silipo A, Mangiapia G, Vitiello G, Radulescu A, Molinaro A, Lanzetta R, Paduano L.

Characterization of liposomes by lipopolysaccharides from *Burkholderia cenocepacia*, *Burkholderia multivorans* and *Agrobacterium tumefaciens*: from the molecular structure to the aggregate architecture. *Phys Chem Chem Phys*. 2010; 12(41):13574-85.

- Din FV, Valanciute A, Houde VP, Zibrova D, Green KA, Sakamoto K et al. Aspirin inhibits mTOR signaling, activates AMP-activated protein kinase, and induces autophagy in colorectal cancer cells. *Gastroenterology* 2012; 142: (7)1504–1515.
- Duan X, Liu D, Chan C, Lin W. Polymeric Micelle-mediated Delivery of DNA-Targeting Organometallic complexes for Resistant Ovarian Cancer Treatment. *Small*. 2015; 11(32):3962-72.
- Dunai Z, Bauer PI, Mihalik R. Necroptosis: biochemical, physiological and pathological aspects. *Pathol Oncol Res*. 2011; 17(4):791-800.

E

- Elmore S. Apoptosis: a review of programmed cell death. *Toxicol Pathol*. 2007; 35(4):495-516
- Estanqueiro M, Amaral MH, Conceição J, Sousa Lobo JM Nanotechnological carriers for cancer chemotherapy: the state of the art. *Colloids Surf B Biointerfaces*. 2015; 126:631-48.
- Eum KH, Lee M. Crosstalk between autophagy and apoptosis in the regulation of paclitaxel-induced cell death in v-Ha-ras-transformed fibroblasts. *Mol Cell Biochem* 2011; 348:61–8.

F

- Falahi F, van Kruchten M, Martinet N, Hospers GA, Rots MG. Current and upcoming approaches to exploit the reversibility of epigenetic mutations in breast cancer. *Breast Cancer Res*. 2014; 16(4):412.
- Farooqi AA, Li KT, Fayyaz S, Chang YT, Ismail M, Liaw CC, Yuan SS, Tang JY, Chang HW. Anticancer drugs for the modulation of endoplasmic reticulum stress and oxidative stress. *Tumour Biol*. 2015; 36(8):5743-52.
- Felsenfeld G. Chromatin. *Nature*. 1978; 271 (5641): 115-22
- Ferlay J, Soerjomataram I, Dikshit R, Eser S, Mathers C, Rebelo M, Parkin DM, Forman D, Bray F. Cancer incidence and mortality worldwide: sources, methods and major patterns in GLOBOCAN 2012. *Int J Cancer*. 2015 Mar 1;136(5):E359-86.
- Flexman JA, Yung A, Yapp DT, Nq SS, Kozłowski P. Assessment of vessel size by MRI in an orthotopic model of human pancreatic cancer. *Conf Proc IEEE Eng Med Biol Soc*. 2008; 2008:851-4.
- Fulda S. Therapeutic exploitation of necroptosis for cancer therapy. *Semin. Cell Dev Biol* 2014; 35: 51–56

- Fulda S., Debatin KM Extrinsic versus intrinsic apoptosis pathways in anticancer chemotherapy. *Oncogene*. 2006; 25: 4798–4811.
- Fulda S, Debatin KM. Apoptosis signaling in tumor therapy. *Ann N Y Acad Sci*. 2004; 1028:150-6.

G

- Gabizon A, Shmeeda H, Horowitz AT, Zalipsky S. Tumor cell targeting of liposome entrapped drugs with phospholipid-anchored folic acid-PEG conjugates. *Adv Drug Deliv Rev*. 2004; 56(8):1177-92.
- Gabler C, Blank N, Hieronymus T, Schiller M, Berden JH, Kalden JR, Lorenz HM. Extranuclear detection of histones and nucleosomes in activated human lymphoblasts as an early event in apoptosis. *Ann Rheum Dis*. 2004; 63(9):1135-44.
- Gabler C, Blank N, Winkler S, Kalden JR, Lorenz HM. Accumulation of histones in cell lysates precedes expression of apoptosis-related phagocytosis signals in human lymphoblasts. *Ann N Y Acad Sci*. 2003; 1010:221-4.
- Gaiddon C., Jeannequin P., Bischoff P., Pfeiffer M., Sirlin C., Loeffler, J. P. Ruthenium(II)-derived organometallic compounds induce cytostatic and cytotoxic effects on mammalian cancer cell lines through p53-dependent and p53-

- independent mechanisms. *J Pharmacol Exp Ther*. 2005; 315(3): 1403-1411.
- Galanski M, Arion VB, Jakupec MA, Keppler BK. Recent developments in the field of tumor-inhibiting metal complexes. *Curr Pharm Des*. 2003; 9(25):2078-89.
- Gallinari P, Di Marco S, Jones P, Pallaoro M, Steinkühler C. HDACs, histone deacetylation and gene transcription: from molecular biology to cancer therapeutics. *Cell Res*. 2007; 17(3):195-211.
- Galluzzi L, Vitale I, Senovilla L, Eisenberg T, Carmona-Gutierrez D, Vacchelli E, Robert T, Ripoche H, Jägemann N, Paccard C, Servant N, Hupé P, Lazar V, Dessen P, Barillot E, Zischka H, Madeo F, Kroemer G. Independent transcriptional reprogramming and apoptosis induction by cisplatin. *Cell Cycle*. 2012; 11(18):3472-80.
- Ganesan A, Nolan L, Crabb SJ, Packham G. Epigenetic therapy: histone acetylation, DNA methylation and anti-cancer drug discovery. *Curr Cancer Drug Targets*. 2009; 9(8):963-81.
- Garrard WT, Nobis P, Hancock R. Histone H3 disulfide reactions in interphase, mitotic, and native chromatin. *J Biol Chem*. 1977; 252(14):4962-7
- Gill KK, Kaddoumi A, Nazzal S. PEG-lipid micelles as drug carriers: physicochemical attributes, formulation principles and biological implication. *J Drug Target*. 2015; 23(3):222-31.

- Gissot A, Camplo M, Grinstaff MW, Barthélémy P. Nucleoside, nucleotide and oligonucleotide based amphiphiles: a successful marriage of nucleic acids with lipids. *Org Biomol Chem*. 2008; 6(8):1324-33.
- Glick D, Barth S, Macleod KF. Autophagy: cellular and molecular mechanisms. *J Pathol* 2010; 221(1): 3–12.
- Glozak MA, Seto E. Histone deacetylases and cancer. *Oncogene*. 2007; 26(37):5420-32.
- Gołąbek K, Strzelczyk JK, Wiczkowski A, Michalski M. Potential use of histone deacetylase inhibitors in cancer therapy. *Contemp Oncol (Pozn)*. 2016; 19(6):436-40.
- Green DR, Llambi F. Cell Death Signaling. *Cold Spring Harb Perspect Biol*. 2015; 7(12).
- Gregoriadis G, Wills EJ, Swain CP, Tavill AS. Drug-carrier potential of liposomes in cancer chemotherapy. *Lancet*. 1974; 1(7870):1313-6.
- Grobden B, De Deyn PP, Slegers H. Rat C6 glioma as experimental model system for the study of glioblastoma growth and invasion. *Cell Tissue Res*. 2002; 310(3):257-70.
- Groessl M, Terenghi M, Casini A, Elviri L, Lobinski R, Dyson PJ. Reactivity of anticancer metallodrugs with serum proteins: new insights from size exclusion chromatography-ICP-MS. *J Anal At Spectrom*. 2010; 25(3): 305-313
- Groessl M, Zava O, Dyson PJ. Cellular uptake and subcellular distribution of ruthenium-based metallodrugs under clinical investigation versus cisplatin. *Metallomics*. 2011; 3(6):591-9.
- Gryder BE, Sodji QH, Oyelere AK. Targeted cancer therapy: giving histone deacetylase inhibitors all they need to succeed. *Future Med Chem*. 2012; 4(4):505-24.

H

- Hanif M, Babak MV, Hartinger CG. Development of anticancer agents: wizardry with osmium. *Drug Discov Today*. 2014; 19(10):1640-8.
- Hankins HM, Baldrige RD, Xu P, Graham TR. Role of flippases, scramblases and transfer proteins in phosphatidylserine subcellular distribution. *Traffic*. 2015; 16(1):35-47.
- Hartinger C.G., Zorbas-Seifried S., Jakupec M.A., Kynast B., Zorbas H., Keppler B.K. From bench to bedside--preclinical and early clinical development of the anticancer agent indazolium trans-[tetrachlorobis(1H-indazole)ruthenate(III)] (KP1019 or FFC14A). *Journal Inorg Biochem*. 2006; 100 (5-6) 891–904
- Hayes ME, Drummond DC, Hong K, Park JW, Marks JD, Kirpotin DB. Assembly of nucleic acid-lipid nanoparticles from aqueous-organic

- monophases. *Biochim Biophys Acta*. 2006; 1758(4):429-42.
- Hayes P, Knaus UG. Balancing reactive oxygen species in the epigenome: NADPH oxidases as target and perpetrator. *Antioxid Redox Signal*. 2013; 18(15):1937-45.
 - Heacock AM, Agranoff BW. CDP-diacylglycerol synthase from mammalian tissues. *Biochim Biophys Acta*. 1997; 1348(1-2):166-72.
 - Hearn JM, Romero-Canelón I, Munro AF, Fu Y, Pizarro AM, Garnett MJ, McDermott U, Carragher NO, Sadler PJ. Potent organo-osmium compound shifts metabolism in epithelial ovarian cancer cells. *Proc Natl Acad Sci U S A*. 2015; 112(29):E3800-5.
 - Hillaireau H, Couvreur P. Nanocarriers' entry into the cell: relevance to drug delivery. *Cell Mol Life Sci*. 2009; 66(17):2873-96.
 - Holden P., Horton WA. Crude subcellular fractionation of cultured mammalian cell lines. *BMC Res Notes*. 2009; 2: 243.
 - Hosta-Rigau L, Zhang Y, Teo BM, Postma A, Städler B. Cholesterol-a biological compound as a building block in bionanotechnology. *Nanoscale*. 2013; 5(1):89-109.
 - Hutchinson L. Gastrointestinal cancer: a step closer to combating acquired resistance in CRC. *Nat Rev Clin Oncol*. 2012; 9(8):428.
- I**
- Immordino ML, Dosio F., and Cattel L. "Stealth liposomes: review of the basic science, rationale, and clinical applications, existing and potential" *Int J Nanomedicine*. 2006; 1(3): 297–315.
 - Izuishi K, Kato K, Ogura T, Kinoshita T, Esumi H. Remarkable tolerance of tumor cells to nutrient deprivation: possible new biochemical target for cancer therapy. *Cancer Res*. 2000; 60(21):6201-7.
- J**
- Jahr S, Hentze H, Englisch S, Hardt D, Fackelmayer FO, Hesch RD, Knippers R. DNA fragments in the blood plasma of cancer patients: quantitations and evidence for their origin from apoptotic and necrotic cells. *Cancer Res*. 2001; 61(4):1659-65.
 - Janib SM, Moses AS, MacKay JA. Imaging and drug delivery using theranostic nanoparticles. *Adv Drug Deliv Rev*. 2010; 62(11):1052-63.
 - Jänicke RU, Sprengart ML, Wati MR, Porter AG. Caspase-3 is required for DNA fragmentation and morphological changes associated with apoptosis. *J Biol Chem*. 1998; 273(16):9357-60.
 - Jenuwein T, Allis CD. Translating the histone code. *Science*. 2001; 293(5532):1074-80.
 - Jhaveri A, Torchilin V. Intracellular delivery of nanocarriers and targeting to

subcellular organelles. *Expert Opin Drug Deliv.* 2016;13(1):49-70.

- Jiang C, Pugh BF. Nucleosome positioning and gene regulation: advances through genomics. *Nat Rev Genet* 2009; 10(3): 161–172
- Jögi A, Vaapil M, Johansson M, Pählman S. Cancer cell differentiation heterogeneity and aggressive behavior in solid tumors. *Ups J Med Sci.* 2012; 117(2):217-24.

K

- Kang C, Song JJ, Lee J, Kim MY. Epigenetics: an emerging player in gastric cancer. *World J Gastroenterol.* 2014; 20(21):6433-47.
- Kapitza S, Pongratz M, Jakupec MA, Heffeter P, Berger W, Lackinger L, Keppler BK, Marian B. Heterocyclic complexes of ruthenium(III) induce apoptosis in colorectal carcinoma cells. *J Cancer Res Clin Oncol.* 2005; 131(2):101-10
- Kapitza S., Jakupec M.A., Uhl M., Keppler B.K., Marian B., The heterocyclic ruthenium(III) complex KP1019 (FFC14A) causes DNA damage and oxidative stress in colorectal tumor cells. *Cancer Letters* 2005; 226(2):115–121.
- Kasinsky HE, Lewis JD, Dacks JB, Ausio J Origin of H1 linker histones. *FASEB J* 2001; 15(1): 34–42.
- Katayama M, Kawaguchi T, Berger MS, Pieper RO. DNA damaging agent-induced autophagy produces a cytoprotective adenosine triphosphate surge in malignant glioma cells. *Cell Death Differ.* 2007; 14(3):548-58
- Kersten L, Bräunlich H, Keppler BK, Gliesing C, Wendelin M, Westphal J. Comparative nephrotoxicity of some antitumour-active platinum and ruthenium complexes in rats. *J Appl Toxicol.* 1998; 18(2):93-101.
- Khalaila I, Bergamo A, Bussy F, Sava G, Dyson PJ. The role of cisplatin and NAMI-A in relation to combination therapy. *Int J Oncol.* 2006; 29(1):261-8.
- Kim B, Srivastava SK, Kim SH. Caspase-9 as a therapeutic target for treating cancer. *Expert Opin Ther Targets.* 2015; 19(1):113-27.
- Klajner M., Hebraud P., Sirlin C., Gaiddon C., Harlepp P. DNA binding to an anticancer organo-ruthenium complex. *J Phys Chem. B* 2010; 114 (44): 14041–14047
- Klajner M., Licon C., Fetzler L., Hebraud P., Mellitzer G., Pfeiffer M., Harlepp S., Gaiddon, C. Subcellular localization and transport kinetics of ruthenium organometallic anticancer compounds in living cells: a dose-dependent role for amino Acid and iron transporters. *Inorg Chem* 2014; 53(10): 5150-8
- Knop K, Hoogenboom R, Fischer D, Schubert US. Poly(ethylene glycol) in drug delivery: pros and cons as well as potential alternatives. *Angew Chem Int Ed Engl.* 2010; 49(36):6288-308.

- Köberle B, Tomicic MT, Usanova S, Kaina B. *Biochim Biophys Acta*. Cisplatin resistance: preclinical findings and clinical implications. 2010; 1806(2):172-82.
- Kocoglu M., Badros A. The Role of Immunotherapy in Multiple Myeloma. *Pharmaceutics* 2016; 9(1).
- Koff JL, Ramachandiran S, Bernal-Mizrachi L. A time to kill: targeting apoptosis in cancer. *Int J Mol Sci*. 2015; 16(2):2942-55.
- Kouzarides T. Chromatin modifications and their function. *Cell*. 2007; 128(4): 693-705
- Kraft JC, Freeling JP, Wang Z, Ho RJ. Emerging research and clinical development trends of liposome and lipid nanoparticle drug delivery systems. *J Pharm Sci*. 2014; 103(1):29-52.
- Krieg AM, Tonkinson J, Matson S, Zhao Q, Saxon M, Zhang LM, Bhanja U, Yakubov L, Stein CA. Modification of antisense phosphodiester oligodeoxynucleotides by a 5' cholesteryl moiety increases cellular association and improves efficacy. *Proc Natl Acad Sci U S A*. 1993; 90(3):1048-52.
- Krysko DV, Vanden Berghe T, D'Herde K, Vandenabeele P. Apoptosis and necrosis: detection, discrimination and phagocytosis. *Methods*. 2008; 44(3):205-21.
- Kuhn PS, Büchel GE, Jovanović KK, Filipović L, Radulović S, Raptap P, Arion VB. Osmium(III) analogues of KP1019: electrochemical and chemical synthesis, spectroscopic characterization, X-ray crystallography, hydrolytic stability, and antiproliferative activity. *Inorg Chem*. 2014; 53(20):11130-9.
- Kumar B, Yadav A, Lang JC, Teknos TN, Kumar P. Suberoylanilide hydroxamic acid (SAHA) reverses chemoresistance in head and neck cancer cells by targeting cancer stem cells via the downregulation of nanog. *Genes Cancer*. 2015; 6(3-4):169-81.
- Kumar R, Li DQ, Müller S, Knapp S. Epigenomic regulation of oncogenesis by chromatin remodeling. *Oncogene*. 2016. [Epub ahead of print]
- Kurosaka K, Takahashi M, Watanabe N, Kobayashi Y. Silent cleanup of very early apoptotic cells by macrophages. *J Immunol*. 2003; 171(9):4672-9.

L

- Lacko AG, Nair M, Prokai L, McConathy WJ. Prospects and challenges of the development of lipoprotein-based formulations for anti-cancer drugs. *Expert Opin Drug Deliv*. 2007; 4(6):665-75.
- Lam J, Herant M, Dembo M, Heinrich V. Baseline mechanical characterization of J774 macrophages. *Biophys J*. 2009; 96(1):248-54.
- Lambert LA, Qiao N, Hunt KK, Lambert DH, Mills GB, Meijer L, Keyomarsi K. Autophagy: a novel mechanism of synergistic cytotoxicity between doxorubicin and roscovitine in a sarcoma

- model. *Cancer Res.* 2008; 68(19):7966-74.
- Lammers M., Follmann, H. "The ribonucleotide reductases - a unique group of metalloenzymes essential for cell-proliferation" *Struct. Bonding* 1983; 54: 27–91
 - Latham JA, Dent SY. Cross-regulation of histone modifications. *Nat Struct Mol Biol* 2007; 14(11): 1017–1024.
 - Lawaczeck R, Nandi PK, Nicolau C. Interaction of negatively charged liposomes with nuclear membranes: adsorption, lipid mixing and lysis of the vesicles. *Biochim Biophys Acta.* 1987; 903(1):123-31.
 - Lee SB, Tong SY, Kim JJ, Um SJ, Park JS. Caspase-independent autophagic cytotoxicity in etoposide-treated CaSki cervical carcinoma cells. *DNA Cell Biol* 2007; 26(10):713–20.
 - Leijen S., Burgers S. A., Baas P., Pluim D., Tibben M., van Werkhoven E., Alessio E., Sava G., Beijnen J. H. and Schellens J. H. M., Preliminary Phase II studies in combination with gemcitabine in non-small cell lung cancer patients, *Invest. New Drugs.* 2015; 33(1): 201–214.
 - Levina A, Mitra A, Lay PA. Recent developments in ruthenium anticancer drugs. *Metallomics.* 2009; 1(6):458-70.
 - Liang Y, Yan C, Schor NF. Apoptosis in the absence of caspase 3. *Oncogene.* 2001; 20(45):6570-8.
 - Liu HK, Berners-Price SJ, Wang F, Parkinson JA, Xu J, Bella J, Sadler PJ. Diversity in guanine-selective DNA binding modes for an organometallic ruthenium arene complex. *Angew Chem Int Ed Engl.* 2006; 45(48):8153-6.
 - Liu P, Wu BY, Liu J, Dai YC, Wang YJ, Wang KZ. Inorg Chem. DNA Binding and Photocleavage Properties, Cellular Uptake and Localization, and in-Vitro Cytotoxicity of Dinuclear Ruthenium[II] Complexes with Varying Lengths in Bridging Alkyl Linkers. *Inorg Chem.* 2016; 55(4):1412-22.
 - Lu C, Stewart DJ, Lee JJ, Ji L, Ramesh R, Jayachandran G, Nunez MI, Wistuba II, Erasmus JJ, Hicks ME, Grimm EA, Reuben JM, Baladandayuthapani V, Templeton NS, McMannis JD, Roth JA. Phase I clinical trial of systemically administered TUSC2(FUS1)-nanoparticles mediating functional gene transfer in humans. *PLoS One.* 2012; 7(4):e34833.
 - Lu H, Blunden BM, Scarano W, Lu M, Stenzel MH Anti-metastatic effects of RAPTA-C conjugated polymeric micelles on two-dimensional (2D) breast tumor cells and three-dimensional (3D) multicellular tumor spheroids. *Acta Biomater.* 2015; 32:68-76.
 - Luger K, Mäder AW, Richmond RK, Sargent DF, Richmond TJ Crystal structure of the nucleosome core particle at 2.8 Å resolution. *Nature.* 1997; 389(6648):251-60.
 - Lum JJ, DeBerardinis RJ, Thompson CB. Autophagy in metazoans: cell survival in

the land of plenty. *Nat Rev Mol Cell Biol.* 2005; 6:439–448.

- Luo Y, Ziebell MR, Prestwich GD. “A hyaluronic acid-taxol antitumor bioconjugate targeted to cancer cells”. *Biomacromolecules.* 2000;1(2): 208-18

M

- Mabrey S., Mateo PL, Sturtevant JM. High-sensitivity scanning calorimetric study of mixtures of cholesterol with dimyristoyl- and dipalmitoylphosphatidylcholines. *Biochemistry.* 1978; 17(12):2464-8
- Maillet A, Yadav S, Loo YL, Sachaphibulkij K, Pervaiz S. A novel Osmium-based compound targets the mitochondria and triggers ROS-dependent apoptosis in colon carcinoma. *Cell Death Dis.* 2013; 4:e653.
- Maiuri MC, Zalckvar E, Kimchi A, Kroemer G. Self-eating and self killing: crosstalk between autophagy and apoptosis. *Nat Rev Mol Cell Biol.* 2007; 8(9):741-52.
- Mangiapia G, Accardo A, Lo Celso F, Tesauro D, Morelli G, Radulescu A, et al. Mixed micelles composed of peptides and gadolinium complexes as tumorspecific contrast agents in MRI: a SANS study. *J Phys Chem B* 2004;108: 17611e7
- Mangiapia G, D'Errico G, Simeone L, Irace C, Radulescu A, Di Pascale A, Colonna A, Montesarchio D, Paduano L. Ruthenium-based complex

nanocarriers for cancer therapy. *Biomaterials.* 2012; 33(14):3770-82.

- Marks P, Rifkind RA, Richon VM, Breslow R, Miller T, Kelly WK. Histone deacetylases and cancer: causes and therapies. *Nat Rev Cancer.* 2001; 1(3):194-202.
- Marnett LJ. Oxyradicals and DNA damage. *Carcinogenesis.* 2000; 21:361–370
- Marsh D. Thermodynamics of phospholipid self-assembly. *Biophys J.* 2012; 102(5):1079-87.
- Maruyama K., “Intracellular targeting delivery of liposomal drugs to solid tumors based on EPR effects” *Adv Drug Deliv Rev.* 2011; 63(3):161-9.
- Masood R, Husain SR, Rahman A, Gill P. Potentiation of cytotoxicity of Kaposi's sarcoma related to immunodeficiency syndrome (AIDS) by liposome-encapsulated doxorubicin. *AIDS Res Hum Retroviruses.*1993; 9:741–6.
- Matougui N, Boge L, Groo AC, Umerska A, Ringstad L, Bysell H, Saulnier P. Lipid-based nanoformulations for peptide delivery. *Int J Pharm.* 2016; 502(1-2):80-97.
- Meek DW, Regulation of the p53 response and its relationship to cancer. *Biochem J.* 2015; 469(3):325-46.
- Mendes F., Groessl M., Nazarov AA., Tsybin YO, Sava G., Santos I., Dyson PJ, Casini A. Metal-based inhibition of poly(ADP-ribose) polymerase--the

- guardian angel of DNA. *J. Med. Chem.*, 2011; 54(7): 2196-2206.
- Meng X, Leyva ML, Jenny M, Gross I, Benosman S, Fricker B, Harlepp S, Hébraud P, Boos A, Wlosik P, Bischoff P, Sirlin C, Pfeffer M, Loeffler JP, Gaiddon C. A ruthenium-containing organometallic compound reduced tumor growth through induction of the endoplasmic reticulum stress gene CHOP. *Cancer Res.* 2009 Jul 1; 69(13):5458-66.
 - Messori L, Merlino A. Ruthenium metalation of proteins: the X-ray structure of the complex formed between NAMI-A and hen egg white lysozyme. *Dalton Trans.* 2014; 43(16):6128-31.
 - Midorikawa K, Murata M, Kawanishi S. Histone peptide AKRHRK enhances H₂O₂-induced DNA damage and alters its site specificity. *Biochem Biophys Res Commun.* 2005; 333(4):1073-7.
 - Mikhed Y, Görlach A, Knaus UG, Daiber A. Redox regulation of genome stability by effects on gene expression, epigenetic pathways and DNA damage/repair. *Redox Biol.* 2015; 5:275-89.
 - Mikkelsen TS, Ku M, Jaffe DB, et al. Genome-wide maps of chromatin state in pluripotent and lineage-committed cells. *Nature.* 2007; 448(7153):553–560
 - Moghaddam B, Ali MH, Wilkhu J, Kirby DJ, Mohammed AR, Zheng Q, Perrie Y. The application of monolayer studies in the understanding of liposomal formulations. *Int J Pharm.* 2011; 417(1-2):235-44.
 - Molinaro A, Holst O, Di Lorenzo F, Callaghan M, Nurisso A, D'Errico G, Zamyatina A, Peri F, Berisio R, Jerala R, Jiménez-Barbero J, Silipo A, Martín-Santamaría S. Chemistry of lipid A: at the heart of innate immunity. *Chemistry.* 2015; 21(2):500-19.
 - Monneret C. Platinum anticancer drugs. From serendipity to rational design. *AnnPharm Fr.* 2011; 69(6):286-95
 - Monteiro N, Martins A, Reis RL, Neves NM. Liposomes in tissue engineering and regenerative medicine *J R Soc Interface.* 2014; 11(101): 20140459.
 - Moran AP. Relevance of fucosylation and Lewis antigen expression in the bacterial gastroduodenal pathogen *Helicobacter pylori*. *Carbohydr Res.* 2008; 343(12):1952-65.
 - Muggia FM, Bonetti A, Hoeschele JD, Rozenzweig M, Howell SB. Platinum antitumor complexes: 50 year since Barnett Rosenberg's discovery. *J Clin Oncol.* 2015; 33(35):4219-26.
 - Mukubou H, Tsujimura T, Sasaki R, Ku Y. The role of autophagy in the treatment of pancreatic cancer with gemcitabine and ionizing radiation. *Int J Oncol* 2010; 37:821–8.
 - Muralidharan S, Sasi SP, Zuriaga MA, Hirschi KK, Porada CD, Coleman MA, Walsh KX, Yan X, Goukassian DA. Ionizing Particle Radiation as a Modulator of Endogenous Bone Marrow

- Cell Reprogramming: Implications for Hematological Cancers. *Front Oncol.* 2015; 5:231.
- Muratani M, Deng N, Ooi WF, Lin SJ, Xing M, Xu C, Qamra A, Tay ST, Malik S, Wu J, Lee MH, Zhang S, Tan LL, Chua H, Wong WK, Ong HS, Ooi LL, Chow PK, Chan WH, Soo KC, Goh LK, Rozen S, Teh BT, Yu Q, Ng HH, Tan P. Nanoscale chromatin profiling of gastric adenocarcinoma reveals cancer-associated cryptic promoters and somatically acquired regulatory elements. *Nat Commun.* 2014; 5:4361.
 - Murray BS, Babak MV, Hartinger CG, Dyson PJ. The development of RAPTA compounds for the treatment of tumors *Coordination Chemistry Reviews* 2016; 306: 86–114
 - Murtola TJ, Syväälä H, Pennanen P, Bläuer M, Solakivi T, Ylikomi T, Tammela TL. The importance of LDL and cholesterol metabolism for prostate epithelial cell growth. *PLoS One.* 2012; 7(6):e39445.
 - Musumeci D, Montesarchio D. Synthesis of a cholesteryl-HEG phosphoramidite derivative and its application to lipid-conjugates of the anti-HIV 5'TGGGAG^{3'} Hotoda's sequence. *Molecules.* 2012; 17(10):12378-92.
 - Musumeci D, Rozza L, Merlino A, Paduano L, Marzo T, Massai L, Messori L, Montesarchio D. Interaction of anticancer Ru(III) complexes with single stranded and duplex DNA model systems. *Dalton Trans.* 2015; 44(31):13914-25.
- ## N
- Nikolettou V, Markaki M, Palikaras K, Tavernarakis N. Crosstalk between apoptosis, necrosis and autophagy. *Biochim Biophys Acta.* 2013; 1833(12):3448-59.
 - Notte A., Leclere L., Michiels C. Autophagy as a mediator of chemotherapy-induced cell death in cancer. *Biochemical Pharmacology.* 2011; 82(5): 427–434.
 - Nowak-Sliwinska P, van Beijnum JR, Casini A, Nazarov AA, Wagnieres G, van den Bergh H, Dyson PJ, Griffioen AW. Organometallic ruthenium(II) arene compounds with antiangiogenic activity. *J Med Chem.* 2011; 54(11):3895-902.
 - Nunes AM, Zavitsanos K, Del Conte R, Malandrinos G, Hadjiliadis N *Inorg Chem.* The possible role of 94-125 peptide fragment of histone H2B in nickel-induced carcinogenesis. 2010; 49(12):5658-68
- ## O
- Oberoi HS, Nukolova NV, Kabanov AV, Bronich TK. Nanocarriers for delivery of platinum anticancer drugs. *Adv Drug Deliv Rev.* 2013; 65(13-14):1667-85.
 - Okamura M, Hashimoto K, Shimada J, Sakagami H. Apoptosis-inducing

- activity of cisplatin (CDDP) against human hepatoma and oral squamous cell carcinoma cell lines. *Anticancer Res.* 2004; 24(2B):655-61.
- Olive PL, Banáth JP. The comet assay: a method to measure DNA damage in individual cells. *Nat Protoc.* 2006; 1(1):23-9.
- P**
- Pacher P, Beckman JS, Liaudet L. Nitric oxide and peroxynitrite in health and disease. *Physiol Rev.* 2007; 87(1):315-424.
 - Palade C, Ciurea AV, Nica DA, Savu R, Moisa HA. Interference of apoptosis in the pathophysiology of subarachnoid hemorrhage. *Asian J Neurosurg.* 2013; 8(2): 106-11
 - Parker JP, Ude Z, Marmion CJ. Exploiting developments in nanotechnology for the preferential delivery of platinum-based anti-cancer agents to tumours: targeting some of the hallmarks of cancer. *Metallomics.* 2016; 8(1):43-60.
 - Peacock AF, Sadler PJ. Medicinal organometallic chemistry: designing metal arene complexes as anticancer agents. *Chem Asian J.* 2008; 3(11):1890-9.
 - Pelillo C, Bergamo A, Mollica H, Bestagno M, Sava G. Colorectal Cancer Metastases Settle in the Hepatic Microenvironment Through $\alpha 5\beta 1$ Integrin. *J Cell Biochem* 2015; 116(10): 2385-96.
 - Philpott NJ, Elebute MO, Powles R, Treleaven JG, Gore M, Dainton MG, Min T, Swansbury GJ, Catovsky D. Platinum agents and secondary myeloid leukaemia: two cases treated only with platinum-based drugs. *Br J Haematol.* 1996; 93(4):884-7
 - Pluim D, van Waardenburg RC, Beijnen JH and Schellens JH: Cytotoxicity of the organic ruthenium anticancer drug NAMI-A is correlated with DNA binding in four different human tumour cell lines. *Cancer Chemother Pharmacol* 2004; 54: 71-78.
 - Poon RT, Borys N. Lyso-thermosensitive liposomal doxorubicin: a novel approach to enhance efficacy of thermal ablation of liver cancer. *Expert Opin Pharmacother.* 2009; 10(2):333-43.
 - Postberg J, Forcob S, Lipps HJ The evolutionary history of histone H3 suggests a deep eukaryotic root of chromatin modifying mechanisms. *BMC Evol Biol* 2010; 10: 259.
 - Presant CA, Scolaro M, Kennedy P, Blayney DW, Flanagan B, Lisak J, et al. Liposomal daunorubicin treatment of HIV-associated Kaposi's sarcoma. *Lancet.* 1993; 341:1242-3.
- R**
- Ramachandran S, Temple BR, Chaney SG, Dokholyan NV. Structural basis for the sequence-dependent effects of platinum-DNA adducts. *Nucleic Acids Res.* 2009; 37(8):2434-48.

- Ramakrishnan V. Histone structure and the organization of the nucleosome. *Annu Rev Biophys Biomol Struct.* 1997; 26:83-112.
- Reedijk J, Platinum Anticancer Coordination Compounds: Study of DNA Binding Inspires New Drug Design *Eur. J. Inorg. Chem.* 2009; 10: 1303-1312
- Ricci MS, Wei-Xing Zong Chemotherapeutic Approaches for Targeting Cell Death Pathways *Oncologist.* 2006; 11(4): 342–357.
- Robles SJ, Adami GR. Agents that cause DNA double strand breaks lead to p16INK4a enrichment and the premature senescence of normal fibroblasts. *Oncogene.* 1998; 16:1113–1123.
- Roque A, Ponte I, Suau P Macromolecular crowding induces a molten globule state in the C-terminal domain of histone H1. *Biophys J* 2009; 93(6): 2170–2177.
- Rosenberg B, VanCamp L, Trosko JE, Mansour VH. «Platinum compounds: a new class of potent antitumor agents” *Nature* 1969; 222(5191):385-6.
- Rubas W, Supersaxo A, Weder HG, Hartmann HR, Hengartner H, Schott H, Schwendener R, *Int. J. Cancer,* 1986; 37(1): 149–154.
- Ryabov AD, Soukharev VS, Alexandrova L, Le Lagadec R, Pfeffer M. Low-Potential Cyclometalated Osmium(II) Mediators of Glucose Oxidase. *Inorg. Chem.* 2003; 42(21): 6598–6600.
- Sabnis N, Lacko AG. Drug delivery via lipoprotein-based carriers: answering the challenges in systemic therapeutics. *Ther Deliv.* 2012; 3(5):599-608.
- Saelens X, Festjens N, Vande Walle L, van Gurp M, van Loo G, Vandenameele P. Toxic proteins released from mitochondria in cell death. *Oncogene* 2004; 23(16):2861-74.
- Saikusa K, Shimoyama S, Asano Y, Nagadoi A, Sato M, Kurumizaka H, Nishimura Y, Akashi S. Charge-neutralization effect of the tail regions on the histone H2A/H2B dimer structure. *Protein Sci.* 2015; 24(8):1224-31.
- Sava G, Bergamo A. Ruthenium-based compounds and tumour growth control (review). *Int J Oncol.* 2000; 17(2):353-65.
- Sava G, Zorzet S, Turrin C, Vita F, Soranzo M, Zabucchi G, Cocchietto M, Bergamo A, DiGiovine S, Pezzoni G, Sartor L, Garbisa S. Dual Action of NAMI-A in inhibition of solid tumor metastasis: selective targeting of metastatic cells and binding to collagen. *Clin Cancer Res.* 2003; 9(5):1898-905.
- Sava G, Gagliardi R, Cocchietto M, Clerici K, Capozzi I, Marrella M, Alessio E, Mestroni G, Milanino R. Comparison of the effects of the antimetastatic compound ImH[trans-RuCl₄(DMSO)Im] (NAMI-A) on the arthritic rat and on MCa mammary carcinoma in mice. *Pathol Oncol Res.* 1998; 4(1):30-6.

- Savill J, Fadok V. Corpse clearance defines the meaning of cell death. *Nature*. 2000; 407(6805):784-8.
- Schulga P, Hartinger CG, Egger A, Reisner E, Galanski M, Jakupec MA, Keppler BK. Redox behavior of tumor-inhibiting ruthenium(III) complexes and effects of physiological reductants on their binding to GMP. *Dalton Trans*. 2006; (14):1796-802.
- Schmitt CA, Fridman JS, Yang M, Lee S, Baranov E, Hoffman RM, Lowe SW. A senescence program controlled by p53 and p16INK4a contributes to the outcome of cancer therapy. *Cell*. 2002; 109:335–346
- Schwendener RA., Supersaxo A., Rubas W., Weder HG, Hartmann HR, Schott H., Ziegler A., Hengartner H., *Biochem. Biophys. Res. Commun.*, 1985; 126(2): 660–666.
- Seymour LW, Ulbrich K, Steyger PS, Brereton M, Subr V, Strohal J, Duncan R. Tumour tropism and anti-cancer efficacy of polymer based doxorubicin prodrugs in the treatment of subcutaneous murine B16F10 melanoma. *Br J Cancer*. 1994; 70(4):636-41.
- Sharma R, Graham J, Blagden S, Gabra H Sustained platelet-sparing effect of weekly low dose paclitaxel allows effective, tolerable delivery of extended dose dense weekly carboplatin in platinum resistant/refractory epithelial ovarian cancer. *BMC Cancer*. 2011; 11:289.
- Shinjo K., Kondo Y. Targeting cancer epigenetics: Linking basic biology to clinical medicine. *Adv Drug Deliv Rev* 2015; 95:56-64.
- Shintani T, Klionsky DJ. Autophagy in health and disease: a double-edged sword. *Science*. 2004; 306:990–995.
- Shubassi G, Robert T, Vanoli F, Minucci S, Foiani M. Acetylation: a novel link between double-strand break repair and autophagy. *Cancer Res* 2012; 72: 1332–1335
- Siddik ZH. Cisplatin: mode of cytotoxic action and molecular basis of resistance. *Oncogene*. 2003; 22(47):7265-79.
- Simeone L, Mangiapia G, Irace C, Di Pascale A, Colonna A, Ortona O, De Napoli L, Montesarchio D, Paduano L. Nucleolipid nanovectors as molecular carriers for potential applications in drug delivery. *Mol Biosyst*. 2011; 7(11):3075-86.
- Simeone L, Mangiapia G, Vitiello G, Irace C, Colonna A, Ortona O, Montesarchio D, Paduano L. Cholesterol-based nucleolipid-ruthenium complex stabilized by lipid aggregates for antineoplastic therapy. *Bioconjug Chem*. 2012; 23(4):758-70.
- Singh V, Azad GK, Mandal P, Reddy MA, Tomar RS. Anti-cancer drug KP1019 modulates epigenetics and induces DNA damage response in *Saccharomyces cerevisiae*. *FEBS Lett*. 2014; 588(6):1044-52.

T

- Slesarev AI, Belova GI, Kozyavkin SA, Lake JA. Evidence for an early prokaryotic origin of histones H2A and H4 prior to the emergence of eukaryotes. *Nucl Ac Res* 1998; 26(2): 427–430.
- Soori H, Rabbani-Chadegani A, Davoodi J. Exploring binding affinity of oxaliplatin and carboplatin, to nucleoprotein structure of chromatin: spectroscopic study and histone proteins as a target. *Eur J Med Chem.* 2015; 89:844-50.
- Stano P, Bufali S, Pisano C, Bucci F, Barbarino M, Santaniello M, Carminati P, Luisi PL, Novel camptothecin analogue (gimatecan)-containing liposomes prepared by the ethanol injection method. *J Liposome Res.* 2004; 14(1-2):87-109
- Stebelska K, Wyrozumska P, Sikorski AF. PS exposure increases the susceptibility of cells to fusion with DOTAP liposomes. *Chem Biol Interact.* 2006; 160(2):165-74.
- Sui X, Chen R, Wang Z, Huang Z, Kong N, Zhang M, Han W, Lou F, Yang J, Zhang Q, Wang X, He C, Pan H. Autophagy and chemotherapy resistance: a promising therapeutic target for cancer treatment. *Cell Death Dis.* 2013;4:e838
- Sun Y, Zhang J, Peng ZL. Beclin1 induces autophagy its potential contributions to sensitizes SiHa cells to carboplatin therapy. *Int J Gynecol Cancer* 2009; 19(4):772–6.
- Tan C, Wu S, Lai S, Wang M, Chen Y, Zhou L, Zhu Y, Lian W, Peng W, Ji L, Xu A. Synthesis, structures, cellular uptake and apoptosis-inducing proprieties of highly cytotoxic ruthenium-Norharm-an complexes. *Dalton Trans.* 2011; 40(34):8611-21.
- Tang N, Du G, Wang N, Liu C, Hang H, Liang W. Improving penetration in tumors with nanoassemblies of phospholipids and doxorubicin. *J Natl Cancer Inst.* 2007; 99(13):1004-15.
- te Poele RH, Okorokov AL, Jardine L, Cummings J, Joel SP. DNA damage is able to induce senescence in tumor cells in vitro and in vivo. *Cancer Res.* 2002; 62:1876–1883
- Teicher BA, Linehan WM, Helman LJ. Targeting cancer metabolism. *Clin Cancer Res.* 2012 ; 18(20):5537-45.
- Tessarz P, Kouzarides T. Histone core modifications regulating nucleosome structure and dynamics. *Nat Rev Mol Cell Biol.* 2014; 15(11):703-8.
- Theeler BJ, Gilbert MR. Advances in the treatment of newly diagnosed glioblastoma. *BMC Med.* 2015; 13:293.
- Thornberry NA, Lazebnik Y. Caspases: enemies within. *Science.* 1998; 281:1312–1316.

- Toh HS, Compton RG Electrochemical detection of single micelles through 'nano-impacts' *Chem. Sci.* 2015; 6: 5053-5058

V

- Vaccaro M, Accardo A, Tesaro D, Mangiapia G, Lof D, Schillen K, et al. Supramolecular aggregates of amphiphilic gadolinium complexes as blood pool MRI/MRA contrast agents: physicochemical characterization. *Langmuir* 2006; 22:6635e43
- van den Berg HW, Roberts JJ Investigations into the mechanism of action of anti-tumour platinum compounds: time- and dose-dependent changes in the alkaline sucrose gradient sedimentation profiles of DNA from hamster cells treated with cis-platinum (II) diamminedichloride. *Chem Biol Interact.* 1975; 11(6):493-9.
- van Rijt SH, Sadler PJ. Current applications and future potential for bioinorganic chemistry in the development of anticancer drugs. *Drug Discov Today.* 2009; 14(23-24):1089-97.
- van Rijt SH, Peacock AF, Johnstone RD, Parsons S, Sadler PJ. Organometallic osmium(II)arene anticancer complexes containing picolinate derivatives. *Inorg Chem.* 2009; 48(4):1753-62.
- Vandenplas ML, Carlson RW, Jeyaretnam BS, McNeill B, Barton MH, Norton N, Murray TF, Moore JN. Rhizobium sin-1 lipopolysaccharide (LPS) prevents

enteric LPS-induced cytokine production. *J Biol Chem.* 2002; 277(44):41811-6.

- Vergara A, D'Errico G, Montesarchio D, Mangiapia G, Paduano L, Merlino A. Interaction of anticancer ruthenium compounds with proteins: high-resolution X-ray structures and raman microscopy studies of the adduct between hen egg white lysozyme and AziRu. *Inorg Chem.* 2013; 52(8):4157-9.
- Vergara A, Russo Krauss I, Montesarchio D, Paduano L, Merlino A. Investigating the ruthenium metalation of proteins: X-ray structure and Raman microspectroscopy of the complex between RNase A and AziRu. *Inorg Chem.* 2013; 52(19):10714-6
- Vertut-Doi A, Ishiwata H, Miyajima K. Binding and uptake of liposomes containing a poly(ethylene glycol) derivative of cholesterol (stealth liposomes) by the macrophage cell line J774: influence of PEG content and its molecular weight. *Biochim Biophys Acta.* 1996; 1278(1):19-28.
- Vidimar V, Meng X, Klajner M, Licon C, Fetzer L, Harlepp S, Hebraud P, Sidhoum M, Sirlin C, Loeffler JP, Mellitzer G, Sava G, Pfeffer M, Gaiddon C. Induction of caspase 8 and reactive oxygen species by ruthenium-derived anticancer compounds with improved water solubility and cytotoxicity. *Biochem Pharmacol* 2012; 84 (11): 1428-1436.

W

- Waddington CH. The epigenotype. 1942. *Int J Epidemiol.* 2012; 41(1):10-3.
- Walczak H, Krammer PH. The CD95 (APO-1/Fas) and the TRAIL (APO-2L) apoptosis systems. *Exp Cell Res.* 2000; 256(1):58-66.
- Wang M, Thanou M. Targeting nanoparticles to cancer. *Pharmacol Res.* 2010; 62(2):90-9.
- Waring P. Redox active calcium ion channels and cell death. *Arch Biochem Biophys.* 2005; 434:33-42.
- Webster BR, Lu Z, Sack MN, Scott I. The role of sirtuins in modulating redox stressors. *Free Radic Biol Med.* 2012; 52(2):281-90.
- White AE, Hieb AR, Luger K. A quantitative investigation of linker histone interactions with nucleosomes and chromatin. *Sci Rep.* 2016; 6:19122.
- Wiethoff CM, Smith JG, Koe GS, Middaugh CR. The potential role of proteoglycans in cationic lipid-mediated gene delivery. Studies of the interaction of cationic lipid-DNA complexes with model glycosaminoglycans. *J Biol Chem.* 2001; 276(35):32806-13.
- Wilson C, Keefe AD. Building oligonucleotide therapeutics using non-natural chemistries. *Curr Opin Chem Biol.* 2006; 10(6): 607-14.
- Wlodkovic D., Skommer J., Darzynkiewicz Z. Flow cytometry-based

apoptosis detection. *Methods Mol Biol.* 2009;559:19-32.

- Wood CM, Sodngam S., Nicholson JM, Lambert SJ, Reynolds CD, Baldwin JP. The oxidised histone octamer does not form a H3 disulphide bond. *Biochim Biophys Acta.* 2006; 1764(8):1356-62.
- Wu B, Ong MS, Groessl M, Adhireksan Z, Hartinger CG, Dyson PJ, Davey CA. A ruthenium antimetastasis agent forms specific histone protein adducts in the nucleosome core. *J. Chem. Eur.* 2011; 17(13): 3562-3566.
- Wu D, Ingram A, Lahti JH, Mazza B, Grenet J, Kapoor A, Liu L, Kidd VJ, Tang D. Apoptotic release of histones from nucleosomes. *J Biol Chem.* 2002; 277(14):12001-8.

X

- Xiong F, Mi Z, Gu N. Cationic liposomes as gene delivery system: transfection efficiency and new application. *Pharmazie.* 2011; 66(3):158-64.
- Xu WS, Parmigiani RB, Marks PA. Histone deacetylase inhibitors: molecular mechanisms of action. *Oncogene.* 2007; 26(37):5541-52.

Y

- Yang WY, Gu JL, Zhen TM Recent advances of histone modification in gastric cancer. *J Cancer Res Ther.* 2014; of histone modification in gastric cancer. 10 Suppl:240-5.
- Yoon S, Eom GH. HDAC and HDAC inhibitor: From Cancer to Cardiovascular

- Diseases. *Chonnam Med J.* 2016; 52(1):1-11
- Yu L, McPhee CK, Zheng L, Mardones GA, Rong Y, Peng J et al. Termination of autophagy and reformation of lysosomes regulated by mTOR. *Nature* 2010; 465: (7300)942–946.

Z

- Zabner J, Fasbender AJ, Moninger T, Poellinger KA, Welsh MJ. Cellular and molecular barriers to gene transfer by a cationic lipid. *J Biol Chem.* 1995; 270(32):18997-9007.
- Zeiss CJ. The apoptosis-necrosis continuum: insights from genetically altered mice. *Vet Pathol.* 2003; 40(5):481-95.
- Zhang D, Fan D. New insights into the mechanism of gastric cancer multidrug resistance and future perspectives. *Future Oncol.* 2010; 6(4):527-37.
- Zhang T, Cooper S, Brockdorff N. The interplay of histone modifications – writers that read *EMBO Rep.* 2015; 16(11): 1467–1481.
- Zhang X, Jiang SJ, Shang B, Jiang HJ. Effects of histone deacetylase inhibitor trichostatin A combined with cisplatin on apoptosis of A549 cell line. *Thorac Cancer.* 2015; 6(2):202-8.
- Zong WX, Thompson CB. Necrotic death as a cell fate. *Genes Dev.* 2006; 20:1–15
- Zoroddu MA, Peana M, Medici S, Casella L, Monzani E, Costa M. Dalton Trans. Nickel binding to histone H4. 2010; 39(3):787-93.
- Zou CF, Jia L, Jin H, Yao M, Zhao N, Huan J, et al. Re-expression of ARHI (DIRAS3) induces autophagy in breast cancer cells and enhances the inhibitory effect of paclitaxel. *BMC Cancer* 2011;11:22

Web sites:

<http://globocan.iarc.fr>

<http://uniprot.org>

<http://nano.cancer.gov/>

<http://lifesci.dundee.ac.uk/technologies/flow-cytometry-cellsorting/techniques/cell-death-and-apoptosis>

Books:

Laurence Brunton, Bruce Chabner, Bjorn Knollman. Goodman and Gilman's. *The Pharmacological Basis of Therapeutics.* 12th Edition.

ACKNOWLEDGEMENTS

I wish to tell thanks to all the colleagues and supervisors with whom I had the pleasure of working during my Ph.D., for their friendly assistance.

First of all, I want to express my gratitude for my tutor Prof. Rita Santamaria, for her constant and careful support during my doctorate; it was significant both for my professional and personal growth.

Heartfelt thanks to the Prof. Carlo Irace, for introducing me to the research world and for his valuable advices, and also to all students that, over the years, took part in the F22 Lab, for sharing with me this beautiful experience.

I wish to spare a special thought to the memory of the Prof. Alfredo Colonna.

Moreover, I would like to thank the Prof. Luigi Paduano and Prof. Daniela Montesarchio, for giving me the possibility to test the compounds made by them, and for the excellent "cultural exchange" between biochemists and chemists.

I wish to express my thankfulness to all the people that I have known during the period of my Ph.D. held at the Inserm Institute of Strasbourg, primarily for their great welcome.

I am grateful to my supervisor Dr. Christian Gaidon, not only for allowing me this good experience, but also for his teachings, and for encouraging my enthusiasm during this training.

Sincere thanks to the Dr. Georg Mellitzer for his precious and stimulating suggestions, and to all the members of the Gaidon-Mellitzer Lab, in particular Christophe Orvaine and Veronique Dévignot for their important help.

Finally, I want to address a thought to all the people that are part of my private life, my family and my friends, that always demonstrate their love and believe in me.

To my dad and my mother, simply for being my first mentors.

To Guglielmo, to be always with me.